2022

IL-22 Mediated Host Defense During Attaching-Effacing Pathogen Infection

Baiyi Cai
University Of Alabama At Birmingham

IL-22 MEDIATED HOST DEFENSE DURING ATTACHING-EFFACING PATHOGEN INFECTION

by

BAIYI CAI

CASEY T. WEAVER, COMMITTEE CHAIR
CHARLES O. ELSON
HUI HU
LAURIE E. HARRINGTON
ROBERT S. WELNER

A DISSERTATION

Submitted to the graduate faculty of The University of Alabama at Birmingham,
in partial fulfillment of the requirements for the degree of
Doctor of Philosophy

BIRMINGHAM, ALABAMA

2022

IL-22 MEDIATED HOST DEFENSE DURING ATTACHING-EFFACING PATHOGEN INFECTION

BAIYI CAI

IMMUNOLOGY

ABSTRACT

Intestinal infections are a cause of morbidity and mortality worldwide and remain a public threat. Interleukin (IL)-22 is central to host immune responses in the intestine during infection and inflammation. IL-22 can be produced by both innate and adaptive immune cells, yet their relative contributions to host protection remain unclear.

Here we demonstrated the specific role and mechanism for IL-22 from innate and adaptive sources to protect the host. Using the *Citrobacter rodentium* (*C.r*) model, we found that IL-22 from innate cell, protect the host during early infection. IL-22 induces epithelial production of polymorphonuclear neutrophils (PMN) recruiting chemokine CXCL1, CXCL2 and CXCL5 through IL-22 receptor signaling on intestinal epithelial cells, to promote PMN recruitment into the colon during early infection. We showed that PMN protects the host by limiting *C.r* load and preventing crypt invasion. PMNs are recruited to both intestinal epithelium and lamina propria during infection and prevent *C.r* from invading colonic crypts.

We also found that IL-22 from $CD4^+$ T cells is important during the late phase response. Uniquely, mice with IL-22 deficiency from $CD4^+$ T cells suffered massive *C.r* invasion into the colonic crypts. In line with this, we found IL-22 provided more systematic

activation of STAT3 at both surface and cryptal epithelial cells, and IL-22 producing $CD4^+$ T cells are located in close proximity to colonic crypt cells. $CD4^+$ T cell derived IL-22 activates host-protective transcriptome programs from intestinal epithelial cells, including AMPs and chemokines.

Lastly, our research specified the role of IL-22 mediated antimicrobial responses during *C.r* infection. We found Lcn2 protects the host by limiting bacterial load during early infection. Since PMNs are required for host protection against *C.r* and are recruited by the IL-22 response, we examined the role of neutrophil elastase (NE) and ROS production, in *C.r* infection. We found NE protects the host from early infection by limiting *C.r* load and prevent *C.r* from invading the crypt region. Meanwhile, NOX2 mediated ROS production is required to protect the host from fatality caused by *C.r* infection. We also found IL-22 induced iNOS production is required for bacterial load control during early infection.

DEDICATION

This work is dedicated to my parental grandmother Cuilan Wan,
who teaches me to face the world with courage and kindness,
and for her unconditional love and support

ACKNOWLEDGEMENT

This work is by no means achieved solely by myself, but a collective result of many kind and smart persons, whom I feel lucky and blessed to encounter during my life.

First, this work won't be formed without my mentor, Dr. Casey Weaver. He is kind enough to allow me to board his voyage of science expedition and guides through the fascinating yet challenging field of immunology research. I am also grateful to have Dr. Carlene Zindl to teach me benchwork, scientific thinking, and many other skills without which I won't be an immunology scientist today. Thank you, Carlene, for all the 'come in' you said that saved my life.

I am lucky to be in a fun, creative and helpful group. Here I would like to thank our current and past lab members: Daniel Silberger, Jeffery Singer, Daniel Ditoro, David Figge, Stacey Harbour, Blake Frey, Duy Pham, Garret Wilson, Emma Dean, Lennard Duck, Robin Hatton, and Awal Chadha. Those people really sparked the lab with their brilliant mind to push my research forward. I would like to thank Yoshiko Nagaoka-Kamata, Emma Higginbotham, Kim Nguyen for their kind support with the mouse work and Henrietta Turner, Elaina Harris, and Constance Rutledge for all the help with paperwork.

Also, I appreciate the support of my committee: Dr. Charles Elson, Dr. Hui Hu, Dr. Laurie Harrington, and Dr. Robert Welner. Thank you for sharing your expertise and teaching me to be a critical and logical researcher.

I can’t imagine me going through Graduate School without my friends: Joe Gould, Fangming Zhu, Xianyou Xia, Kai Qin, Hairui Su, Victor Du, Yuge Wang, Mingyong Liu, Jun Wang, Zhang Li, Zhaoqi Yan, Shijie Wang, Samuel Medlin, Ashley Connelly, Katundu Katundu, Alex Aquilino and many others. You guys really make my graduate school life more colorful.

I would like to thank my father Wenjun Cai, my mother Sumei Zhang and all other family members for their love and support.

Last but not least, my life will never be happy and peaceful without my beloved wife Xiaorui Zhang. Thank you for always having faith in me and helping me while going through many obstacles in my life.

TABLE OF CONTENTS

LIST OF FIGURES

A NON-REDUNDANT ROLE FOR T CELL-DERIVED INTERLEUKIN 22 IN ANTIBACTERIAL DEFENSE OF COLONIC CRYPTS

INNATE CELL-DERIVED INTERLEUKIN (IL)-22 PROMOTES EARLY PMN RECRUITMENT FOR ANTIBACTERIAL DEFENSE OF COLONIC SURFACE EPITHELIUM

LIST OF ABBREVIATIONS

A/E lesions	Attaching and effacing intestinal lesions
AMP	Antimicrobial peptide
C.r	*Citrobacter rodentium*
CD	Crohn's disease
CX3CR1	CX3C chemokine receptor 1
CXCL	C-X-C motif chemokine ligand
CXCR2	CXC chemokine receptor 2
DAPI	4′,6-diamidino-2-phenylindole
DARC	Duffy antigen receptor
DC	Dendritic cells
EHEC	Enterohemorrhagic *Escherichia coli*
EPEC	Enteropathogenic *Escherichia coli*
GWAS	Genome-wide association studies
HNE	Host nutrient extraction
IBD	Inflammatory bowel disease
IE	Intestinal epithelium
IEC	Intestinal epithelial cells
IFN	Interferon
Ig	Immunoglobulin

ILC	Innate lymphoid cell
iNOS	Inducible nitric oxide synthase
KO	Knockout
Lcn2	Lipocalin-2
LD	Live/Dead dye
LEE	Locus of enterocyte effacement
LP	Lamina propria
LTi	Lymphoid tissue inducer
Mac/Mo	Macrophage and monocytes
MPAK	Mitogen-activated protein kinase
NET	Neutrophil extracellular traps
Plzf	Promyelocytic leukemia zinc finger
PMN	Polymorphonuclear neutrophils
RORγt	Retinoic-acid-receptor-related orphan nuclear receptor gamma
ROS	Reactive oxygen species
SFB	Segmented filamentous bacteria
SNP	Single nuclear polymorphisms
STAT3	Signal transducer and activator of transcription 3
Stx	Shiga toxin
T3SS	Type III secretion system
Tir	Translocated intimin receptor
TNF	Tumor Necrosis Factor alpha

UC	Ulcerative colitis

INTRODUCTION

Intestinal infection and inflammation

Enteropathogenic *Escherichia coli* (EPEC) and enterohemorrhagic *E. coli* (EHEC) cause over 300 million illnesses and 200,000 deaths each year, and remain a threat to public health in developing countries[1–3]. Both EPEC and EHEC cause diarrhea which can lead to life-threatening complications, especially in children under the age of 2 years old[4]. EPEC and EHEC share many similar features with commensal *E. coli* but express unique virulence factors, primarily the locus of enterocyte effacement (LEE) pathogenicity island[5,6]. LEE encodes a type III secretion system (T3SS) that allows EPEC and EHEC to form attaching and effacing intestinal lesions (A/E lesions)[7,8], a process whereby bacteria attach and establish a pedestal-like structure through the effacement of microvilli on the surface of epithelial cells, to establish their colonization[9].

EPEC injects various effector molecules such as translocated intimin receptor (Tir) into the host cell upon attachment, to facilitate adhesion to the epithelial cells by binding to intimin located on the EPEC[10]. This leads to increased cellular permeability and actin rearrangement resulting in A/E lesion formation. EPEC attachments activate several immune pathways including NF-kB[11], IL-8 production[12] and polymorphonuclear neutrophils (PMN) recruitment[13] in the host. EHEC also requires LEE for its initial attachment in the colon but produces Shiga toxin (Stx) as its main virulence factor[14]. Stx

can directly damage colonic epithelial cells by inducing cell apoptosis[15], and after epithelial translocation of bacteria, damages renal epithelial cells through both direct toxicity and induction of local inflammatory cytokine and chemokines[16]. However, the mechanism by which EPEC and EHEC induce host chemokine production and PMN recruitment in the colon remains largely unknown.

Inflammatory bowel disease (IBD), which includes Crohn's disease (CD) and ulcerative colitis (UC), is another gastrointestinal complication that threats human health[17]. IBD affects over 3.5 million people in the USA and Europe combined and caused more than $6 billion in medical expenses[18]. IBD is characterized by chronic inflammation in the gastrointestinal tract and causes diarrhea, abdominal pain rectal bleeding and weight loss[19]. CD affects both small and large intestine but can also extend to other parts of the gastrointestinal tract in a patchy fashion[20]. In contrast, UC occurs in the colon and rectum with a continuous pattern[21]. Pathologically, CD is characterized by thickened submucosa, transmural inflammation, fissuring ulceration, and granulomas[22], whilst UC inflammation is limited to the mucosa and submucosal region with cryptitis and crypt abscesses[17,23].

The exact cause of IBD remains unknown but several factors are shown to contribute to the pathogenesis of IBD including gut microbiota, host genetics, and environment[17]. Composition of the microbiota has been shown to correlate with IBD progression in patients[24–26], often linked to dysregulation of immune tolerance to commensal microbes. Host genetics also correlate with IBD development, as GWAS studies have identified single nuclear polymorphisms (SNP) in multiple loci including *NOD2* and *IL-23r* genes that are associated with IBD[27]. NOD2 is a pattern recognition receptor expressed by immune cells to detect muramyl peptide during an innate immune response[28], and IL-23R

is one of the key cytokine receptors expressed by $CD4^+$ T cells that promotes the production of proinflammatory cytokines IL-17 and IL-22[29,30]. Understanding how the host innate and adaptive immune system coordinate a response to intestinal infection can provide key information on the pathogenesis of IBD.

Citrobacter rodentium model for EPEC, EHEC and IBD

Citrobacter rodentium (C.r) is a naturally occurring A/E mouse pathogen and was first discovered in the mid-1970s[31]. *C.r* shares many similarities with EPEC and EHEC including its expression of LEE pathogenicity island as well as its ability to establish intestinal A/E lesions[32]. *C.r* strains with selective deletions of LEE and non-LEE encoded genes (such as *Tir* and *EspA*) allow us to study the role of each *C.r* virulence factor and how they interact with the host epithelium and host immune system[33]. An Stx-expressing strain of *C.r* was also developed to study Shiga-toxin-producing *E. coli*[34]. Since human EPEC and EHEC strains are unable to infect mice without antibiotic pre-treatment, *C.r* has become a principal model bacterium to study pathogenesis and host immune responses against A/E pathogens in mice[35,36]. Furthermore, *C.r* provides a valuable tool to dissect some fundamental immune mechanism in the gut, which could potentially help to expand our vision and knowledge on pathogenesis of IBD.

Infection cycle of C.r

C.r infection in the host is often categorized into 4 phases based on bacteria growth and clearance:[36]

The Establishment phase (1-3d p.i.): Orally inoculated *C.r* initially colonizes the cecum where it adapts to the microenvironment of the gastrointestinal tract. During this phase,

host and microbiota-derived environmental factors, including temperature[37], fluid sheer force[38], sulfate and phosphate[39], and butyrate[40], regulate the expression LEE in *C.r*. Interestingly, very small *C.r* microcolonies are established in the colon during the first 18 hours of infection. These early microcolonies spread during later infection and solely dictate A/E lesion pathogenesis, rather than through the reinfection by planktonic bacteria[41].

The Expansion phase (4-8d p.i.): *C.r* colonizes the distal colon where it attaches to the luminal surface of epithelial cells and forms A/E lesions, marked by the effacement of the brush border microvillous structure of intestinal epithelial cells (IEC)[42]. This is a hallmark that *C.r* has fully adapted to the gut environment and upregulates virulence factors such as intimin to facilitate their colonization[43]. During this stage of the infection, *C.r* inject Tir and other effectors into the host epithelial cells, to facilitate bacterial adhesion through binding to intimin located on the bacterial surface. This step activates the rearrangement of host epithelial actin to form a pedestal like structure and induces the effacement of microvilli on the epithelial cells (A/E lesion).

However, recent data have shown that intimin-Tir interaction is not sufficient for A/E lesion formation and additional non-LEE encoded effectors are needed[44]. *C.r* attachment induces tissue damage and activates an IEC repair response, resulting in proliferation of $Lgr5^+$ intestinal stem cells, increase of $Ki67^+$ transit amplifying cells, and elongation of the colonic crypts, defined as hyperplasia[45]. Notably, in scenarios where naïve mice infected with fecal *C.r* from other infected animals, *C.r* will bypass the establishment phase and start from the expansion phase[46].

The Steady-state phase (8-12d p.i.): *C.r* load in the colon reaches a plateau with 10^9 cfu/g of *C.r* in the feces. *C.r* utilizes T3SS to inject various effector proteins into host IECs that

manipulate innate and cell death pathways to promote further infection[47]. Recent studies have found that *E. coli* can also use a unique inner membrane protein complex named CORE, along with T3SS, to extract nutrients from host cells through a process defined as host nutrient extraction (HNE)[48]. It remains unclear what host nutrients uniquely support *C.r* colonization and whether the host immune response targets HNE to limit *C.r* infection.

The final Clearance phase (12-21d p.i.): clearance of *C.r* is mediated by an IgG antibody response[49,50], during which antibody-opsonized *C.r* will be engulfed by neutrophils[51]. Gut microbiota also compete with *C.r* at this phase to contribute to their eradication[52].

Host immunity against C.r

Host immunity against *C.r* requires the spatiotemporal coordination among epithelium, innate and adaptive immune cells[32].

Innate immune response to C.r. Initial *C.r* attachments activate epithelial production of antimicrobial molecules that includes AMPs, serum amyloid A and ROS as a first line of defense[53,54]. Subsequently, early pattern recognition receptors TLR2 and NOD2 respond to *C.r* derived peptidoglycan and LPS and promote the recruitment of protective $CCR2^{+}$ $CD11b^{+}$ $F4/80^{+}$ $Gr1^{+}$ macrophages[55], through induction of stromal production of CCL2. TLR-MyD88 dependent signaling induces anti-bacterial molecules Lcn2 and iNOS, as well as pro-inflammatory molecules in IL-6 and TNF-α[56]. In the absence of MyD88 signaling, colonic barrier function is negatively affected as evidenced by a reduction in epithelial integrity and a reduction in epithelial cell proliferation, resulting in severe mucosal injury[56].

Cells from the myeloid lineage, including PMNs, macrophages, and monocytes (Mac/Mono) are required for host protection against *C.r*[51,57,58]. PMNs are recruited to the

colon during *C.r* infection through CXCR2 receptor signaling, which is crucial for host protection. CXCR2-deficient mice show neutropenia in the colon and suffer from crypt invasion, increased bacterial load, and delayed clearance after *C.r* infection[57]. PMNs are uniquely able to engulf *C.r* opsonized by IgG antibody at later stages of infection[51]. More functions of PMNs and their roles will be discussed in the following chapter.

Mac/Monos are critical in assisting other immune cells to mediate host protection: $CX3CR1^+$ macrophages produce IL-1β to induce IL-22 production from ILC3 cells[59]. Mac/Monos are also important in supporting IFN- γ response from $CD4^+$ T cells, through their production of IL-12[58,60]. Both IL-12 and IFN-γ is required for host protection against *C.r* and mice with IL-12 deficiency suffered from cryptal invasion, increased hyperplasia and partially (10-15%) succumb to the infection, whilst IFN-γ KO mice have increased bacteria load increase and moderate hyperplasia but survive the infection and clear the bacteria eventually.

Meanwhile, dendritic cells (DCs) are also critical for host protection: mice depleted of colonic DCs show decreased survival and increased bacterial burden in response to *C.r*., likely due to a reduction in priming of $CD4^+$ T cells[58]. It was shown that Notch2-dependent intestinal $CD11b^+$ $CD103^+$ DCs are important source of IL-23, which promote protective IL-22 production from innate lymphoid cells and T cells.

RORγt– and IL-23–dependent IL-22-producing innate cells are required for the host protection against *C.r*[30,61,62]. These cells include γδT cells, $CD4^+$ lymphoid tissue inducer cells (LTi; a subset of ILC3s) and other ILC3s, which are found to provide host protection independently of adaptive immune cells[62].

Adaptive immune response to C.r. $CD4^+$ T and B cells are critical for host protection; mice deficient in either $CD4^+$ T cells or B cells (μMT mice) show delayed clearance and succumb to infection[63,64]. $CD8^+$ T cells are dispensable for the host protection[64]. Th17 and Th22 cells that produce IL-17 and IL-22, respectively, are important mediators of host defense at barrier sites and are the primary T helper subset involved in host protection against *C.r*. Deficiency in Th17 pathway genes, including IL-23 leads to increased susceptibility to *C.r* infection[29]. Interestingly, mice with either IL-17A or IL-17F deficiency suffer from increased *C.r* load and local bacterial expansion but are ultimately able to survive and clear the infection[65], suggesting these cytokines can be important for restricting bacterial growth but are not required for clearance. In contrast, mice deficient in IL-22 succumb to infection beginning on day 8 post infection[30,66] and suffer from increased dissemination of bacteria into the spleen and liver[67]. Notably, though innate cells can produce IL-22, IL-6–dependent IL-22 production from $CD4^+$ T cells is non-redundant and provides host protection during later infection[30], indicating a spatiotemporal coordination of IL-22 producing innate and adaptive immune cells during *C.r* infection.

The final clearance of *C.r* requires a robust humoral response as evidenced by the increased susceptibility of B cell-deficient mice to infection[64]. The interplay between $CD4^+$ T cells, B cells and phagocytes is important for clearance. $CD4^+$ T cell-dependent IgG, but not IgA or IgM, is critical for this clearance[49]. Antibody binding opsonizes *C.r* which can then be recognized by phagocytes (including PMNs), to engulf the bacteria[51].

IL-22 mediated host immunity

IL-22 was discovered in 2000 as a gene differentially express in IL-9 treated BW5147 murine T lymphoma cells[68]. IL-22 belongs to the IL-10 family of cytokines, which includes IL-10, IL-19, IL-20, IL-22, IL-24, IL-26, and the more distantly related IL-28A, IL-28B, and IL-29[69]. IL-22 is a secreted protein with α-helical structure, a shared feature among all IL-10 family cytokines[70], and signals through the IL-22 receptor consisting of two subunits: IL-22RA1 and IL-10RB. While IL-10RB is ubiquitously expressed, IL-22RA1 expression is limited to epithelial cells and stromal cells[71]. These two subunits are not exclusive for IL-22 and can form new cytokine receptors with other subunits: IL-22RA1 also forms a heterodimer with IL-20RB to detect IL-20 and IL-24[72]; IL-10RB can form heterodimers with IL-10RA, IL-28R and IL-20RA to detect IL-10, IL-28/IL-29, and IL-26, respectively[73]. IL-22RA2, also called IL-22BP, is another secreted, soluble IL-22 receptor subunit that negatively regulates IL-22 signaling by binding to IL-22 to prevent it from interact with IL-22RA1, which may play a role in the regulation of inflammatory responses at epithelial surfaces[74].

The master cytokine that regulates IL-22 production is IL-23. Notch2-dependent $CD11b^+$ DCs are one of the major sources of IL-23 during C.r infection to promote IL-22 production from ILC3s, Th17 and Th22 cells[75]. Myeloid cells also produce other inflammatory cytokines, including IL-1β, IL-6, TNFα, and IL-12, to promote IL-22 production[76].

IL-22 signaling Upon activation by IL-22, the IL-22 receptor complex approximates (Janus kinase 1) JAK1 and tyrosine kinase 2 (TYK2)[77], which leads to the phosphorylation of signal transducer and activator of transcription 3 (STAT3)[78,79]. MPAK, Akt and P38

pathways are also involved in IL-22 signaling[80]. Among those pathways, STAT3 is one of the key pathways in maintaining epithelium integrity and barrier functions by promoting Wnt-dependent intestinal crypt regeneration and AMP Reg3g and Pla2g2a production[79,81,82]

IL-22 mediated immune responses

IL-22 was initially found to be critical in innate immune responses in keratinocytes, where it induces the production of the antimicrobial peptide (AMP) β-defensin and activates STAT3[83]. In the intestine, IL-22 plays an indispensable role in protecting the colon from attaching/effacing pathogens. This protective role comes via multiple mechanisms: inducing antimicrobial molecules[66,84] and chemokines[85,86], as well as promoting epithelial regeneration and proliferation[87].

IL-22 promotes epithelial regeneration and barrier function Pathogen infections in the intestine can induce intestinal epithelial damage and cause disruption of epithelial barrier[88]. IL-22 activates $Lgr5^+$ intestinal stem cells located at bottom of the crypt and activate STAT3 to promote IEC regeneration and expansion of proliferating $KI67^+$ IECs[87]. This leads to the increase of transient amplifying (TA) cells that replace epithelial cells lost during infection[87,89,90] Meanwhile, IL-22 promotes cell survival by inducing pro-survival genes, including BCL_{XL}, *Mcl1* and *Hsp70*[79,91]. Some studies suggest that IL-22 stimulate TA cells through activation of Wnt and Notch pathway to promote intestine regeneration[89,92]. IL-22 also promotes wound healing in skin and colon tissues by inducing extracellular matrix and tissue formation downstream of STAT3. Mucus is usually stored in goblet cell vacuoles and acts as a static battier at the epithelial surface to isolate the intestinal epithelial cells from commensal and pathogenic microbiota[93]. IL-22 enhances

mucus secretion by goblet cells in the intestinal epithelium during infection by upregulating mucus associated genes, including *Muc1*, *Muc3*, *Muc10* and *Muc13*[94].

IL-22 induces PMN recruiting chemokines. IL-22 has been shown to induce neutrophil recruiting chemokines including CXCL1[95,96], CXCL2[97] and CXCL5[86] from hepatic cells, stromal cells and IECs. It has been shown that IL-22 mediated neutrophil recruitment through chemokine induction is one of the key contributing factors of epidermal alterations in psoriasis[98]. In a viral infection model, IL-22 promotes CXCL1 production in stromal nonhematopoietic tissue to recruit antiviral PMNs to infected tissue[86]. However, no studies have explored the role of IL-22–mediated neutrophil recruitment in colonic infection.

IL-22 induces production of AMPs IL-22 induces the production of several antimicrobial peptides (AMPs) including Reg3β, Reg3γ, Lcn2, S100A8, S100A9 and β-defensins[66,84,99–101]. Reg3β and Reg3γ belong to the Reg3 protein family that contain a C-type lectin domain, which facilitates peptidoglycan carbohydrate binding to kill bacteria[102]. Reg3β targets Gram negative pathogens including *Salmonella*[103], whilst Reg3γ targets Gram positive pathogens[104]. Interestingly, exogenous delivery of Reg3γ improved the survival the IL-22 KO mice during *C.r* infection[66]. This could due to a role for Reg3γ to maintain proper thickness of the mucus to reduce epithelial contact with pathogens[105]. The specific role of this family of AMPs on *C.r* infection remain largely unknown.

Lcn2, S100A8 and S100A9 are all AMPs that limit bacterial growth through metal sequestering, which is a common host immune strategy called nutritional immunity[106]. Lcn2 limits bacterial access to iron through binding to bacterial siderophores used to chelate iron for bacterial uptake[107]. S100A8 and S100A9 form a heterodimer called calprotectin in the presence of calcium. Calprotectin's bactericidal property comes from its

ability to sequester iron, manganese, and zinc through chelation[108]. Inability of access to these ions by bacteria disrupts the formation of several enzymes essential to bacterial metabolism[109]. Other than being an antimicrobial component, S100A8 and S100A9 also induce secretion of cytokines such as IL-1β, IL-6, IL-8 and TNF-α, to promote local inflammation[110,111].

The role of neutrophils during intestinal infection and inflammation

Polymorphonuclear neutrophils (PMN) are the most abundant leukocyte population in blood[112], comprising 50-60% of total leukocytes[113]. The number of PMNs produced daily is approximately 10^7 and 10^{11} in mice and humans, respectively[114]. PMNs are generated in the bone marrow and remain there for up to 6-7 days from last cell division to release into the blood stream[115]. Once released from the bone marrow, PMNs have a short life span with an average half-life of less than 24 hours, although they can live up to 5.4 days in humans[116]. PMNs are professional phagocytes but their role is far greater than just phagocytosis: they can release chemokines to facilitate the recruitment of other immune cells including macrophages[117], they also produce local inflammatory molecules[118]. The multiple roles of PMNs and their abundance in the gut during intestinal inflammation makes them an important target to study in order to fully understand the colonic immune response.

Life cycle of PMNs

PMN development starts from granulocyte-monocyte progenitors (GMPs) and goes through a series of maturation stages, with each stage marked by defined granulocyte-committed precursors: myeloblasts, promyelocytes, myelocytes, metamyelocyte, banded

neutrophil, mature neutrophil and finally circulating neutrophils[119]. Recent studies have also categorized PMNs as pre-, immature and mature neutrophils based on several surface markers including CXCR4, CXCR2, CD11b and Ly6G in mouse, or CD66b in human. In mice, pre-neutrophils are CD117+, CD11b+ and CXCR4+ cells; immature neutrophils are defined as $CD11b^+$, $Ly6g^+$ but CD101- and CXCR2- cells and mature neutrophils are $CD11b^+$, $Ly6G^+$, $CXCR2^+$ and $CD101^+$[120].

Mature neutrophils are released to the bloodstream and circulate around the body. During homeostasis, most 'unused' PMNs will undergo an aging process, marked by the downregulation of CXCR2 and upregulation of CXCR4[121]. A portion of aging PMNs will traffic back to the bone marrow, liver or spleen[122,123], with each of these organs contributing 30% of PMN clearance[124]. In response to inflammation, PMNs can be rapidly mobilized by chemokine gradients and other inflammation cues to the inflamed tissue, where they perform their immune function[125]. These tissue infiltrating PMNs are cleared via several pathways: they can be recruited to bone marrow, liver or spleen, similar to ageing circulating PMNs[124], via the CXCR4 receptor; or they will undergo apoptosis and clearance by other phagocytes including macrophage and monocytes[126]. Lastly, in the context of mucosal infection/inflammation, some PMNs migrate across the epithelium into luminal space where they bind pathogens or allergens and are carried away by mucus[127].

PMN recruitment

During PMN maturation, PMNs downregulate CXCR4 and upregulate chemokine receptor CXCR2 to leave bone marrow and enter the bloodstream[128]. During intestine infection, PMNs first cross the blood vessel through transendothelial migration, then moving through

tissue cells and eventually undergo transepithelial migration to pass intestinal epithelium to reach the pathogen in the lumen[129].

The initial neutrophil recruitment starts from tethering, rolling, adhesion, crawling and transmigration of circulation PMNs across the endothelium[125]. Endothelial cells around inflamed tissue upregulate adhesion molecules including P-selectin, E-selectins[130], and ICAM2[131]. These adhesion molecules bind to PMN surface glycosylated ligands, such as P-selectin glycoprotein ligand 1 (PSGL1), to capture circulating PMNs and facilitate their tethering and rolling[132]. PMNs will then come in contact with chemokines that decorate the endothelial cell surface, and other inflammatory cytokines (e.g., TNFα and IL-1β) to become activated[133]. The major PMN chemokines are positively charged molecules and anchored on negatively charged heparan sulphates on endothelium[134], thus creating an intravascular chemotactic gradient. Upon binding with its ligand, CXCR2, as a G-protein-coupled chemokine receptor, will induce changes in the conformation of PMN surface integrins, such as LFA1 (CD11a-CD18 complex) and MAC1 (CD11b-CD18 complex), to bind with ICAM1 and ICAM2 molecules to promote PMN adhesion to endothelial cells[135]. Recent studies also reveal that CXCL1 decorates endothelial cells and pericytes, to facilitate PMN crawling during transmigration[136].

After establishing adhesion to endothelial cells, PMNs transmigrate across the endothelium. This step requires multiple integrins, cell adhesion molecules (ICAM1 ICAM2, and VCAM1), and junctional proteins (PECAM1, CD99, JAMs and ECAMs)[137]. CXCL2 binds with ACKR1 receptor at the endothelial cell junction to aid PMN paracellular transmigration[136]. During this process, endothelial cells also rearrange cytoskeletal structures to change their attachments to the extracellular matrix, thereby facilitating PMN

transendothelial migration[138]. Meanwhile, PMNs utilize a group of proteases, including matrix metalloproteases and serine proteases (e.g. neutrophil elastase) to potentially degrade the extracellular matrix and migrate through endothelial junctions[139].

Extravasated PMNs then follow chemokine gradients to reach inflamed sites. PMNs need to be recruited by other chemokines that override the existing gradient, which is dictated by chemoattractant hierarchy[140]. Various PMN chemokine receptors and corresponding ligands have been found including: CXCR2-CXCL8 (in mice CXCR2 can bind CXCL1 (KC), CXCL2 (MIP-2), and CXCL5 (LIX))[141], BLT1-LTB4[142], and FRP1-fMLP[143]. These chemokine receptors can have parallel functions for PMN recruitment: CXCR2 can augment the function of BLT1 to enhance PMN migration, for instance[144]. On the other hand, some 'end target' chemokine receptor such as FRP1 can override other chemokine functions. For instance, bacterial derived molecules such as N-formyl-methionyl-leucyl-phenylalanine (fMLP) or the complement component C5a can act as 'end-target' chemokines and override CXCL8 or BLT1 gradients on endothelial cells[145]. Chemokines with different hierarchies also activate different signal pathways: most 'intermediate' chemokines activate PI3K to promote the phosphorylation of PIP2 into PIP3 to mediate PMN directional migration[146]. However, 'end-target' chemokines activate p38 MAPK to direct PMN recruitment[147].

Among these chemokine receptors, CXCR2 has been shown to be critical for protection of *C.r* infection. Global CXCR2 knockout mice fail to recruit PMNs to the colon during infection and have an increased bacterial load, more severe diarrhea and crypt invasion by *C.r*[57]. A study using bone marrow chimera model revealed that CXCR2 can be expressed by both endothelial cells and PMNs in the lung and both cell types are equally important

for PMN recruitment. Hematopoietic or non-hematopoietic knockout of CXCR2 lead to a 50% reduction in PMN recruitment in a lung infection model, suggesting that CXCR2 ligands not only act as a chemoattractant to recruit PMN into the tissue but also facilitate chemokine decoration on the endothelial cells to help PMN establish adhesion and rolling[148]. CXCR2 can bind to multiple ligands, including CXCL1, 2, 3 and 5[141]. So far, no evidence has shown a differential role of these ligands in directly signaling through CXCR2.

Immune function of PMN

PMNs are critical phagocytes that are capable of eliminating pathogens through three major killing mechanisms: phagocytosis, degranulation, and neutrophil extracellular trap (NET) formation (netosis). PMNs can also recruit and prime other immune cells and release pro-inflammatory molecules.

Phagocytosis Phagocytosis is initiated by dedicated receptors that sense particles as targets that activate signaling pathways which favor phagocytosis. Phagocytic receptors can be categorized into non-opsonic and opsonic receptors, based on their targets. Non-opsonic receptors, such as Dectin-1, Mincle, MCL and DC-SIGN[149,150], can directly bind to PAMPs to induce phagocytosis. Other non-opsonic receptors, include TIM-1, TIM-4, stabilin-2 and BAI-1[151–153]. Once phagocytic receptors are bound to targets, a series of downstream signals are activated, including phosphatidylinositol 3-kinase (PI3-K), GTPase, and protein kinase C (PKC), to promote actin polymerization that drive the formation of phagosomes[154,155]. This will promote the internalization of phagocytic receptors and initiate the phagocytosis process, followed by lipid composition changes to generate membrane protrusions that finalize phagosome formation[156]. Fresh phagosomes combine with endosomes to form phagolysosomes in a process that involves the accumulation of V-

ATPase and NADPH oxidase complex on the phagosome membrane to generate ROS[157,158]. Phagolysosomes also contain several hydrolytic enzymes, including cathepsins, proteases and lysozymes and lipases for its bactericidal function[159].

Degranulation Part of the PMNs host defense function relies on granules that store molecules with antimicrobial and inflammatory functions. PMN granules are categorized into 4 types: primary granules (azurophilic granules, markers: MPO and CD63), secondary granules (specific granules, markers: Lcn2 and CD66b), tertiary granules (gelatinase granules, marker: gelatinase B and CD11b), and secretory vesicles. Primary granules store hydrolytic enzymes such as elastase, and myeloperoxidase. The secondary and tertiary granules contents often overlap with each other, including lactoferrin, matrix metalloprotease 9 (gelatinase B), and Lcn2. The secretory vesicles contain mostly serum albumin[160].

NET formation. PMN NET formation is another major PMN defense mechanism to eliminate pathogens during infection. NETs are web-like structures that consist of de-condensed chromatin and mitochondrial DNA[161] decorated with bactericidal granule components, including calprotectin[162]. NET release depends on various PMN stimuli, including bacterial derived molecules (lipopolysaccharide), viruses, and cytokines[163]. ROS is also indispensable for netosis, and a recent study suggests that ROS mediates DNA damage and subsequently repair pathways leading to chromatin decondensation, which may be important for NET formation[164]. Based on the source of ROS, NET formation can be characterized by the requirement of NOX2. NOX2-dependent NET formation utilizes ROS from NOX2, and NOX2-independent NET formation uses ROS derived from mitochondrial. Recently, studies have found that PAD4 is required for the histone H3 de-

condensation during NOX-independent NET formation, and mice with PAD4 deficiency suffer from increase bacterial load and inflammation during *C.r* infection, suggesting a critical role for NET in protecting mice from *C.r* infection[165].

It has to be noted that these killing mechanisms often rely on mutual pathways and molecules to realize their function. For instance, ROS formation is required by all three-killing mechanisms upon neutrophil activation; neutrophil elastase not only digests engulfed targets during phagocytosis but also decorates NET to kill potential trapped pathogens. However, the specific role of these PMN effectors during *C.r* infection and whether they protect epithelial crypts remains unknown.

PMN pro-inflammatory functions Other than direct killing of targets, PMNs can also produce cytokines and chemokines to mediated inflammatory response and prime other immune cells.

PMNs have been shown to produce IL-22 during inflammation. In DSS induced colon inflammation, IL-22 producing PMNs are recruited into the colon upon IL-23 stimulation and protect the colon by inducing AMPs Reg3β and S100A8, to reduce epithelial damage[84]. Neutrophils can also produce IL-17 to promote self-recruitment during lung inflammation and induce IL-12/IFN-γ which promotes kidney ischemia-reperfusion injury[166] in mice but human PMNs don't produce IL-17A or IL-17F[148], shown by a recent *in vitro* study. PMN derived matrix metalloproteases (MMPs) also increase the activity of CXCL1 and CXCL5 through molecule cleavage to increase their chemoattractant activity [167–169]. PMNs are also the dominant source of IL-1β during *S. aureus* infection and form abscesses to control the spread of bacteria, a process which relies on PMN surface innate receptors including TLR2, NOD2, FPR1 and ASC/NLRP3[170].

PMNS also actively recruit themselves and other immune cells by producing various chemokines. PMN can produce CXCL1, CXCL2 and LTB4[171] to promote self-recruitment and PMN swarming during acute infection or inflammation, where PMN derived chemokines decorate surrounding tissue cells to create a 'passage' which allows rapid PMN recruitment to the infection site[172]. PMNs also produce macrophage and monocyte chemoattractants, such as CAP18, cathepsin G and azurocidin to recruit macrophages in the surrounding tissue[173]. PMNs can also produce CCL8 to promote the recruitment of ILC2s[174]. PMNs can prime the function of surrounding immune cells: PMN derived inflammatory molecules, including certain AMPs and ROS can prime the inflammasome and IL-1β production from alveolar macrophages[175].

Overall research goal

IL-22 is critical for immune defense at mucosal sites. A number of cell types including $CD4^+$ T cells, ILCs, NK, NKT cells, γδT cells and neutrophils have been shown to produce IL-22, but the relative contributions of innate vs adaptive cell IL-22 to intestinal immunity is unclear. IL-22 induces both antimicrobial peptides as well as neutrophil and other innate cell-recruiting chemokines from IECs, but their kinetics, role in protection against *C.r*. and regulation by IL-22 are not well understood. PMNs recruited by IL-22-induced chemokines are critical for host defense and are thought to protect epithelial crypts from bacterial invasion, preventing systemic dissemination of bacteria and controlling bacterial burden until an effective adaptive immune response is initiated, after which they become important in assisting antibody mediated clearance of bacteria by phagocytosis.

This study aims to address three main questions:

1. What is the relative contribution of innate v adaptive IL-22 to host protection in *C.r* infection?
2. How does IL-22 mediate PMN recruitment into the colonic mucosa and which chemokines are critical for this process?
3. What are the antimicrobial peptides involved in host protection in C.r. infection and how does IL-22 regulate their expression?

A NON-REDUNDANT ROLE FOR T CELL-DERIVED INTERLEUKIN 22 IN ANTIBACTERIAL DEFENSE OF COLONIC CRYPTS

By

CARLENE L. ZINDL, STEVEN J. WITTE, VINCENT A. LAUFER, MIN GAO, ZONGLIANG YUE, KAREN M. JANOWSKI, BAIYI CAI, BLAKE FREY, DANIEL J. SILBERGER, STACEY N. HARBOUR, JEFFREY R. SINGER, HENRIETTA TURNER, FRAN E. LUND, BRUCE A. VALLANCE, ALEXANDER F. ROSENBERG, TRENTON R. SCHOEB, JAKE Y. CHEN, ROBIN T. HATTON AND CASEY T. WEAVER

Immunity. 2022 Mar 8;55(3):494-511.e11

Format adapted for dissertation

Summary

Interleukin (IL)-22 is central to immune defense at barrier sites. In response to attaching and effacing enteropathogenic bacteria, IL-22 produced by type 3 innate lymphoid cells (ILC3s) is thought to act early to protect intestinal epithelial cells (IECs) in advance of T cell-derived IL-22, although specific contributions of ILC versus T cell-derived IL-22 are unknown. Here, using mice that both report IL-22 and allow its lineage-specific deletion, we identified spatiotemporal differences in the production and actions of IL-22 by innate immune cells and T cells that led to geographically distinct responses of IECs during infection by *Citrobacter rodentium (C.r)*. Innate cell-derived IL-22 activated STAT3 in *C.r*-colonized surface IECs and initially restrained bacterial growth but its actions were not sustained as infection progressed. T cell-derived IL-22 induced more robust and extensive activation of STAT3 in IECs and was required for STAT3 signaling in IECS lining colonic crypts; T cell-specific deficiency of IL-22 led to pathogen invasion of the crypts and increased mortality. This reflected a requirement for T cell-derived IL-22 to upregulate a diversity of host-protective genes, including those encoding AMPs, neutrophil-recruiting chemokines, and mucin-related molecules, while also restricting IFN□–induced pro-inflammatory genes. Thus, IL-22–producing T cells are indispensable for protection of the intestinal crypts via their activation of crypt-lining epithelium.

Introduction

Host defense against extracellular bacteria is orchestrated by type 3 immunity, which employs cells of the innate and adaptive immune systems that share responsiveness to IL-23 and production of IL-17 family cytokines and the IL-10 family cytokine, IL-22 (Mangan et al., 2006; Sonnenberg et al., 2011a; Zheng et al., 2008). *Citrobacter rodentium* (*C.r*) is an attaching and effacing (AE) enteric pathogen that models human disease caused by enteropathogenic and enterohemorrhagic *E. coli* (EPEC and EHEC) (Collins et al., 2014; Mundy et al., 2005; Silberger et al., 2017). These Gram-negative bacteria use a type III secretion system to inject effectors into apical surfaces of intestinal epithelial cells (IECs), allowing them to attach and efface IEC microvilli and establish colonization (Donnenberg et al., 1997; Frankel et al., 1998). Clearance of *C.r* occurs when bacterial-laden IECs are shed into the lumen (Barker et al., 2008; Clevers, 2013). However, (AE) pathogens have evolved mechanisms to inhibit apoptosis and turnover of IECs to prolong colonization (Hemrajani et al., 2010; Kim et al., 2010; Nougayrède et al., 2005). Moreover, *C.r* manipulates host IEC metabolism for its growth and evasion from innate immune responses (Berger et al., 2017). Therefore, antigen-specific CD4 T-cell and B-cell responses are ultimately required for pathogen eradication (Bry et al., 2005; Maaser et al., 2004; Simmons et al., 2003; Vallance et al., 2002).

Histopathological hallmarks of *C.r* infection are elongation of crypts due to epithelial hyperplasia and goblet cell depletion (hypoplasia) in the distal colon (Berger et al., 2017; Bergstrom et al., 2008; Borenshtein et al., 2009; Chan et al., 2013; Ma et al., 2006; Papapietro et al., 2013), which is the infectious niche of *C.r*. Similar changes are induced by pathogenic *E. coli* infection of the ileum (EPEC) or transverse colon (EHEC) in humans

(Croxen et al., 2013). Elongation of the crypts is thought to distance intestinal stem cells (ISCs) residing in the base of crypts from physical and metabolic damage that result from infection, thereby protecting progenitors that give rise to all IEC subsets (Kaiko et al., 2016; Liang et al., 2017; Matsuki et al., 2013; Okada et al., 2013). Infection-induced accelerated production of IEC progenitors, or transient-amplifying (TA) cells, correlates with increased shedding of *C.r*-laden IECs (Collins et al., 2014; Higgins et al., 1999); however, mechanisms by which IEC differentiation is altered during *C.r* infection are incompletely defined.

STAT3 activation is a major output of the liganded IL-22 receptor, composed of IL-22Ra1 and IL-10Rb subunits that are expressed by IECs (Lindemans et al., 2015). IL-22 signaling into IECs has been shown to be important for mucosal barrier protection and restitution of the intestinal epithelium during infection (Basu et al., 2012; Pickert et al., 2009; Wittkopf et al., 2015; Zheng et al., 2008). IL-22R signaling upregulates host defense molecules, such as antimicrobial peptides (e.g., Reg3 and S100a family members) (Liang et al., 2006; Wolk et al., 2006; Zheng et al., 2008), inflammatory reactive proteins (e.g., Lbp, Saa, complement, chemokines) (Aujla et al., 2008; Boniface et al., 2005; Hasegawa et al., 2014; Liang et al., 2010), and proteins that alter the mucus layer (e.g., Muc1, Fut2) (Pham et al., 2014; Sugimoto et al., 2008). Different types of innate cells, including ILC3s, NK cells, NKT cells, γδT cells and neutrophils (Cella et al., 2008, 2010; Chen et al., 2016; Colonna, 2009; Lee et al., 2012, 2015; Satpathy et al., 2013; Sonnenberg et al., 2011b, 2011a; Spits et al., 2013; Zheng et al., 2008; Zindl et al., 2013) can respond to IL-23 to produce IL-22 that acts on IECs. CD4 T cells of the Th17 pathway—Th17 and Th22—also produce IL-22, whether induced by IL-23 or TCR signaling (Akdis et al., 2012; Basu et al.,

2012; Guo et al., 2014; Kim et al., 2012; Trifari et al., 2009). ILC3s are thought to be the major source of IL-22 contributed by innate cells and are crucial for early host protection (Rankin et al., 2016; Sonnenberg et al., 2011a; Spits et al., 2013). Th17 and Th22 cells contribute to IL-22 following recruitment to the intestinal mucosa later in *C.r* infection (Liang et al., 2006; Zheng et al., 2007) and are important for enhancing barrier protection and limiting IEC damage. (Basu et al., 2012; Silberger et al., 2017; Zenewicz et al., 2008). T cell-dependent, *C.r*-specific IgG is also required to eradicate virulent *C.r* (Kamada et al., 2015). Studies using mice with deficiency of *Ahr* in RORγ^+ innate cells in the presence or absence of T cells shows both ILC3s and T cells contribute to antimicrobial defense during *C.r* infection (Song et al., 2015). However, relative contributions of IL-22$^+$ innate cells and CD4 T cells in the context of an intact immune system including B cells and all T-cell subsets, and the mechanisms by which IL-22$^+$ T cells control *C.r* infection are unclear.

Using new IL-22 reporter/conditional knockout mice to identify IL-22 producers and target deficiency of IL-22 to different cell populations, we have found that ILC3s and Th17/Th22 cells have distinct roles in activating IECs during *C.r* infection. Whereas innate cell-derived IL-22 dominates first and targets superficial IECs early in infection to limit the initial wave of *C.r* colonization and spread, T cell-derived IL-22 is indispensable later for induction of heightened and sustained STAT3 activation in both superficial and crypt IECs to prevent bacterial invasion of colonic crypts and limit bacterial dissemination as infection progresses. RNA-seq analysis of colonic IECs indicated that IL-22$^+$ T cells uniquely mobilize multiple mechanisms that underlie their essential role in protecting the crypts and preserving ISCs that provide progeny for restitution of the infected intestinal epithelium.

Results

Distinct spatiotemporal distribution of IL-22$^+$ innate and adaptive immune cells during *C.r* infection

Multiple immune cell types can produce IL-22 in the intestines (Basu et al., 2012; Cella et al., 2008; Colonna, 2009; Silberger et al., 2017; Sonnenberg et al., 2011a; Spits et al., 2013; Trifari et al., 2009; Zindl et al., 2013). To better characterize dynamics of the location and number of IL-22$^+$ cells during *C.r* infection, we developed gene-targeted IL-22 reporter/conditional (cKO) mice to track and delete specific subsets of IL-22$^+$ cells (*Il22*$^{hCD4.fl}$ mice, hereafter labeled *Il22*^{hCD4}; **Figures S1A-S1D**). Using the reporter read-out, we found that type 3 innate lymphoid cells (ILC3s) were the dominant IL-22$^+$ cells at steady state (**Figures 1A-1E**). During early *C.r* infection (d3-6), mCD4$^+$TCRβ$^-$ ILC3s (LTi cells) expressed the greatest amount of hCD4 (IL-22) (**Figures 1A-1C**) on a per-cell basis, albeit similar numbers of IL-22$^+$ mCD4$^-$TCRβ$^-$ cells (non-LTi ILC3s) were present. Interestingly, no significant change in numbers of IL-22$^+$ ILCs was observed throughout infection, suggesting either these cells did not proliferate or alter their turnover rates during infection. This is consistent with recent reports that ILCs populate non-lymphoid tissues early in life and remain largely static (Ahlfors et al., 2014; Gasteiger et al., 2015) (**Figures 1A-1B**). In contrast, rapid increases in hCD4$^+$ (IL-22$^+$) CD4 T cells in the infected mucosa after the first week resulted in their outnumbering all IL-22$^+$ innate cells combined, and they produced increased IL-22 on a per-cell basis compared to innate cells (**Figures 1A**, **1B** and **S1E**).

Because *in situ* detection of hCD4/IL-22 by immunostaining proved unreliable using available antibodies, *Rorc*/EGFP BAC reporter mice (Lochner et al., 2008) were used to

identify and localize colonic RORγt$^+$ cells, including IL-22$^+$ ILC3s and Th17/Th22 cells (**Figures 1D, 1E** and **S1F-S1H**). Notably, while some IL-22$^+$RORγt$^+$ cells were found within the intestinal epithelium during infection, the great majority were found within non-epithelial tissue compartments, and ILC3s were mostly NKp46$^-$ (**Figures S1I-S1K**). In naïve mice and during *C.r* infection, RORγt$^+$ CD3$^-$ ILC3s were clustered within colonic lymphoid tissues (i.e., solitary intestinal lymphoid tissues, or SILTS, and colonic patches); few ILC3s were found in the lamina propria (LP) and redistribution of these cells outside of ILFs did not change during infection, in agreement with recent studies (Ahlfors et al., 2014; Colonna, 2018; Gasteiger et al., 2015) (**Figures 1D-1E**). Similarly, there were no significant changes in the few RORγt$^+$ T cells found in ILFs in naïve mice and during infection. In marked contrast, RORγt$^+$ CD4 T cells increased dramatically (>50-fold) in the LP with numerous T cells found in close apposition to crypt IECs. Collectively, these findings indicate IL-22$^+$ ILC3s and CD4 T cells occupy distinct microanatomic niches over the course of *C.r* infection: IL-22$^+$ ILC3s are restricted to ILFs and static in number, whereas IL-22$^+$ CD4 T cells populate the LP in increasing numbers to become the dominant IL-22 producers, with more uniform distribution and in closer proximity to the epithelial monolayer relative to ILC3s.

IL-22 produced by either ILCs or T cells is required to restrain bacterial burden at different times during *C.r* infection

The distinct spatial and temporal deployment of IL-22$^+$ ILCs and T cells during *C.r* infection suggested the possibility of complementary or unique functions for these cells in mucosal barrier defense. To evaluate their relative contributions, we crossed the *Il22*^{hCD4} mice with different Cre recombinase lines to target IL-22 deficiency to all cells, innate cells

or T cells (**Figure 2A**). Using a bioluminescent strain of *C.r* (ICC180) that allowed real-time visualization of colonization in the whole animal (Wiles et al., 2006), we found infected global KO (gKO) mice (*EIIa-cre* x *Il22*^{hCD4}; *Il22*^{EIIa}) had increased burden of *C.r* compared to controls as early as 3 days after inoculation and all gKO mice succumbed (**Figures 2B-2D**), in accord with previous results (Zheng et al., 2008). Similar to *Il22*^{EIIa} gKO mice, innate cell-specific deficiency of IL-22 (*Zbtb16/Plzf)-cre* x *Il22*^{hCD4}; *Il22*^{Plzf} cKO)—in which *Il22* is deleted in all γδ T cells and iNKT cells, and ~80% of all colonic ILC3s (**Figure S2D**) (Constantinides et al., 2014; Kovalovsky et al., 2008; Lu et al., 2015; Savage et al., 2008)—succumbed to *C.r* infection with similar kinetics to gKO mice, correlating with heightened *C.r* burden around d3 compared to controls (**Figures 2B, 2E** and **2F**). However, ~40% of *Il22*^{Plzf} cKO mice survived infection, presumably rescued by influx of IL-22^{+} T cells not present in gKO mice. Clearance of *C.r* progressed with the same kinetics as WT controls over the late course of infection (**Figures 2B**, **1A** and **1B**). This contrasted with T cell-specific deficiency of IL-22 (*Cd4-cre* x *Il22*^{hCD4}; *Il22*$^{\Delta Tcell}$ cKO), in which there was no increase in *C.r* burden early, but ~40% of mice succumbed late with delayed clearance of *C.r* compared to controls (**Figures 2B, 2G** and **2H**). Because *C.r* colonization of colonic IECs is detectable around d3 and crests by d5-7 after inoculation (**Figures S2A-S2C**), these data establish that innate cell-derived IL-22 acts to limit *C.r* colonization during the early phase of infection, but is unable to compensate for T cell-derived IL-22 in bacterial restraint and host protection later.

T cell-derived IL-22 is essential for protection of colonic crypts against bacterial invasion

In view of the foregoing results, we postulated that IL-22 delivered by T cells played a non-redundant role in barrier defense against *C.r* infection. To elucidate potential

mechanisms, we examined the dynamics and distribution of bacterial epithelial attachment using GFP-expressing *C.r* (*C.r*-GFP; Bergstrom et al., 2010), and assessed histopathologic features of tissue injury over the course of infection in IL-22 cKO mice. Coincident with onset of death in infected *Il22*^{EIIa} gKO mice (d8), we observed heightened epithelial injury in the middle and distal colon with increased goblet cell (GC) and crypt cell loss, and depletion of crypts (**Figures 3A** and **S3A**). This was accompanied by multifocal ulcerations of the mucosa and mass translocations of *C.r* cells (**Figure 3A**, and data not shown), consistent with our previous findings in IL-23- and IL-22-deficient mice (Basu et al., 2012; Mangan et al., 2006). During early phase of infection (d3/4) in *Il22*^{hCD4} mice, isolated microcolonies of *C.r* were attached to luminal surfaces of IECs; in contrast, gKO mice showed uniform spread of *C.r* over the epithelial surface (**Figures 3B-3C**), indicating that following early *C.r* colonization, IL-22 produced by ILC3s acted to limit *C.r* growth at the luminal surface. As infection progressed, there was uniform distribution of *C.r* on the epithelium in control mice (d9), with extension focally into luminal openings of the crypts, but no penetration deeper into the crypts (**Figure 3B**). In marked contrast, *C.r* invaded deep into colonic crypts in gKO mice by d9, coinciding with influx of CD4 T cells into the LP (**Figure 1**). Accordingly, the number of *C.r* cells attached to IECs was >10-fold higher compared to controls (**Figure 3C**) indicating that in global absence of IL-22, there was loss of protection of crypts against *C.r* invasion. Consistent with these findings, the bacterial burden in livers of infected *Il22*^{EIIa} gKO mice was increased compared to controls (**Figure S3C**). Thus, IL-22 is required to control the progressive spread of *C.r* from small microcolonies attached to surface IECs to the depths of crypts and into the periphery.

To define the contributions of IL-22^{+} ILCs and T cells to restraint of the spread of *C.r*, parallel studies were performed in *Il22*$^{\text{Plzf}}$ and *Il22*$^{\Delta\text{Tcell}}$ cKO mice. Similar to gKO mice and consistent with our bioluminescent studies, infected *Il22*$^{\text{Plzf}}$ cKO mice had enhanced *C.r* colonization of surface IECs with ~10-fold higher *C.r* burden compared to controls on d4 of infection (**Figures 2E, 2F, 4A** and **4B**). However, our tissue staining and bioluminescent studies showed no significant differences in distribution and *C.r* load on d9 of infection, consistent with a dominant influence of IL-22^{+} CD4 T cells by this stage of infection (**Figures 1, 2E, 2F, 4A** and **4B**). This correlated with significant *C.r* burden in the liver of *C.r*-GFP-infected *Il22*^{Plzf} cKO mice compared to controls on d6 but not on d9 post-infection (**Figure S3D**). Importantly, and in contrast to *Il22*$^{\text{EIIa}}$ gKO mice, there was no significant extension of *C.r* into the crypts of infected *Il22*$^{\text{Plzf}}$ cKO mice either in mice that died or in the fraction of mice that survived the innate phase infectious "crisis" (**Figure 4A**). Moreover, histopathologic exam of *Il22*$^{\text{Plzf}}$ cKO mice that survived did not show significant differences from controls in colitis scores at the peak of infection (**Figures S2E** and **S3B**). These data reinforced the importance of innate cell-derived IL-22 in restraining bacterial proliferation and spread across the superficial epithelium, but suggested ILC3-derived IL-22 might be inadequate for protection of the crypts.

The discrepancy in crypt invasion by *C.r* between *Il22*$^{\text{EIIa}}$ gKO and *Il22*$^{\text{Plzf}}$ cKO mice suggested that T cell-derived IL-22 might be required for crypt protection. This proved to be the case. While there was no significant difference in *C.r* load in control and *Il22*$^{\Delta\text{Tcell}}$ mice early due to an intact ILC response (**Figure 2H**), at later time points, which correlated with influx of T cells in the LP, *C.r* cells extended into the colonic crypts (d9; **Figure 4C**), spreading to the bases of crypts by days 12-14 of infection (**Figure 4C**, right panels)—

similar to our findings in gKO mice (**Figure 3B**). In accord with extension of *C.r* into crypts and whole-body imaging data (**Figures 2G-2H**), flow cytometric quantitation of *C.r* attachment to IECs was ~100-fold higher in *Il22*$^{\Delta Tcell}$ cKO mice compared to controls (**Figure 4D**), corresponding with more severe histopathologic findings prior to death (**Figure 2B**), including increased hyperplasia, GC loss, and crypt cell injury in the middle and distal colon compared to controls (**Figures S4A-S4B**). This paralleled significant *C.r* burden in the liver and spleens of infected *Il22*$^{\Delta T\ cell}$ cKO mice compared to controls (**Figure S4C**).

The lack of crypt protection in *Il22*$^{\Delta Tcell}$ cKO mice could not be attributed to altered production of protective antibodies against *C.r*, which are required for complete clearance of infection (Bry and Brenner, 2004; Maaser et al., 2004; Simmons et al., 2003), as infected mice with normal B cell numbers but deficiency of both Ig class-switching and secreted IgM (*Aicda*$^{-/-}$.*μs*$^{-/-}$) showed protection of crypts comparable to controls (**Figure 4E**). Moreover, total and anti-*C.r* specific fecal IgG was elevated in *Il22*$^{\Delta Tcell}$ cKO mice, perhaps reflecting increased bacterial load (**Figure S4D**). Loss of crypt protection was also not due to deficiency of non-IL-22 producing effector CD4 T cells in *Il22*$^{\Delta Tcell}$ cKO mice, as the number and effector phenotype of LP T cells did not differ from controls (**Figure 4F**). Collectively, these data establish that while ILC3s were sufficient to restrain *C.r* colonization early, they were unable to protect the crypts; only IL-22^{+} T cells could protect colonic crypts from *C.r* invasion, consistent with previous findings that crypts are not protected in *C.r*-infected Rag1$^{-/-}$ (Bergstrom et al., 2015; Chan et al., 2013) (**Figure S4E**). Thus, IL-22^{+} innate and adaptive immune cells have distinct, specialized roles in the clearance of attaching/effacing enteric pathogens.

IL-22–producing innate and adaptive immune cells target different IEC subsets

Because our findings implied a different capacity of IL-22^{+} ILC3s and CD4 T cells to activate a protective response in colonic crypts, we reasoned this might reflect differential IL-22 signaling into IEC subsets. Although STAT3 signaling is crucial for the protective effects of IL-22 on IECs (Pickert et al., 2009; Sovran et al., 2015; Wittkopf et al., 2015), details on which subsets of IECs are activated by IL-22 and from what cellular source are unclear. We therefore surveyed the colonic mucosa of *Il22*^{hCD4} WT and *Il22*^{EIIa} gKO mice for STAT3 activation by immunostaining for pTyr705-STAT3 at steady state and during infection. In naïve control mice, pSTAT3 was undetectable in either colonic IECs or LP cells (**Figures 5A** and **5C**); i.e., no baseline activation of STAT3 was evident. During the innate phase of *C.r* infection (d4), low-intermediate intensity pSTAT3 activation (pSTAT3^{dim}) was detected in the nuclei of surface (s)IECs (i.e., IECs facing the lumen or lining the mouth of crypts) and in LP immune cells of control mice (**Figures 5A-5B**, see insets). Global deficiency of IL-22 eliminated detectable pSTAT3 in IECs, which was preserved in LP cells, indicating IL-22 is non-redundant in its activation of IECs during the innate phase of *C.r* infection, whereas other STAT3-activating cytokines signal into LP cells.

In contrast to sIECs, most IECs lining the crypts showed no or minimal pSTAT3 during the innate phase of infection (d4). This changed dramatically with the influx of IL-22^{+} CD4 T cells (d8) (**Figures 5A-5B**). While there was no significant difference in the number of pSTAT3^{+} sIECs, the average intensity of staining increased ~3-fold, reflecting higher amplitude pSTAT3 signaling (pSTAT3^{bright}). Notably, IECs now became pSTAT3-bright at all levels of the crypts, with comparable frequencies and staining intensities to those of

sIECs. Strikingly, STAT3 activation was ablated in all IECs in *Il22*^{EIIa} gKO mice compared to controls, indicating that IL-22 is also indispensable for STAT3 activation of crypt cells during *C.r* infection. Also, as noted above, no discernable decrement in the frequency or intensity of pSTAT3 staining was evident in LP immune cells consequent to loss of IL-22 during the adaptive phase of infection. Thus, whereas IL-22 is indispensable for activation of IECs, other STAT3-activating cytokines (e.g., IL-6, IL-23) act on immune cells in the involved mucosa.

To extend these findings, we examined IL-22–dependent activation of STAT3 in IECs contingent on the source of IL-22, whether from ILC3s or T cells. During early stages of infection when ILC3-derived IL-22 was dominant in limiting *C.r* colonization of the luminal surface, STAT3 activation was diminished in sIECs of infected *Il22*^{Plzf} cKO mice compared to controls (**Figures 5C-5D**, see insets). During late phase of infection when T cell-derived IL-22 was required for crypt protection, both the frequency and intensity of pSTAT3 positivity was markedly reduced in crypt (c)IECs of infected *Il22*$^{\Delta Tcell}$ cKO mice compared to controls (**Figures 5E-5F**, see insets). Deficiency in T cell-derived IL-22 also ablated STAT3 activation in sIECs, indicating that late in infection all IECs were dependent on T cell-derived IL-22 for STAT3 activation and thus protective responses, irrespective of the continued production of IL-22 by non-T cells.

Together with our previous findings, these data establish that ILC-derived IL-22 is the principal cytokine driving STAT3 activation in sIECs necessary for restraint of *C.r* colonization and host survival during the early course of infection, but its effectiveness is limited to superficial IECs. As infection progresses, T cell-derived IL-22 is indispensable for driving STAT3 activation that underpins resistance of cIECs to *C.r* invasion and for

sustaining and amplifying STAT3 activation of sIECs. Thus, the non-redundant function of IL-22 in host protection against attaching/effacing bacteria reflects the unique ability of this cytokine to activate STAT3 in IECs, and CD4 T cells are indispensable for protection of both the colonic crypts and surface barrier as *C.r* infection progresses.

T cell-derived IL-22 promotes a shift in IEC functional programming to protect intestinal crypts

All IEC subsets arise from intestinal stem cells (ISCs) sequestered from the lumen—and potential pathogens—in the base of intestinal crypts (Barker et al., 2007; Chang and Leblond, 1971; Flier and Clevers, 2009; Hua et al., 2012). The differentiation and specialization of IECs occur as progeny of ISCs divide and transit along the crypt-surface axis, giving rise to absorptive enterocytes (ECs), the major surface IEC, and secretory IECs, including goblet cells (GC), tuft cells, enteroendocrine cells (EECs), and, in the colon, deep secretory cells (DSCs, or Paneth-like cells), which appear to share ISC-supportive functions similar to Paneth cells in the small intestine (Rothenberg et al., 2012; Sasaki et al., 2016). Because we identified a unique role for IL-22^{+} T cells in activating STAT3 in crypt IECs—including those residing in the IEC "incubator" at the base of crypts—during *C.r* infection, we sought to understand how T cell-derived IL-22 might reprogram developing IECs to protect the crypts.

Genes differentially expressed (DEGs) contingent on T cell-derived IL-22 were identified by RNA-seq analysis of three subsets of IECs sorted from mid-distal colons of naïve (d0) and d9 *C.r*-infected control (*Il22*^{hCD4}; Cntrl) and T cell cKO (*Il22*$^{\Delta Tcell}$) mice. Subsets were defined by differential cell size/complexity and expression of EpCAM1 and CEACAM1: Small crypt (SC) cells (EpCAM1^{+}CEACAM1^{lo} FSC^{lo}SSC^{lo}); large crypt (LC) cells (EpCAM1^{+}CEACAM1^{int}FSC^{hi}SSC^{int}); and superficial, or surface, cells (Srf)

(EpCAM1^{+}CEACAM1^{hi}FSC^{hi}SSC^{hi}) (**Figures 6A-6D**); which correlated with lower crypt cells, upper crypt cells, and surface cells, respectively, based on correlative gene expression from RNA-seq and laser capture microdissection (LCM)/RT-PCR analyses (**Figures S5A-S5D).** At the peak of *C.r* infection (d9), 739 DEGs were identified in colonic IECs from control versus *Il22*$^{\Delta Tcell}$ cKO mice (**Figures 6D-6F** and **S5E-S5G**).

Transcripts of genes involved in host defense were up-regulated by T cell-derived IL-22, whether predominantly in surface (s)IECs (e.g., *Sting1*), crypt (c)IECs (e.g., *Lcn2*, *Lbp*, *Muc1*) or all IEC subsets (e.g., *S100a8*, *Lrg1*, *Tac1*) (**Figures 6D, 6E** and **S5E-S5G**). The striking induction in cIECs of transcripts that encode lipocalin 2, a principal sequestrator of iron-binding siderophores expressed by pathogenic *E. coli* and *C.r* (Berger et al., 2006; Goetz et al., 2002), and S100a8, a component of the metal-chelator calprotectin (Brandtzaeg et al., 1995; Clohessy and Golden, 1995), is consistent with an important role of these antimicrobial peptides (AMPs) in defense of the colonic crypts. Moreover, IL-22^{+} T cells up-regulated several phospholipase A2 (PLA2) genes encoding phospholipid-hydrolyzing enzymes that have bactericidal activity and contribute to IL-22/STAT3-dependent host defenses (Harwig et al., 1995; Okita et al., 2016; Wittkopf et al., 2015; Yamamoto et al., 2015) (**Figures 6D, S5E-S5G**, **7B**, **7C** and **S6**) and transcripts for the Reg family AMPs, Reg3β and Reg3γ—implicated as important IL-22-dependent AMPs in *C.r* infection (Zheng et al., 2008) (**Figures 6D** and **S5E-S5G**). Up-regulation in cIECs of transcripts encoding the LPS-binding protein (*Lbp*), a key factor in enhanced recognition of Gram-negative bacterial cell wall components by TLR2 and TLR4 (Medzhitov et al., 1997; Poltorak et al., 1998; Pugin et al., 1993; Schletter et al., 1995), suggests potentiation

of recognition of this pathogen-associated molecular pattern (PAMP) by cIECs may contribute to crypt defense in *C.r* infection.

T cell-derived IL-22 also amplified neutrophil-attractant chemokines and shifted mucin production and modification by IECs that contribute to host defense during *C.r* infection (Aujla et al., 2008; Bergstrom et al., 2008; Hopkins et al., 2019; Liang et al., 2010; Lindén et al., 2008) (**Figures 6D, 6E** and **S5E-S5G**). Transcripts for *Cxcl1*, *Cxcl2* and *Cxcl5*, which are recognized by neutrophils via CXCR2, were induced in both sIECs and cIECs, suggesting a central role for IL-22 signaling into IECs to regulate recruitment of neutrophils in the infected crypts, where they contribute to clearance of *C.r* (Kamada et al., 2015). Previous studies have identified an IL-22–induced shift in mucin production and its altered mucin fucosylation by IECs (Pham et al., 2014; Sugimoto et al., 2008; Turner et al., 2013), which we found was dependent on IL-22$^+$ T cells. Thus, in addition to amplifying antimicrobial recognition and AMPs, T cell-derived IL-22 may also coordinate neutrophil recruitment to infected IECs and the colonic lumen, direct a shift in mucin production from Muc2 to Muc1 (**Figures 6D, 6E**, **S5E-S5G** and **S4F**), and alter mucin fucosylation, which may deprive *C.r* of an important energy source (Pham et al., 2014).

Genes repressed by T cell-derived IL-22 were a major component of the DEG profile (**Figures 6D-6H** and **S5E-S5G**). Notable from a combined gene set, network and pathway analysis (GNPA) were genes induced by TNFα and IFNγ (**Figures 7A, 7B** and **S6**). This included genes of the antigen processing and presentation (APP) pathway, particularly MHC class I and II genes, and the central transactivator of APP, *Ciita* (Martin et al., 1997; Steimle et al., 1993). Proinflammatory genes were also repressed (**Figures 6D-6H, 7A-7B**, **S5E-S5G** and **S6A-S6B**), including IFNγ-dependent chemokines *Cxcl9* and *Cxcl10*, which

recruit immune cells in type I responses, including Th1 cells. (Loetscher et al., 1996; Luster and Ravetch, 1987). Because IFNγ is required for GC loss and IEC proliferation during *C.r* infection (Chan et al., 2013), heightened IFNγ responses due to IL-22 deficiency may have contributed to enhanced GC hypoplasia and IEC damage, as well as increased crypt hyperplasia observed in *Il22*$^{\Delta Tcell}$ cKO mice (**Figures S4A-S4B**). IL-22 is required to initiate DNA damage response (DDR) induced by ionizing radiation (Gronke et al., 2019); however, during *C.r* infection we found enhanced apoptosis and DDR in IECs from *Il22*$^{\Delta Tcell}$ cKO mice (**Figures S6D-S6E**) perhaps reflective of elevated TNF and IFNγ responses. Moreover, DEGs repressed by IL-22 were characteristic of absorptive enterocytes (ECs; e.g., *Ces2c*, *Cyp3a13*, *Ubd*, *Ugdh*, *Noct*) (**Figures 6D**, **7B-7C**, **S5E-S5G** and **S6**), as reflected in the enhanced EC signature by GNPA analysis (**Figures 7B, 7C** and **S6**). Strikingly, many genes characteristic of mature ECs were enriched in Srf IECs from infected *Il22*$^{\Delta Tcell}$ cKO mice compared to controls, suggesting T cell-derived IL-22 acts to repress maturation of ECs driven by IFNγ-driven hyperproliferation during infection, perhaps as a measure to deprive *C.r* of its cellular host for attachment and colonization. This was contrasted by enhancement of EEC gene signature in Srf IECs (e.g., *Tac1*, *Adgrl1*, *Celf3*, *Myt1*, *Sct*) (**Figures 6D, 7B- 7C, S5E-S5G** and **S6**), implicating a regulatory role for T cell-derived IL-22 in programming EEC differentiation and/or function to alter local hormones. Collectively, these findings indicate, in addition to shifting the type of mucus produced by IECs and enhancing expression of a select set of AMPs and chemokines, IL-22 signaling provided by T cells plays an important role in modulating development of IECs that may restrain *C.r* invasion of the crypts—whether by promoting STAT3 activation to induce gene expression or repress aspects of IFN and TNF signaling.

Discussion

In this study we define a non-redundant role for IL-22$^+$ T cells in antibacterial defense of colonic crypts. Our findings address a central, unresolved issue regarding the coordination of innate and adaptive immunity and specialization of ILCs and CD4 T cells. Since the discovery of ILC subsets and appreciation of their functional parallels with T-cell subsets (Bando and Colonna, 2016; Huntington et al., 2016; Song et al., 2015; Spits et al., 2013), it has been unclear what functions are unique to each immune cell population. Here we find that, despite their critical role in restraining bacterial colonization over the early course of enteropathogenic bacterial infection, ILC3s—and other IL-22-producing innate immune cells—induce weak STAT3 signaling that is limited to surface IECs. In contrast, T cells are uniquely charged with delivery of IL-22 to crypt and surface IECs as infection progresses, inducing robust, sustained STAT3 signaling in both IEC populations that is required to amplify programs essential for host defense against bacterial invasion.

Although the mechanisms by which IL-22–producing T cells achieve heightened activation of IECs are not yet fully defined, a major, if not sole, contributor would appear to be the geography of immune-cell positioning relative to the intestinal epithelium. Whereas most ILC3s are sequestered in lymphoid tissues and fail to increase their local numbers throughout infection (Ahlfors et al., 2014; Gasteiger et al., 2015), effector CD4 T cells generated in response to infection become the major population of IL-22$^+$ cells in the inflamed mucosa and are positioned subadjacent to IECs they are charged with protecting, most notably in the crypts. Here they uniquely activate IL-22/STAT3 signaling into cIECs and become the sole source for sustained activation of sIECs as the quality of these cells is altered by a shift in IEC maturation during infection. It will be important to determine

whether this is due to increased local concentrations of IL-22, directed delivery of IL-22 to IECs in the context of MHCII-mediated non-classical antigen presentation, delivery of co-signals that amplify IL-22-mediated STAT3 activation, or a combination of these. Irrespective of mechanism, T cells would appear to deliver IL-22 to IECs on-site, whereas ILCs must deliver IL-22 long-range.

The host-protective effects of T cell-derived IL-22 on IECs are diverse and non-redundant. Consistent with a previous study showing IL-22 and not IL-6 activates IECs (Pickert et al., 2009), we found IL-22 induced STAT3 activation during each phase of *C.r* infection, reflective of IL-22's critical role in antibacterial host defense (Basu et al., 2012; Sonnenberg et al., 2011a; Zheng et al., 2008). RNA-seq analyses revealed that T cell-derived IL-22 augments antimicrobial peptides (AMPs) and neutrophil-recruiting chemokines (Aujla et al., 2008; Boniface et al., 2005; Liang et al., 2010; Okita et al., 2016; Wittkopf et al., 2015; Wolk et al., 2006; Yamamoto et al., 2015; Zheng et al., 2008), alters mucin production and fucosylation (Pham et al., 2014; Sugimoto et al., 2008), and enhances expression of genes that restrain bacterial growth (e.g., *Sting1*, *Lbp*) (Aden et al., 2018; Wolk et al., 2006, 2007). Based on whole colon analyses from global IL-22–deficient mice, it has been proposed that IL-22–mediated host protection is due to upregulation of the Reg3 family of AMPs (Zheng et al., 2008) particularly Reg3β(Waldschmitt et al., 2019), which, unlike Reg3γ (Cash et al., 2006; Pham et al., 2014), has anti-microbial actions against Gram-negative bacteria (Miki et al., 2012; Stelter et al., 2011). Although we found that *Reg3b* and *Reg3g* transcripts were up-regulated in areas of *C.r* colonization—mid-distal colon—their expression was far greater in the proximal colon, which is not colonized during *C.r* infection (Basu et al., 2012; Wiles et al., 2004; data not shown). In contrast, IL-

22-induced *S100a* family of AMPs and *Lcn2* occurs in areas colonized by *C.r*. It is unclear if this reflects a particularly potent effect of IL-22–induced Reg3□ in colonization resistance or rather a limited role for this AMP in protection against *C.r*, as has been shown for Reg3b (Pham et al., 2014). In this regard, we found that neither *S100a9* nor IEC-derived *Sting1* was required for crypt protection, leaving open the question of which factor, or combination of factors, induced by T cell-derived IL-22 support this critical function.

Invasion of colonic crypts by *C.r* has been observed in *Cxcr2*$^{-/-}$ mice, which have impaired neutrophil recruitment to the infected colon (Spehlmann et al., 2009). Our finding that T cell-derived IL-22 upregulated several CXCL chemokines that are ligands of CXCR2 (e.g., *Cxcl1*, *Cxcl2*, *Cxcl5*) provides a mechanism by which neutrophil recruitment during *C.r* infection may be orchestrated, and, in view of the important role for neutrophils in eradicating luminal bacteria (Kamada et al., 2015) suggests that this pathway may participate in antibacterial defense of crypts. Because neutrophils are themselves an important source of CXCL2 (Li et al., 2016), these findings implicate a possible feed-forward mechanism whereby recruitment of neutrophils to the infected mucosa is initiated by T cell-derived IL-22 activation of IECs and then amplified by incoming neutrophils. In preliminary studies, we have found *Cxcl5* expression was limited to IECs (Cai et al., unpublished observation), suggesting that *Cxcl5* may be important in directing neutrophils to sites of *C.r*-infected IECs. This will require further study. In any case, our findings identify a potential link between T cell-derived IL-22 and neutrophil recruitment that may aid in limiting *C.r* invasion of crypts. Interestingly, however, despite the important role for *C.r*-specific IgG responses in the ultimate clearance of infection (Bry and Brenner, 2004; Maaser et al., 2004)—thought to be due in part to antibody-dependent opsonization of the

bacterium to enhance neutrophil-mediated phagocytosis(Kamada et al., 2015)—we found no requirement for antibody-dependent protection of the crypts. Thus, any actions of neutrophils in defense of colonic crypts may be adequate without requirement for IgG-mediated bacterial opsonization, although this, too, will require further study.

Notably, T cell-derived IL-22 tempered pro-inflammatory and developmental programming effects on IECs exerted by TNF and IFN signaling. The actions of IFNγ on IECs have been shown to result in acceleration of IEC proliferation (hyperplasia) and goblet cell loss thought to protect the crypts from bacterial incursion (Chan et al., 2013) and further distance ISCs in the crypt bases from invading pathogens and their products (Kaiko et al., 2016; Liang et al., 2017; Matsuki et al., 2013; Okada et al., 2013). However, we find that, in the absence of T-cell production of IL-22, the crypts are not protected despite unopposed actions of IFN signaling that result in increased goblet cell loss and crypt hyperplasia. Accordingly, the alterations in IEC developmental programming induced by IFN signaling are inadequate without coordinate actions of IL-22 delivered by T cells. Thus, IFN and IL-22 must cooperate in defense of the crypts as deficiency of either leads to bacterial invasion.

Deficiency of IL-22 resulted in enhanced IFNγ-dependent expression of *Ciita* and thus major components of the antigen processing and presentation pathway by IECs, raising the intriguing possibility that, in addition to its other actions, IFNγ acts to promote the function of IECs as non-classical APCs in order to recruit more potent, protective IL-22 signaling from Th17 and Th22 cells. Furthermore, IL-22 deficiency resulted in enhanced expression of IFNγ-induced IEC-derived chemokines (i.e. *Cxcl9, Cxcl10*) and enhanced recruitment of T cells to IECs. Together, these data suggest IFNγ–induced T cell recruitment and

activation may potentiate protective IL-22 signals to crypt IECs resulting in a feedback loop in which IL-22 then controls IFN-γ signaling in IECs to limit damage caused by chronic stimulation. It was recently reported that antigen presentation by $Lgr5^{+}$ ISCs in the small intestine elicits IL-10 from $Foxp3^{+}$ Tregs that sustains homeostatic ISC self-renewal and during intestinal infections may recruit effector T cell cytokines that shift ISC programming to host-defensive IEC differentiation (Biton et al., 2018). Consistent with this—and extending it—we find that T cell-derived IL-22, also a member of the IL-10 cytokine family, drives strong STAT3 activation in *all* IECs, not just ISCs, thereby restraining IFN□-induced IEC differentiation while promoting antimicrobial defense. Notably, we detect no STAT3 activation in colonic IECs at steady state, including ISCs, suggesting that, in contrast to the small intestine, neither IL-10 nor IL-22 has direct homeostatic actions on colonic IECs. In any case, in its non-redundant role to defend colonic crypts from bacterial invasion, T cell-derived IL-22, like IL-10, would appear to play an essential role in STAT3-dependent maintenance of ISCs to insure restitution of the epithelial barrier and preservation of mucosal integrity. Going forward, it will be important to determine whether recognition of antigen presented on IECs underlies the basis for the unique ability of IL-22-producing T cells, but not innate cells, to activate crypt IECs for antimicrobial defense.

(Format and content adapted for thesis, for more information about this study, please find the full text at: *Immunity,* Volume 55, Issue 3, 8 March 2022, Pages 494-511.e11)

Figures

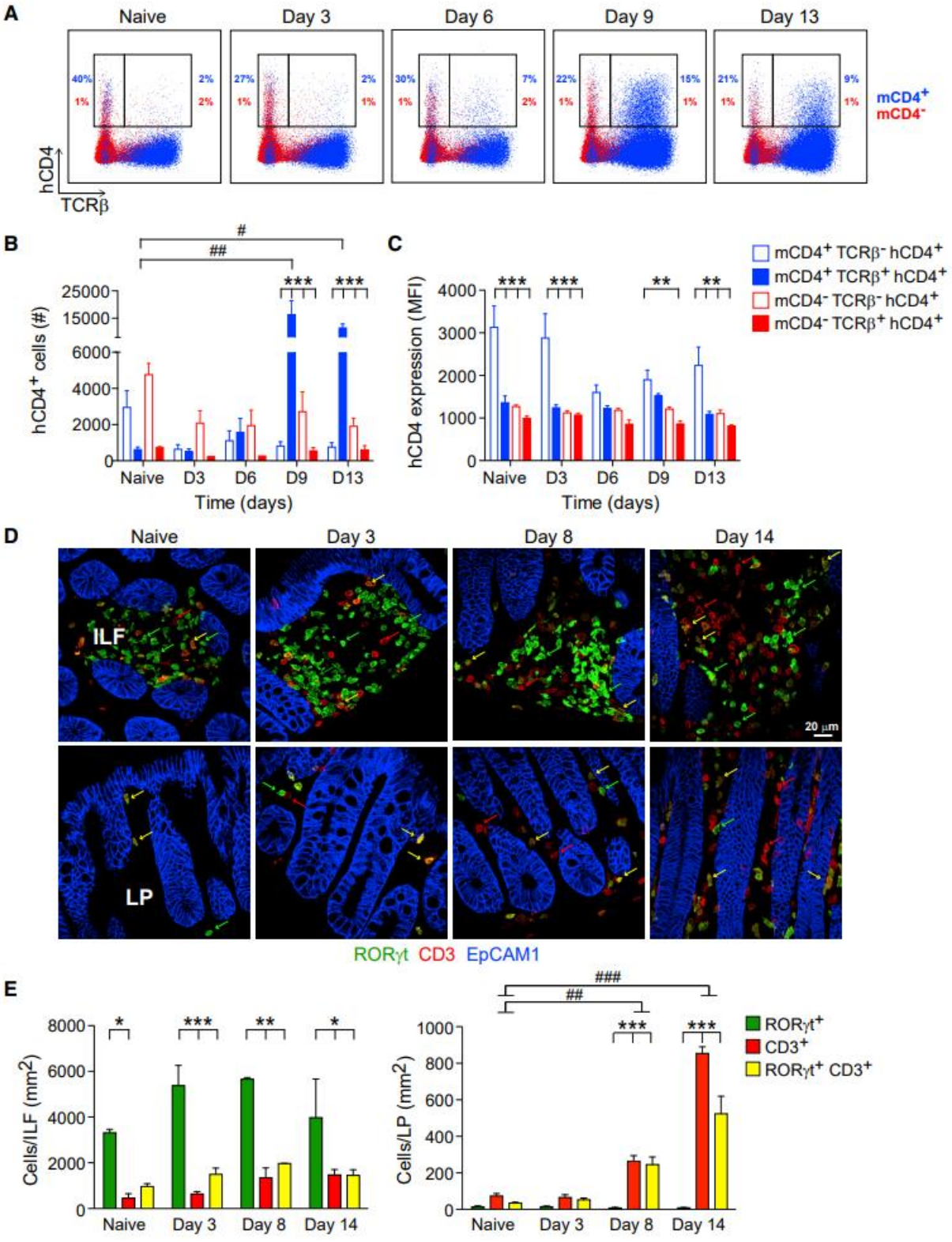
A
Naive
Day 3
Day 6
Day 9
Day 13
40%
1%
2%
2%
27%
1%
2%
1%
30%
1%
7%
2%
22%
1%
15%
1%
21%
1%
9%
1%
mCD4+
mCD4-
hCD4
TCRβ
B
hCD4+ cells (#)
25000
15000
6000
4000
2000
0
#
##
***
***
Naive
D3
D6
D9
D13
Time (days)
C
hCD4 expression (MFI)
4000
3000
2000
1000
0
***
***
**
**
mCD4+ TCRβ- hCD4+
mCD4+ TCRβ+ hCD4+
mCD4- TCRβ- hCD4+
mCD4- TCRβ+ hCD4+
D
Naive
Day 3
Day 8
Day 14
ILF
LP
20 μm
RORγt CD3 EpCAM1
E
Cells/ILF (mm2)
8000
6000
4000
2000
0
*
***
**
*
Naive
Day 3
Day 8
Day 14
Cells/LP (mm2)
1000
800
600
400
200
0
###
##
***
***
RORγt+
CD3+
RORγt+ CD3+

Figure 1. Dynamics of IL-22 expression and cellular localization during *C.r* infection
(A) Colon LP cells from naïve and *C.r*-infected *Il22*^{hCD4} mice stimulated with P/I+IL-23 for 4h, stained for TCRβ**,** hCD4, mCD4, and L/D dye and analyzed by flow cytometry. Numbers represent percentages of hCD4 (IL-22^{+}) innate cells (TCRβ^{-}) or T cells (TCRβ^{+}) and are split into CD4^{+} (blue) and CD4^{-} (red).
(B) Cell numbers and (C) IL-22/hCD4 expression based on MFI. Cells were split into mCD4^{+} (open; blue) and mCD4^{-} (open; red) innate cells, and mCD4^{+} (solid; blue) and mCD4^{-} (solid; red) T cells. Error bars represent mean ± SEM.
(D) Colons from naïve and *C.r*-infected *Rorc*^{EGFP} mice stained for GFP (green)**,** CD3 (red), and EpCAM1 (blue). Arrows depict RORC/GFP^{+} cells (green), CD3^{+} cells (red), and GFP^{+} CD3^{+} cells (yellow). Scale bar, 20 μm.
(E) Quantitation of cells in colonic ILFs and LP. Error bars represent mean ± SEM.
One-way ANOVA, naïve vs infected; $^{\#}p<0.05$, $^{\#\#}p<0.01$ and $^{\#\#\#}p<0.001$. Two-way ANOVA, comparing different cell populations; $*p<0.05$, $**p<0.01$ and $***p<0.001$. 3-4 mice per time point, 3 independent experiments.

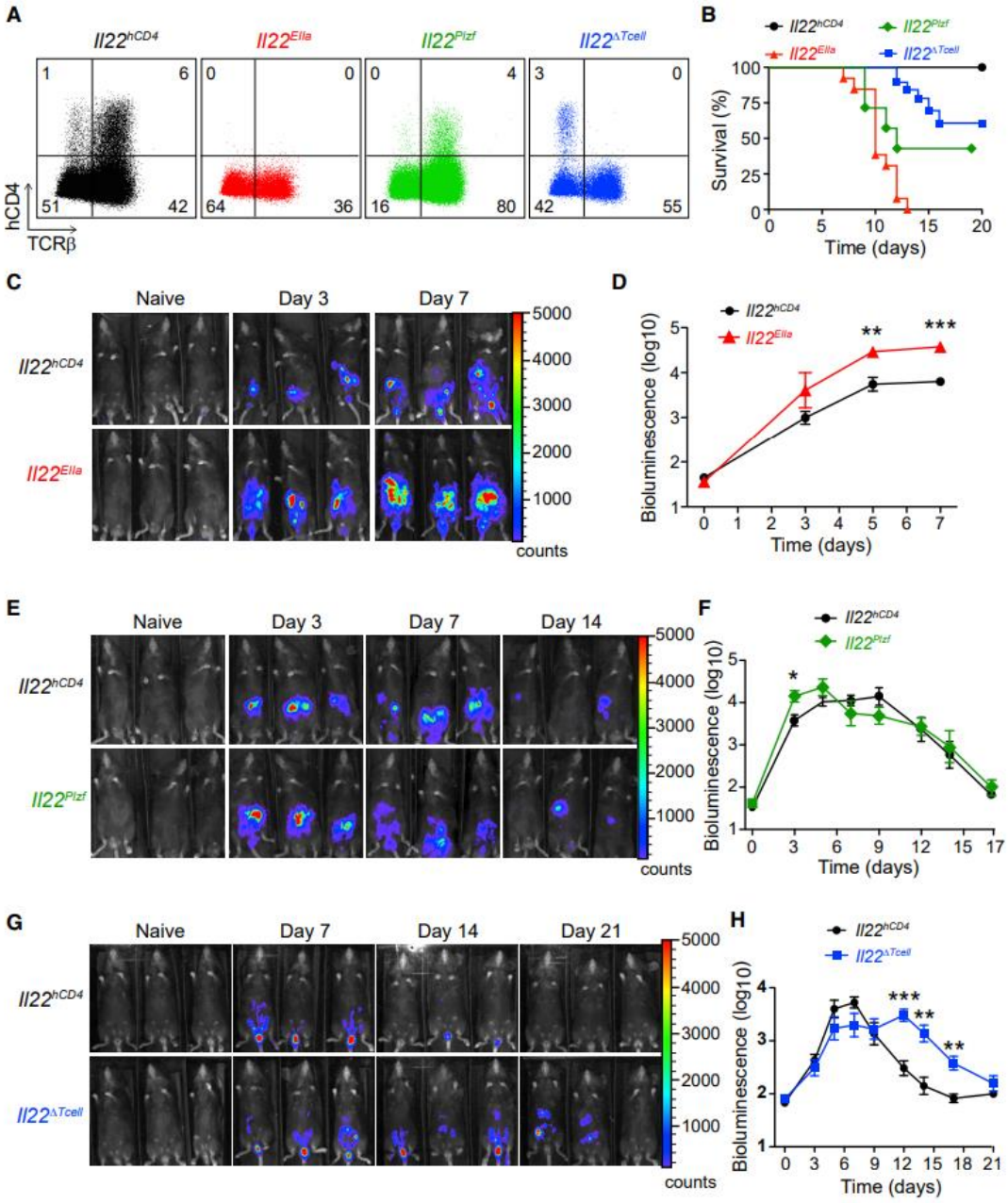

Figure 2. Temporal bacterial burden and fatality in *C.r*-infected *Il22* cKO mice
(A) Colon LP cells from d7 *C.r Il22*^{hCD4} (Cntrl; black), *Il22*^{EIIa} (gKO; red), *Il22*^{Plzf} (Innate cell cKO; green), and *Il22*$^{\Delta Tcell}$ (T cell cKO; blue) mice stained for mCD4, hCD4 (IL-22), L/D dye and TCRβ after P/I+IL-23 stimulation.
(B) Survival kinetics of *C.r*-infected Cntrl, gKO, and cKO mice.
(C, E, G) Serial whole-body imaging and (D, F, H) Colonization kinetics of *C.r*-infected Cntrl, gKO, and cKO mice. Error bars represent mean ± SEM.

Mann Whitney; *p<0.05, **p<0.01, ***p<0.001. 4-5 mice per time point, 2 independent experiments.

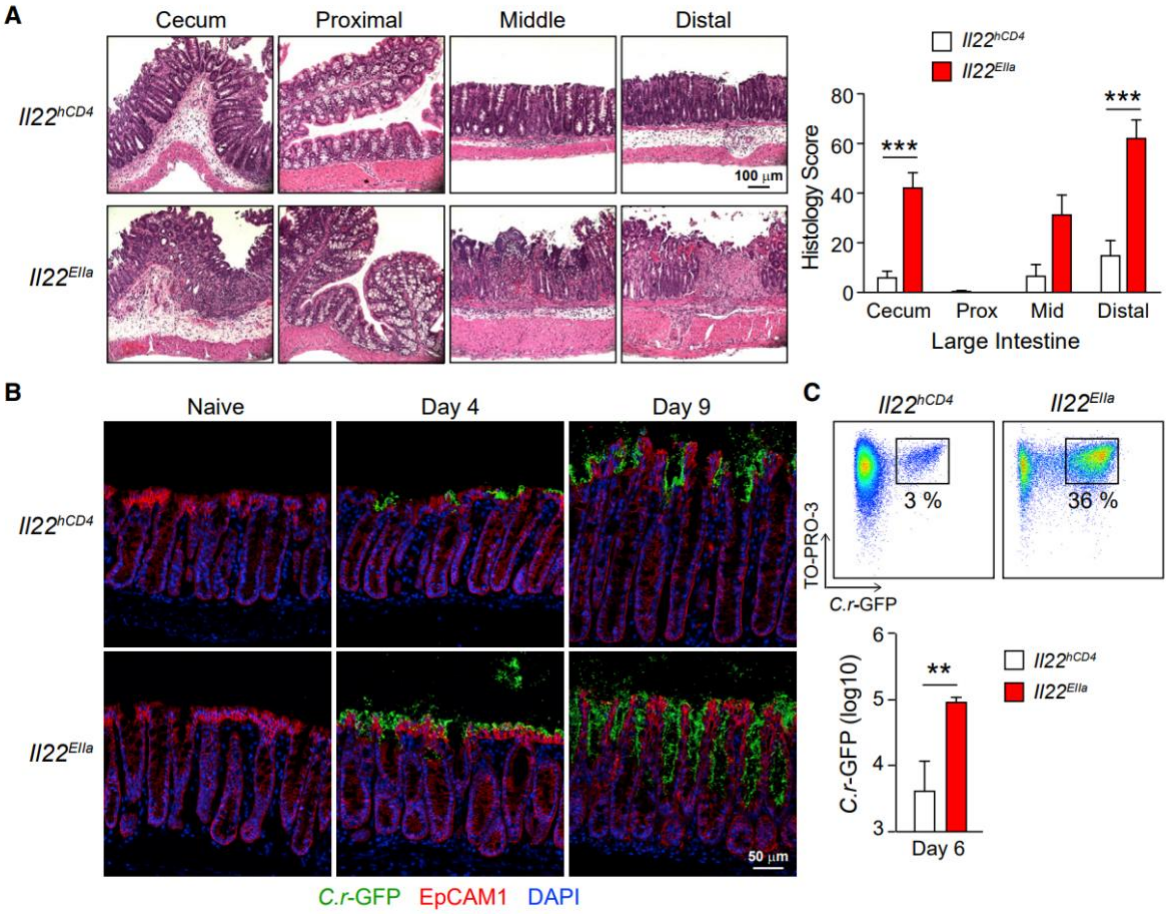

Figure 3. IL-22 protects the colonic crypts from deep bacterial invasion
(A) LI from d8 *C.r Il22*^{hCD4} (Cntrl; white) and *Il22*^{EIIa} (gKO; red) mice stained with H&E (Two-way ANOVA, ***p<0.001). (B) Colons from naïve and *C.r*-GFP-infected Cntrl and gKO mice stained for GFP (green), EpCAM1 (red) and DAPI (blue). Scale bar, 100 μm. (C) *C.r* from supernatants of IEC preps from d6 *C.r*-GFP Cntrl and gKO mice stained with TO-PRO-3 and analyzed by flow cytometry in log scale (Mann Whitney, **p<0.01). Error bars represent mean ± SEM. 3-5 mice per group, 2 independent experiments. Scale bar, 50 μm.

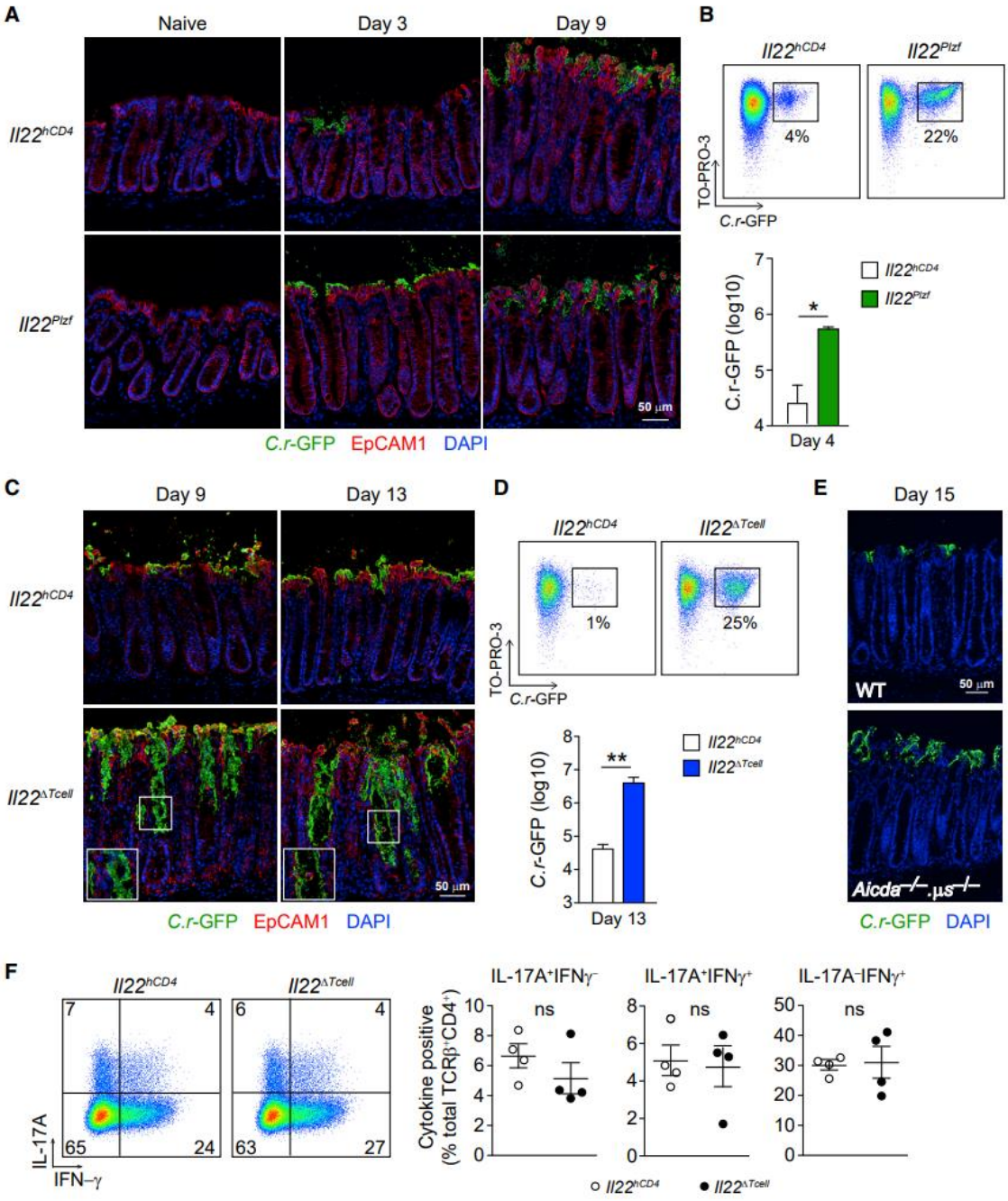

Figure 4. IL-22^{+} innate and adaptive cells protect distinct regions of the colon during *C.r* infection

(A) Colons from naïve and *C.r*-GFP-infected *Il22*^{hCD4} (Cntrl) and *Il22*^{Plzf} (Innate cell cKO) mice stained for GFP (green), EpCAM1 (red) and DAPI (blue). Scale bar, 50 μm.

(B) *C.r* from supernatants of IEC preps from d4 *C.r*-GFP *Il22*^{hCD4} and *Il22*^{Plzf} (green) mice stained with TO-PRO-3 and analyzed by flow cytometry in log scale (Mann Whitney, **p*<0.05). Error bars represent mean ± SEM.
(C) Colons from d9 and d13 *C.r*-GFP *Il22*^{hCD4} and *Il22*$^{\Delta Tcell}$ (T cell cKO) mice stained for GFP (green), EpCAM1 (red) and DAPI (blue). Scale bar, 50 μm.
(D) *C.r* from supernatants of IEC preps from d13 *C.r*-GFP Cntrl and *Il22*$^{\Delta Tcell}$ (blue) mice stained with TO-PRO-3 and analyzed by flow cytometry in log scale (Mann Whitney, ***p*<0.01). Error bars represent mean ± SEM.
(E) Colons from d15 *C.r*-GFP WT and *Aicda*$^{-/-}$ *μs*$^{-/-}$ mice stained for GFP (green) and DAPI (blue). Scale bar, 50 μm.
(F) Colon LPLs from d9 *C.r* Cntrl (open) and *Il22*$^{\Delta Tcell}$ (solid) mice stimulated with P/I+GolgiPlug for 4h and stained for TCRβ**,** mCD4, and L/D dye, followed by IC staining for IL-17A and IFNγ.
ns=not significant, 3-4 mice per group, 2 independent experiments.

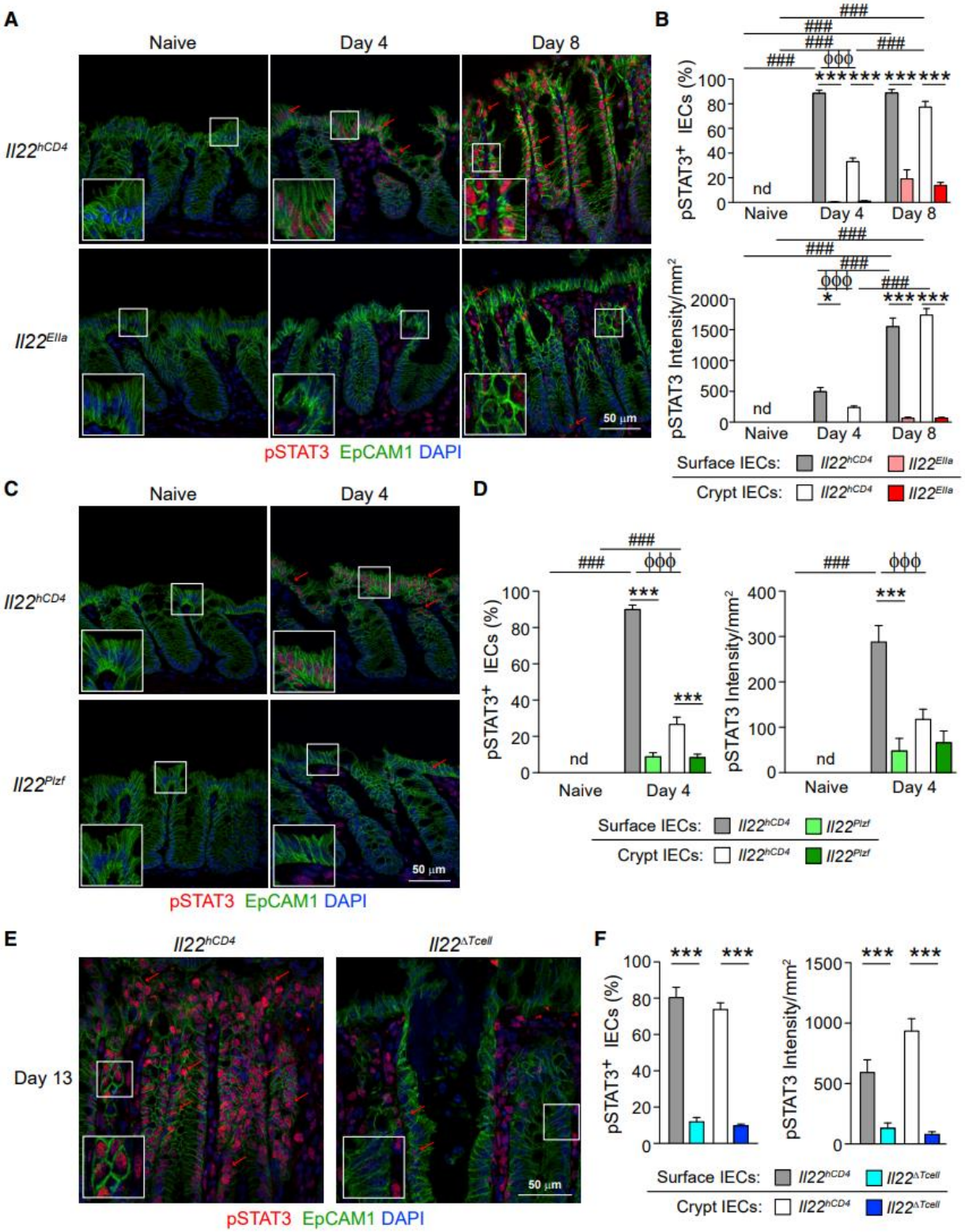
A
Naive
Day 4
Day 8
Il22hCD4
Il22Ella
50 μm
pSTAT3 EpCAM1 DAPI
B
pSTAT3+ IECs (%)
pSTAT3 Intensity/mm2
nd
Naive
Day 4
Day 8
Surface IECs: Il22hCD4 Il22Ella
Crypt IECs: Il22hCD4 Il22Ella
C
Il22Plzf
D
Surface IECs: Il22hCD4 Il22Plzf
Crypt IECs: Il22hCD4 Il22Plzf
E
Il22ΔTcell
Day 13
F
Surface IECs: Il22hCD4 Il22ΔTcell
Crypt IECs: Il22hCD4 Il22ΔTcell

Figure 5. IL-22^{+} T cells induce robust and prolonged STAT3 activation

(A, C, E) Colons from (A) naïve, d4 and d8 *C.r*-infected *Il22*^{hCD4} (Cntrl) and *Il22*^{EIIa} (gKO), and (C) naïve and d4 Cntrl and *Il22*^{Plzf} (Innate cell cKO), and (E) Cntrl and d13 *C.r Il22*$^{\Delta Tcell}$ (T cell cKO) mice stained for EpCAM1 (green), pSTAT3 (red) and DAPI (blue). Red arrows depict pSTAT3^{+} IECs. Scale bar, 50 μm.

(B, D, F) Quantitation of percent pSTAT3^{+} cells and intensity of pSTAT3 in sIECs and cIECs from (B) naïve, d4 and d8 Cntrl and gKO, and (D) naïve and d4 *C.r* Cntrl and *Il22*^{Plzf} and (F) d13 *C.r* Cntrl and *Il22*$^{\Delta Tcell}$ mice.

(B, D) Two-way ANOVA with Bonferroni posttests; $^{\#\#\#}p<0.001$, comparing different time points, $^{*}p<0.05$ and $^{***}p<0.001$, WT vs cKO and $^{\phi\phi\phi}p<0.001$, sIECs vs cIECs.

(F) One-way ANOVA with post-hoc Tukey tests; $^{**}p<0.01$ and $^{***}p<0.001$, WT vs cKO. Error bars represent mean ± SEM. nd=not detected. 4-5 mice per group, 2 independent experiments.

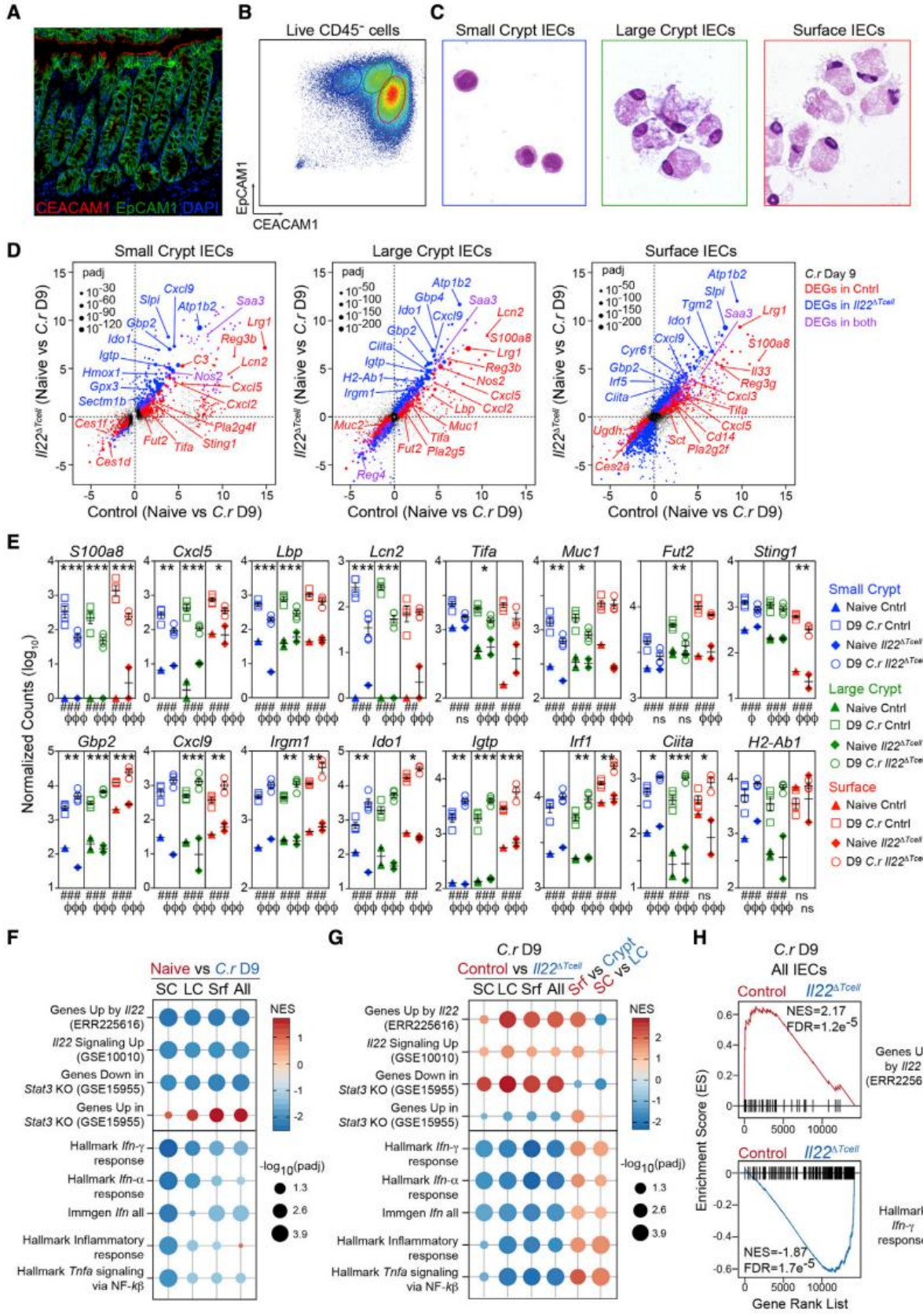
A
CEACAM1 EpCAM1 DAPI
B
Live CD45⁻ cells
EpCAM1
CEACAM1
C
Small Crypt IECs
Large Crypt IECs
Surface IECs
D
Small Crypt IECs
Large Crypt IECs
Surface IECs
padj
Il22ΔTcell (Naive vs C.r D9)
Control (Naive vs C.r D9)
C.r Day 9
DEGs in Cntrl
DEGs in Il22ΔTcell
DEGs in both
E
S100a8
Cxcl5
Lbp
Lcn2
Tifa
Muc1
Fut2
Sting1
Gbp2
Cxcl9
Irgm1
Ido1
Igtp
Irf1
Ciita
H2-Ab1
Normalized Counts (log10)
Small Crypt
Large Crypt
Surface
Naive Cntrl
D9 C.r Cntrl
Naive Il22ΔTcell
D9 C.r Il22ΔTcell
F
Naive vs C.r D9
SC LC Srf All
Genes Up by Il22 (ERR225616)
Il22 Signaling Up (GSE10010)
Genes Down in Stat3 KO (GSE15955)
Genes Up in Stat3 KO (GSE15955)
Hallmark Ifn-γ response
Hallmark Ifn-α response
Immgen Ifn all
Hallmark Inflammatory response
Hallmark Tnfa signaling via NF-kβ
NES
-log10(padj)
G
C.r D9
Control vs Il22ΔTcell
SC LC Srf All
Srf vs Crypt
SC vs LC
H
C.r D9
All IECs
Control
Il22ΔTcell
NES=2.17
FDR=1.2e-5
NES=-1.87
FDR=1.7e-5
Enrichment Score (ES)
Gene Rank List

Figure 6. IL-22^{+} T cells upregulate host defense genes and repress IFNγ–induced genes

(A) Colon stained for EpCAM1 (green), CEACAM1 (red) and DAPI (blue). Scale bar, 50 μm.

(B) IECs from naïve mice stained for EpCAM1, CEACAM1, L/D dye and CD45 and analyzed by flow cytometry or (C) EpCAM1^{+}CD45^{-}LD/dye^{-} cells sorted into small crypt (SC; CEACAM1^{lo}FSC^{lo}SSC^{lo}; blue), large crypt (LC; CEACAM1^{int}FSC^{hi}SSC^{int}; green) and surface IECs (Srf; CEACAM1^{hi}FSC^{hi}SSC^{hi}; red) and stained with H&E.

(D-H) RNA-seq of sorted SC, LC and Srf IECs from mid/distal colons of naïve and *C.r* d9 *C.r Il22*^{hCD4} (Cntrl) and *Il22*$^{\Delta Tcell}$ (T cell cKO) mice.

(D) Two-way scatter plots of DEGs in SC, LC and Srf IECs from naïve vs d9 *C.r* Cntrl (red) & naïve vs d9 *C.r Il22*$^{\Delta Tcell}$ (blue). DEGs in both (purple) (*p*adj<0.05; colored dots).

(E) Count plots of DE host defense genes in SC (blue), LC (green) and Srf (red) IECs from d9 *C.r* Cntrl (solid) and *Il22*$^{\Delta Tcell}$ (open). Normalized by library size. **p*adj<0.1, ***p*adj<0.01, ****p*adj<0.001; d9 *C.r* Cntrl vs *Il22*$^{\Delta Tcell}$. $^{\#\#}$*padj*<0.01, $^{\#\#\#}$*padj*<0.001; naïve Cntrl vs d9 *C.r* Cntrl. $^{\phi}$*p*<0.1, $^{\phi\phi\phi}$*p*<0.001; naïve *Il22*$^{\Delta Tcell}$ vs d9 *C.r Il22*$^{\Delta Tcell}$.

(F,G) GSEA dot plots of IL-22, IFN γ, IFN γ, TNF and Inflammatory pathways in SC, LC, Srf and pooled IECs (All) from (F) naïve (brick) vs *C.r* d9 Cntrl (azure) and (G) d9 *C.r* Cntrl (brick) vs *Il22*$^{\Delta Tcell}$ (azure), Srf (brick) vs pooled Crypt (azure), and SC (brick) vs LC (azure).

(H) GSEA bar code plots of IL-22 and IFN γ pathways in pooled IECs (All) from d9 *C.r Il22*$^{\Delta Tcell}$ (azure) vs Cntrl (brick).

NES, normal enrichment score; FDR, false discovery rate. 2-3 mice per sample, Independent experiments: 1-2 per naïve group and 3-4 per infected group.

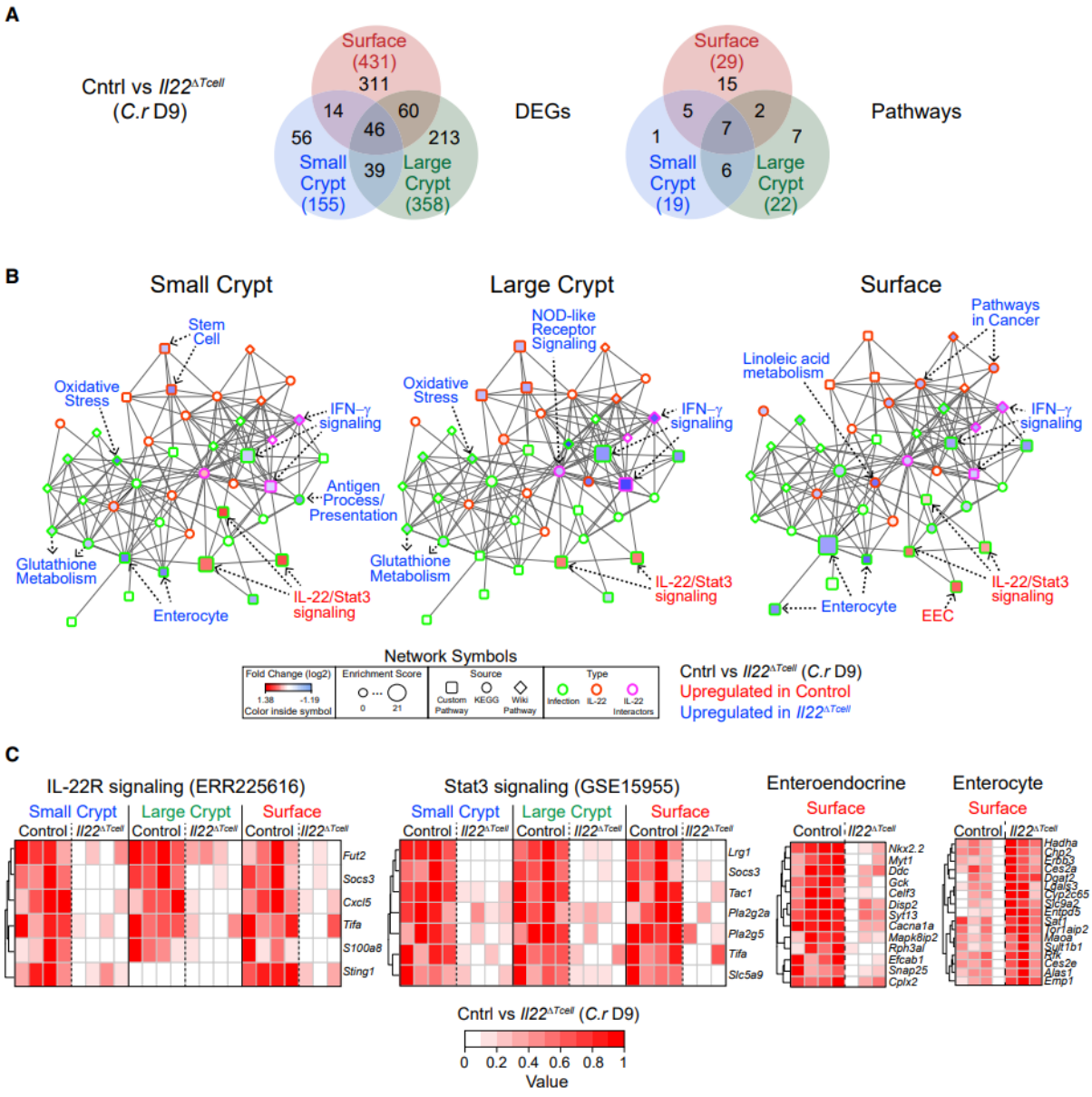

Figure 7. T cell-derived IL-22 promotes a shift in IEC functional programming to protect intestinal crypts

(A-C) RNA-seq of SC, LC and Srf IECs from mid/distal colons of d9 *C.r Il22*^{hCD4} (Cntrl) and *Il22*$^{\Delta Tcell}$ (T cell cKO) mice.

(A) Venn diagram of DEGs and pathways in SC (red), LC (green) and Srf (red) IECs from d9 *C.r* Cntrl and *Il22*$^{\Delta Tcell}$. Total DEGs or Pathways (#).

(B) GNPA of SC, LC and Srf IECs from d9 *C.r* Cntrl and *Il22*$^{\Delta Tcell}$. Log_2 fold change (symbol fill; up in Cntrl (red), down in Cntrl (blue)), Enrichment score (symbol size),

Source: Custom Pathway (square), KEGG (circle), Wiki Pathway (diamond)), and Interaction: (symbol border; Infection (green), IL-22 (orange), IL-22 interactors (pink)).
(C) Heatmaps of top DEGs in IL-22R, STAT3 and custom IEC pathways.
2-3 mice per sample and 3-4 independent experiments per group.

INNATE CELL-DERIVED INTERLEUKIN (IL)-22 PROMOTES EARLY PMN RECRUITMENT FOR ANTIBACTERIAL DEFENSE OF COLONIC SURFACE EPITHELIUM

by

BAIYI CAI, STACEY N. HARBOUR, C. GARRETT WILSON, DANIEL J. SILBERGER, MIN GAO, JEFFREY R. SINGER, SIMON F. MERZ, MATTHIAS GUNZER[4], CARLENE L. ZINDL AND CASEY T. WEAVER

In preparation for *Mucosal Immunology*

Format adapted for dissertation

Abstract

Interleukin (IL)-22 is essential for immune defense against extracellular bacterial pathogens at mucosal barrier sites. In response to the enteric attaching and effacing (A/E) bacteria, *Citrobacter rodentium (C.r)*, IL-22–producing innate cells act early in infection to limit bacterial attachment to surface intestinal epithelial cells (IECs). Yet, the mechanisms by which this protection occurs are not well characterized. Here we show that surface IECs produce neutrophil-recruiting CXC chemokines (CXCL1, CXCL2 AND CXCL5) in response to innate cell-derived IL-22 early in response to infection resulting in increased numbers of polymorphonuclear neutrophils (PMNs) in the lamina propria and neighboring colonic epithelium. Depletion of neutrophils during the early phase of *C.r* infection impaired host defense, resulting in enhanced bacterial burden in the upper crypt regions of the distal colon. Mice with either global or innate cell-specific deficiency of IL-22 had significant deficits in neutrophil-attractant chemokines and recruitment of neutrophils to the colonic LP and epithelium. Mice with deficiency of the IL-22 receptor (IL-22Rα) phenocopied these results, indicating that IL-22 acting on IECs was responsible. Thus, innate cell-driven IL-22/IL-22R signaling in colonic surface IECs is required for early induction of neutrophil-recruiting chemokines that are essential for directing the first wave of PMNs towards the infected epithelium.

Introduction

Enteropathogenic *E. coli* (EPEC) and enterohemorrhagic *E. coli* (EHEC) causes around 0.8 million mortality worldwide and remain a threat to public health[1,2]. Type 3 immune responses govern host defense against extracellular pathogens including EPEC and EHEC by deploying IL-17 and IL-22 from both innate and adaptive immune cells[3]. *Citrobacter rodentium* (*C.r*) is a Gram-negative, attaching and effacing (AE) enteric mouse pathogen that models EPEC and EHEC[3–5]. Similar to EPEC and EHEC, *C.r* expresses a locus of enterocyte effacement (LEE) pathogenicity island[6] and utilizes a type III secretion system to inject its effector molecules such as Tir into host intestinal epithelial cells (IECs)[7], which leads to effacement of IEC microvilli and attachment of *C.r* to the luminal surface of IECs[8,9]. Upon attachment, *C.r* can also cross the epithelial barrier and translocate to the kidney and liver, causing hepatocellular necrosis and ischemic injury[10]. This systemic infection is more pronounced in mice with immune deficiencies such as IL-22 deficiency and is thought to be one of the causes of fatality in *C.r*-infected mice[11–13]. Thus, the host requires a robust immune response to limit the expansion of pathogenic bacteria in the intestines in order to reduce *C.r* translocation into the blood circulation.

Polymorphonuclear neutrophils (PMNs) are important for the clearance of extracellular bacterial pathogens at mucosal barriers[14,15]. PMNs directly kill bacteria through phagocytosis, NET formation, and degranulation[16], mechanisms which require PMNs to be at the approximal location of the pathogen. PMNs circulate in the bloodstream during homeostasis and are recruited to the site of infection through a series of transendothelial and transepithelial cell migration events via CXC chemokine receptor 2 (CXCR2) signaling[17,18]. In contrast to WT animals, mice with global CXCR2 deficiency have

reduced PMN recruitment and suffer from *C.r* invasion into crypts of the colon, emphasizing the importance of PMNs in protection of colonic crypts from *C.r* colonization[17]. Crypt invasion is also observed in IL-22 KO mice[13], suggesting that there might be a link between IL-22–mediated host immunity and PMN recruitment.

During inflammation, epithelial cells produce CXCR2 ligands CXCL1, CXCL2 and CXCL5 to create a chemical gradient that allows PMNs to reach the inflammatory site[19–21]. PMNs themselves are also capable of producing CXCL1 and CXCL2 to promote PMN self-recruitment in a feed-forward loop fashion[22–24]. While CXCL1, CXCL2 and CXCL5 all directly bind to CXCR2, the compartmentalization of these chemokines differs in the local tissue in order to facilitate different stages of PMN migration[22]: CXCL1 and CXCL2 are shown to be produced by endothelial cells and PMN itself, respectively, to promote neutrophil adhesion on endothelial cells and transendothelial cell migration, respectively[22]. Local CXCL1 and CXCL2 concentration also dictates the site of PMN transendothelial migration during intestinal inflammation[25]. However, the geographic distribution of these chemokines in the colon remains unknown during *C.r* infection. Therefore, understanding the temporal and spatial dynamics of different CXC chemokines and their cellular source is crucial to define the mechanisms of PMN migration during *C.r* infection.

IL-22 is indispensable for host protection against *C.r* infection, as mice with IL-22 deficiency rapidly succumb to *C.r* infection. This is in contrast to WT mice, which clear the bacteria at ~3 weeks post-infection[11,13]. IL-22 belongs to the IL-10 cytokine family and is produced by both innate cells (lymphoid cells (ILC3s), natural killer (NK) cells, NKT cells, γδT cells, and PMNs) and CD4 T cells (Th17 and Th22)[26,27]. IL-22 promotes epithelial barrier function[28–30], wound healing[31], and production of defense molecules such

as antimicrobial peptides (Reg3 and calprotectin)[11,32]. Our recent work demonstrated that IL-22 is essential for host protection against *C.r,* with innate cells as important IL-22–producers early in *C.r* infection and T cells as dominant producers at later in infection. In the absence of IL-22, *C.r* invades epithelial crypts and can breach the epithelial barrier. We found that IECs produce CXCL1, CXCL2 and CXCL5 during *C.r* infection but these cytokines are not upregulated in IL-22 knockout mice[13], suggesting a link between IL-22 signaling in IECs and PMN recruitment to the colonic epithelium. However, the mechanism of IL-22–induced chemokine expression on colonic IECs and PMN recruitment remains poorly understood.

In this study we have found that treatment of mice with an αGr-1 antibody reduced the recruitment of PMNs to the colon and led to crypt invasion and increased bacterial load in the *C.r* model. IECs were found to be the major source of PMN recruiting CXC chemokine during early *C.r* infection, which was augmented by CXC chemokine production from PMNs and other immune cells during the later stage of infection. Notably, we found that IECs were exclusive producers of high levels of CXCL5, while PMNs and macrophages produced only CXCL1 and CXCL2 following their recruitment to the colon. IL-22 signaling in the IECs was critical for the recruitment of PMNs, as mice with either IL-22 or IL-22R deficiency had reduced PMN recruitment. We further found that IL-22 from innate cells is required for the initial recruitment of PMNs and production of CXC chemokine from IECs. Our findings reveal a critical role for innate-derived IL-22 in mediating early PMN recruitment for host defense of the colonic crypts during *C.r* infection.

Results

PMNs are required for host defense of colonic epithelial crypts against *C.r* infection

CXCR2-dependent PMN recruitment into the colon is thought to be critical for host defense of colonic crypts during *C.r* infection[17]. To validate the role of PMNs in host defense and crypt protection during *C.r* infection, we depleted PMNs from C57BL/6 mice using αGr-1 (Ly6C/Ly6G) antibody and infected mice with *Citrobacter rodentium* (*C.r*) (Fig. 1a). On day 8 post infection (p.i.), we found a twofold reduction in the relative percentage of $CD11b^+$ $Ly6G^+$ PMNs recruited into the colon (Fig. 1b, c) in mice treated with αGr-1, compared mice treated with isotype control antibody. Using a luminescent strain of *C.r* (ICC180) to allow real-time visualization of bacterial colonization in the whole animal[33], we found that PMN depletion resulted in significantly heightened *C.r* burden on days 8-12 p.i. compared with isotype control treated mice. Notably, there was an approximately 10 times higher *C.r* burden at d10 p.i. in PMN depleted animals.

Next, we assessed how PMN depletion affects crypt protection against *C.r* using immunofluorescence staining of *C.r*-LPS in intestinal tissue from infected animals. On d8 p.i., *C.r* predominately colonized surface epithelial cells in isotype control-treated mice (Figs. 1f, left panel). In contrast, *C.r* colonized deep into the upper crypt region of the colon in αGr-1–treated mice (Fig. 1f, right panel), consistent with a previous study using *Cxcr2* global KO mice[17]. Together, these data confirm that PMNs are critical for host defense against *C.r* to limit bacterial burden and colonization in colonic crypts.

CXCR2 is one of the major chemokine receptors expressed by PMNs to facilitate recruitment into inflamed tissue. To validate if CXCR2 dependent PMN recruitment is

required for crypt protection, we treated mice with CXCR2 antagonist Ladarixin[34], and corresponding control and accessed the PMN recruitment and *C.r* localization. Mice treated with Ladarixin had lower percentage and number of PMN in the IE, and a trend, but non-significant of reduce PMN number in the LP regions of the colon, on d7 p.i. (Fig. S1A-B), suggesting CXCR2 is required for PMN recruitment in the colon, especially IE regions. Ladarixin treated mice have *C.r* colonized deep into the crypt region of the colon on d10 p.i. (Fig. S1D), mirror the phenotype from αGr-1–treated mice (Fig. 1f). Mac/Mono population was also reduced in CXCR2 treated mice (Fig. S1C), suggesting that PMN may also facilitate the recruitment of Mac/Mono. These data shows that PMN recruitment into the colon protects the crypt regions from *C.r* invasion and is dependent on CXCR2.

Dynamics of PMN recruitment into the colon intestinal epithelium and lamina propria during *C.r* infection

Next, we investigated the dynamics and localization of PMN recruitment into the colon during *C.r* infection. Most immune cells (including PMNs) are recruited to the colonic lamina propria after infection, with some PMNs migrating towards the epithelium[35,36]. To assess PMN recruitment into the intestinal epithelium (IE) and lamina propria (LP), we isolated cells from distal colon at different time points post-*C.r*. infection, because PMN mainly infiltrate distal colon during *C.r* infection[33]. Few $CD11b^{+}Ly6G^{+}$ PMNs were found in the distal colon of naïve mice, indicating that PMNs rarely traffic to the colon at steady state (Fig. 2a-d). During the early phase of *C.r* infection (d4 p.i.), where *C.r* starts to establish A/E lesions in the IE, PMNs could be detected at low levels in both the LP and IE. As the infection progressed to peak colonization (d8 p.i.), there was a significant and dramatic increase in PMNs in both the LP and IE compartments compared to naïve and d4

p.i. *C.r*-infected mice (Fig. 2a-c), Notably, PMNs become the dominant myeloid cell in the IE compartment (65% of $CD11b^+$ cells) at the peak of *C.r* infection (d8 p.i.), while the numbers of $CD11b^+Ly6G^-$ monocytes/macrophages (Mac, Mono) remained largely static on d4 and d8 p.i.. To corroborate the localization of PMNs in whole colon tissue of *C.r*-infected mice, we performed immunostaining for $S100a9^+$ PMNs. Consistent with our flow cytometric studies, we found PMNs were located in the LP in between the crypts and at the bottom of the mucosa, with some PMNs infiltrating the epithelium and attached to surface IECs (Fig. 2e, f). The relative abundance of PMNs increased as *C.r*. infection progressed, with both PMN numbers and C. r. colonization being significantly elevated on d8 p.i. (Fig 2e-g). Thus, PMNs are recruited to both the IE and LP compartments in the distal colon in response to *C.r* and are the major myeloid cells associated with the surface and upper-crypt epithelium, suggesting that PMNs may be crucial for limiting bacterial growth at colonic surface and protecting the colonic crypts.

Since *C.r* does not efficiently attach to proximal colon IECs during infection[33,37], we speculated that PMNs may not be recruited to the proximal colon due to the lack of *C.r* colonization and corresponding immune activation. To test this, we isolated cells from both the proximal and distal colon during *C.r* infection and analyzed PMN recruitment by flow cytometry. PMN recruitment in the distal colon increases during the period between naïve and d8 p.i., consisting with our previous data. In contrast, few PMNs are detected in the proximal colon during the same time points post infection in both the IE and LP compartments, coincident with the distribution of *C.r* in the colon. In summary, PMNs are mostly recruited to distal rather than proximal colon (Fig. S2A-E). Our finding as well as other studies[38], suggest that *C.r* local colonization is required for PMN recruitment.

Dynamics of PMN–recruiting chemokines during *C.r* infection

IECs are one of the major producers of CXC chemokines during *C.r* infection to potentially recruit CXCR2^{+} PMNs[13,19–21]. We next investigated the dynamics and cellular sources of CXCR2 ligands: CXCL1, CXCL2 and CXCL5 during *C.r* infection. Cells from distal colon IE and LP compartments were sorted using FACS and chemokine expression was analyzed by RT-PCR. We include PMN and Mac/Mo populations here because they are reported to be able to produce CXCL2[39]. No chemokine expression was detected in IECs from naïve mice, supporting our previous finding that few PMNs exist in the colons of naïve mice. At day 4 p.i., we found strong upregulation of *Cxcl1* and *Cxcl2* expression from Mac/Mo, but not other cellular populations. As the infection progressed (day 8 p.i.), *Cxcl1* expression was observed in all three cell populations while *Cxcl2* was mostly express by PMNs. In contrast, *Cxcl5* was found to be exclusively expressed by IECs at both days 4 and 8 post-infection (Fig. 3a). Our findings reveal that PMN recruiting chemokines Cxcl1 are mostly expressed by IECs, PMNs and Mac/Mo, and Cxcl2 are mostly expressed by PMNs and Mac/Mo, while Cxcl5 is uniquely expressed by IECs. We next investigated the dynamics of CXC chemokine protein production by IECs and PMNs. No chemokines were detected in any cells from naïve mice, consisting with our previous results. IECs and PMNs produced similar levels of CXCL1 during the early stage of infection (day 4 post–infection). On day 8, LP-PMNs become the dominant source of CXCL1 and CXCL2, while CXCL1 production from IECs remain unchanged. Meanwhile, CXCL5 production was found exclusively from IECs as infection progress (Fig 3b).

To confirm these findings, we used immunostaining to localize cells that produce these chemokines in colons from naïve or C.r. infected animals. No CXCL1, CXCL2 or CXCL5

producing cells were found in the distal colon of naïve mice, consistent with our previous gene expression and ELISA data (Fig 3a-b). We found that CXCL1 and CXCL2–producing cells are predominantly located in the LP region of the colon in between the crypts, with a morphology of infiltrating leukocytes. CXCL5-expressing cells were identified as surface and upper crypt epithelial cells (Fig. 3c-d). Together our data demonstrate that CXCL1 and CXCL2 chemokines are predominantly produced by PMNs while the CXCL5 chemokine is expressed by IECs during *C.r* infection, suggesting that CXCL5 could potentially recruit PMNs to the IE in respond to infection.

IL-22 promotes PMN recruitment into the colon LP and IE during *C.r* infection

Study based on viral infection models reveals that IL-22 recruits PMN into the peripheral tissues[40], and our previous study shows that IL-22 promote PMN recruiting chemokine from IECs. Thus, we postulate that IL-22 promotes the recruitment of PMN into the colon during *C.r* infection. To test this, we infected mice with global deficiency of IL-22 (*Il22*^{Ella}) and quantified PMN recruitment into the IE and LP regions by flow cytometry. Strikingly, PMN number and frequency in the colonic IE and LP were reduced in *C.r*-infected *Il22*^{Ella} mice compared to control mice (*Il22*$^{fl/fl}$) at day 7 post-infection (Fig. 4a-c). Next, we employed immunofluorescent staining of colon tissues to validate the frequency and localization of PMNs in *C.r*-infected control and *Il22*^{Ella} mice. In control day 8 *C.r*-infected mice, PMNs were largely found in the LP regions of the colon, with some infiltrating into the epithelium and lumen, and attached to IECs, consistent with our previous findings (Fig. 2e). In marked contrast, we observed an overall PMN number reduction colon tissue from *Il22*^{Ella} mice, with a paucity of PMNs in LP region in between crypts and associated with

surface and upper crypt IECs. (Fig. 4d-e). These data shows that IL-22 can promote PMN recruitment into the colon and colonic epithelium during *C.r* infection.

IL-22 can induce CXCR2 ligands production in colonic epithelial cells during *C.r* infection[13]. The impairment of PMN recruitment in *Il22*^{Ella} mice could result from lack of IL-22-induced chemokine production from IECs. To assess the chemokine production from IECs between control and *Il22*^{Ella} mice, we isolated IECs from both group of mice at day 7 post-infection and analyzed RNA expression of *Cxcl1*, *Cxcl2* and *Cxcl5*. IECs from *Il22*^{Ella} mice have significantly reduced *Cxcl1*, *Cxcl2* and *Cxcl5* mRNA expression, compared with control infected mice. These data conclude that IL-22 production is associated with upregulation of neutrophil-recruiting chemokine expression from IECs during *C.r* infection, which can subsequently promote PMN recruitment to the colon and infected epithelium during *C.r* infection.

It was unclear from these finding whether IL-22 is able to directly recruit neutrophils. To investigate this, we isolated PMNs and IECs from colons of WT mice on day 8 of *C.r* infection and analyzed *Il22ra1* expression by RT-PCR. No *Il22ra1* mRNA expression was detected from PMNs, indicating that IL-22 does not function to directly mediate PMN recruitment (Fig. S3A).

Bactericidal and inflammatory matured PMNs are recruited into the colonic epithelium and their function is independent of IL-22

PMNs recruited to the epithelium are in close proximity to the areas of C.r attachment, and potentially play an important role in bacteria killing and inflammation induction. We next assessed gene expression profiles of PMNs in the IE in both infected control and *Il22*^{Ella}

mice to characterize IE infiltrating PMN and investigated whether IL-22 could impact PMN function. We isolated PMNs from colonic IE regions from both control and *Il22*^{Ella} mice and performed scRNA-Seq analyses. We found a total of 4 groups of PMNs from both control and *Il22*^{Ella} mice that matches the gene expression profiles of G0, G5a, G5b, and G5c PMN populations described by a recent PMN scRNA-Seq study[41] (Fig. S3B). G0 populations are mostly unmature PMN and comprise a small portion of the total PMN. G5a has high expression of bactericidal and inflammatory genes including *Lyz2* and *S100a8*, suggesting they may contribute to host protection against C.r; G5b PMNs express a set of interferon-stimulated genes such as *Gbp5* and *Cxcl10*, and may facilitate the recruitment and activation of other immune cells including Mac/Mo, T cells, NK cells and dendritic cells; G5c PMNs have gene expression of ageing and inflammatory genes, including *Cxcr4*, *Ccrl2*, *Csf1* and *Tnf*, indicating these are ageing PMNs yet still capable of mediating PMN and Mac/Mo activation and recruitment. All 4 group of PMNs are found in both infected control and *Il22*^{Ella} mice. The frequency of effector PMN G5a, G5b and G5c populations are comparable between control and *Il22*^{Ella} mice (Fig. S3C-D), suggesting that the effect of IL-22 is more likely to be related to neutrophil recruitment and less likely to be a direct impact on PMN heterogeneity or function.

PMN, but not IECs, promotes macrophage recruitment during C.r infection

CD11b+ macrophages and monocytes (Mac/Mo) are also reduced in *Il22*^{Ella} infection (Fig. 4a). We hypothesized that these cells could be recruited in response to either IL-22 induction of macrophage/monocyte chemokines, or as a result of IL-22 recruited PMNs subsequently promoting macrophage/monocyte recruitment. To investigate the mechanism of Mac/Mo recruitment during C.r infection and correlation with IL-22, we first tested the

cellular composition of the Mac/Mo populations in naïve and *C.r*–infected mice in the LP region. Using the Ly6C marker, we distinguished monocyte ($CD11b^+$ $Ly6C^+$) and macrophage (CD11b+ $Ly6C^-$) populations (Fig. S4A-B). During homeostasis, macrophages comprise of most of the tissue resident $CD11b^+$ cells. (Fig. S4B, D). As infection progresses, CCR2+ monocytes are recruited into the LP, while the number of macrophages shows marginal increase, suggesting that the infection mostly mobilizes monocytes to the site of the infection (Fig. S3D) and may partially give rise to tissue resident macrophage. In contrast, macrophages and PMNs lack CCR2 expression, suggesting they are recruited through a distinctive pathway independent of monocyte recruitment (Fig. S4C). All together, these findings show that macrophages are one of the major tissue resident cells during homeostasis, and CCR2 expressing monocytes are largely recruited to the colon during *C.r* infection.

Next, we tested the cellular source of CCL2, CCL3 and CCL7, three of the major monocyte chemokines during C.r infection. We isolated cells from the colonic IE at D8 post infection and performed scRNA Seq analysis. We found Mac/Mo uniquely express *Ccl2* and *Ccl7*; with *Ccl3* mostly expressed by PMN and Mac/Mo (Fig. S5A-B). This reveals that monocytes are recruited by both infiltrating PMNs and also self-recruited by existing Mac/Mo. In summary, monocyte recruitment during C.r infection is mostly mediated by PMNs, and tissue-resident Mac/Mo produced chemokines, but not IECs, suggesting that IL-22 is less likely to directly impact Mac/Mo recruitment.

IL-22 signaling to colonic epithelial cells is important for PMN recruitment

Chemokine production from IECs is reduced in $Il22^{Ella}$ mice (Fig. 4f). Giving the fact that IECs are the main target of IL-22 in the colon[42], we hypothesized IL-22 promote

chemokine production from IECs through direct IL-22 receptor signaling. To test this, we infected mice that lack the IL-22 receptor specifically on IECs (*Il22ra1*^{Villin}) and assessed PMN recruitment in the IE and LP regions of the colon from control (*Il22ra1*$^{fl/fl}$) and Il*22ra1*^{Villin} mice. Compared with control mice, PMNs in both the IE and LP compartments of the colon in *Il22ra1*^{Villin} mice were reduced, similar to the phenotype observed in *Il22*^{EIIa} mice (Fig. 5a-c). Histology validation revealed that fewer PMNs were observed in colonic IE and LP in *Il22ra1*^{Villin} mice compared to controls (Fig. 5d-e). To further validate that IL-22 signaling to IECs contribute to chemokine production, which subsequently recruits PMNs, we accessed expression of CXCL5 in colons of day 8 *C.r*-infected control and *Il22ra1*^{Villin} mice by immunofluorescence staining (Fig. 5f). CXCL5 was predominantly found to be expressed by surface IECs in control mice, coincide with our previous data. In contrast, CXCL5 expression was reduced in IECs from *Il22ra1*^{Villin} mice, indicating that IL-22/IL-22R signaling in IECs is required for CXCL5 chemokine production from IECs. These data suggest that IL-22 directly acts on IECs through the IL-22 receptor to promote CXCL5 chemokine production and subsequently recruit PMNs into the infected colon.

IL-22 from innate cells is critical for PMN recruitment during the early phase of *C.r* infection.

During early (days 3-6) *C.r* infection, IL-22 is produced by innate immune cells including ILCs, NK T cells and LTi cells, during which PMNs recruitment is also initiated [13,26](Fig 2a-d). We speculate that IL-22 from innate cells is critical for the early recruitment of PMNs during *C.r* infection. To define a specific role for innate cell-derived IL-22 in facilitating PMN recruitment to the colon, we infected mice that had innate cell-specific deficiency of IL-22 (*Zbtb16/Plzf*)-*cre* x *Il22*^{hCD4}; *Il22*^{Plzf}) and analyzed PMN recruitment

at an early stage of the infection (day 6), when IL-22 is dominantly produced by innate cells (Zindl and others). *Il22*^{Plzf} mice had reduced PMN recruitment in both the IE and LP compartments during *C.r* infection compared with control infected mice (Fig. 6a-c), similar to our previous observation in *Il22*^{EIIa} and *Il22ra1*^{Villin} mice. Immunofluorescence staining confirmed that PMNs attached to or infiltrating into the epithelium, and in the LP were reduced compared to control infected mice (Fig. 6d-e). Next, we evaluated whether IL-22 from innate cell sources induced chemokine production from IECs. As expected, Cxcl1, Cxcl2 and Cxcl5 mRNA expression from colonic IECs was reduced in *Il22*^{Plzf} mice at day 6 of *C.r* infection compared to control infected mice. In addition, immunofluorescence staining revealed that CXCL5 production was predominantly expressed by surface IECs in control infected mice, and Cxcl5 expression was reduced in *Il22*^{Plzf} mice. Together these data establish an important role of IL-22 from innate cells to induce IEC production of chemokines to recruit early PMN recruitment to the colon during *C.r* infection.

Next, we inspected the role of IL-22 from T cells in PMN recruitment. We utilized a mouse with T cell-specific deficiency of IL-22 ((*CD4*)-*cre* x *Il22*^{hCD4}; *Il22*$^{\Delta Tcell}$). *Il22*$^{\Delta Tcell}$ mice were infected with *C.r* and PMN recruitment were assessed at a later phase of infection (day 8) when IL-22–producing T cells start to migrate to the colon and respond to *C.r* infection (Fig. S6A-C). Compared with control (*Il22*$^{fl/fl}$) mice, no major difference in PMN recruitment into either the IE or LP regions was observed in *Il22*$^{\Delta Tcell}$ mice suggesting that other mechanisms control PMN recruitment to the colon during the late phase of *C.r* infection. PMN infiltration to the IE regions and distribution in the LP was also similar between control and *Il22*$^{\Delta Tcell}$ mice, based on immunofluorescent staining (Fig. S6D-E).

Overall, our results suggest that IL-22 from CD4 T cells is not required for PMN recruitment into the IE and LP regions of the colon during peak phase of *C.r* infection.

Discussion

IL-22 is traditionally thought to mediate host defense through direct IEC function, including AMP production, tissue regeneration and barrier function. However, it is unknown whether IL-22 coordinates with other immune cells to provide host protection. Our study highlights the novel function of IL-22 to promote antimicrobial PMN recruitment to mediate host defense during *C.r* infection. Here we have defined a critical role of IL-22 from innate cells to act on IECs through IL-22R signaling to induce epithelial production of CXCR2 ligand CXCL1, CXCL2 and CXCL5 to initiate PMN recruitment. IECs serve as the major producer of the CXCL5 chemokine to promote PMN recruitment specifically to the IE, in order to eliminate bacteria and protect the intestinal crypts from bacterial invasion.

PMNs are phagocytes that have been shown to be important for clearing bacteria from the mucosal surface. PMNs are thought to be critical for clearance of IgG-opsonized *C.r* in the lumen during the last stages of *C.r* infection through phagocytosis[43]. Here, we demonstrate that mice with PMN depletion have increased bacteria load during early-middle stages of infection and *C.r* invasion of the upper crypt region of the colon, indicating that PMNs act during early phase of infection to limit bacterial expansion, before the action of B-cell mediated humoral response. Our results, combined with previous studies, show a full spectrum where PMNs act during the innate phase to limit bacterial expansion, potentially mitigating host damage and immune burden by *C.r*. Once the adaptive system kicks in, PMNs can coordinate with adaptive immune cells to achieve final clearance of *C.r*.

Although PMNs are not grouped into subsets like $CD4^+$ T cells to define their distinctive functions, they are a heterogenous population and can be categorized into different groups

based on their gene expression markers, which reflects their various developmental stages and functional properties[41]. Based on scRNA-Seq analysis, we found that most epithelium-infiltrated PMNs are mature and aging PMNs that express bactericidal and inflammatory genes, including *S100a8, S100A9, Lyz2* and *Ccrl2,* which potentially contribute to the surface and upper crypt defense against *C.r*. Lyz2 is required for lysozyme formation which digest bacteria during phagocytosis[44,45]; S100A8 and S100A9 are secreted antimicrobial peptides through degranulation and limit bacteria growth through iron sequestration[46]. Padi4–mediated PMN NET formation is critical for controlling *C.r* load, but not final clearance of the bacteria[47], suggesting that NET formation may be more important to limit bacterial expansion, but not *C.r*. eradication. Yet, the detailed mechanisms and pathways for PMN limiting bacteria load and protecting the upper crypt remains poorly understood and investigating the specific role of each killing mechanism at difference stages of *C.r* infection will be essential to fully understand how PMNs protect the host from *C.r* infection.

We found that the CXCR2 ligands, CXCL1, CXCL2 and CXCL5, have a distinctive temporospatial distribution during *C.r* infection and that IL-22 promotes production of IECs derived CXCL1, CXCL2 and CXCL5 to promote PMN recruitment into the colon. Although these chemokine actives the same CXCR2 downstream signaling and can act redundantly in the sense of general PMN chemoattractant, their local distribution dictates the unique function of these chemokines. CXCL1 have been shown to be mostly decorating endothelial cells to facilitate PMN adhesion and rolling, whilst CXCL2 are located at cell-cell junctions, to facilitate transendothelial cell migration[22]. A study in a lung inflammation model suggests that CXCL5 can act as both chemoattractant for PMNs as well as bind with

DARC receptor to regulate the local chemokine gradient[48], but this has not been studied in the context of colonic bacterial infection.

Although initially produced by IL-22–activated IECs, CXCL1 and CXCL2 become most abundantly produced by PMNs and Mac/Mo during later stages of infection, where they are located in the LP. This suggests a feed-forward loop for PMNs to be self-recruited into the LP during late infection, independent of IL-22. Though PMNs are the major source of CXCL2 during later infection and may be able to self-recruit independently of IL-22, our data show that few PMNs exist in the colon during very early infection, suggesting IL-22-induced, epithelial-derived chemokines are the major source of PMN chemoattractants that initiate PMN recruitment during early infection.

Interestingly, we find that CXCL5 is uniquely produced mostly by IECs at the luminal surface, suggesting its unique role in PMN recruitment to the epithelium. The role of CXCL5 remains unknown during colon inflammation other than being a CXCR2 ligand to recruit PMNs. In an LPS–induced inflammation model in the small intestine, it was shown that PMN transendothelial cell migration was restricted to submucosal vessels at the bottom of lamina propria but not vascular vessels closer to the lumen, due to the lack of CXC chemokines gradients at luminal surface[25]. It is possible that CXCL5 produced by IECs directs the recruitment of a portion of circulating PMN to cross vessels that feed the surface epithelium more directly, by providing local CXCL5 gradients, instead of requiring their migration from the lower LP.

We initially anticipated that *Il22*$^{\Delta Tcell}$ mice would have reduced PMN recruitment to the epithelium due to lack of epithelium-derived PMN chemokines[13]. However, *Il22*$^{\Delta Tcell}$ mice did not show significant difference in PMN numbers in either lamina propria or the epithelium at d8 of infection. We believe this may be due to the delay in arrival of IL-22–producing T cells until d7-d9 post-infection, well after innate cell-derived IL-22 initially induced chemokine production from IECs. So, the contribution of T cell-derived IL-22 in recruitment of PMNs may not be important until time points later than d8 p.i., at which time mice begin succumbing to infection; at d10-d12 post infection, a portion of *Il22*$^{\Delta Tcell}$ mice suffered from extensive systematic infection with massive infiltration of immune cells including PMN into the colon (data not shown). Based on our previous discovery that *Il22*$^{\Delta Tcell}$ mice begin to succumb to infection around this timepoint[13], we conclude that these data may induce bias by only representing live animals that survived the infection. Considering the important role of T cell derived IL-22 in inducing robust, epithelial-derived PMN recruiting chemokines, future studies will be needed to determine the impact of T cell derived IL-22 on PMN recruitment into the epithelium and PMN transendothelial migration.

Method

List of antibodies used

Antibody	Vender	CAT#
Ultra-LEAF™ Purified anti-mouse Ly-6G/Ly-6C (Gr-1) Antibody (RB6-8C5)	Biolegend	108436
E. coli Polyvalent 8 LPS	Accurate Chemical and Scientific Corp	YCC312-012
EpCAM/CD326 FITC (clone G8.8)	eBioscience/ ThermoFisher	11-5791-82
CD11B Rat anti-Mouse, Brilliant Violet 711, Clone: M1/70, BD	eBioscience/ ThermoFisher	BDB563168

FITC Anti-Mouse CD45.2 (104)	Tombo	35-0454-U500
Ly6G APC (1A8)	Biolegend	127614
S100A9, Mouse, mAb MU14-2A5	Hycult	HM1102
GROα/β/γ Antibody (A-6) FITC	Santa Cruz	sc-365870 FITC
CXCL5 antibody	Biorbyt	orb13450
PerCP/Cy5.5 Ly6C (HK1.4)	Biolegend	128011
APC anti-mouse CD192 (CCR2) Antibody (SA203G11)	Biolegend	150627

List of primers used

Gene	Forward	Reverse
Hprt	GATTAGCGATGATGAACCAGGTT	CCTCCCATCTCCTTCATGACA
Gapdh	ACCACAGTCCATGCCATCAC	CACCACCCTGTTGCTGTAGCC
Cxcl1	CACCTCAAGAACATCCAGAG	TTGAGTGTGGCTATGACTTC
Cxcl2	GCTGTCAATGCCTGAAGA	TTCAGGGTCAAGGCAAAC
Cxcl5	GCCCTACGGTGGAAGTCATA	AGTGCATTCCGCTTAGCTTT

Mice

Il22$^{hCD4.fl}$ were generated by our group previously[13]. C57BL/6 (WT; JAX 000664), EIIa-cre (JAX 003724), Plzf-cre (JAX 024529), mCd4-cre (JAX 022071), and Villin-cre (JAX 021504) mice were purchased from Jackson Laboratory (JAX). In most experiments, littermates were used as controls and experimental adult animals (8-12 wk old) were co-caged in groups of 2-7 mice. Both sexes were used per experimental group whenever possible. All mouse strains were bred and maintained at UAB in SPF environment in accordance with IACUC guidelines.

Citrobacter rodentium infection

Citrobacter rodentium (*C.r*) strain, DBS100 (ATCC 51459) was used for all kinetics experiments. For whole-body imaging experiments, the bioluminescent *C.r* strain ICC180 (derived from DBS100) was used (Wiles et al., 2006) (generously provided by Drs. Gad Frankel and Siouxsie Wiles, Imperial College London). Animals were imaged for bioluminescence using an IVIS-100 Imaging System (Xenogen). For *C.r* inoculation: A fresh, single colony was grown in 10 ml LB overnight at 37ºC with agitation for 12-14 hrs. Next day, 1 ml of overnight culture was added to 250 ml LB, incubated at 37ºC with agitation for 4-5 hrs and then stopped when OD600 reached 1.0 on ThermoFisher SPECTRONIC™ 200 spectrophotometer. Bacteria was pelleted at 25ºC, 3000 rpm for 15 minutes and then resuspended in 5 ml sterile 1x PBS. Mice were inoculated in a total volume of 100 µl via gastric gavage.

Isolation of Intestinal cells

Intestinal tissues were flushed, opened longitudinally and then cut into strips of 0.5 cm length. Tissue pieces were incubated for 40 min at 37ºC with 1 mM DTT (Sigma) and 2 mM EDTA (Invitrogen) in H5H media (1x HBSS, 5% FBS, 20 mM Hepes, and 2.5 mM 2-b-ME), cells from the DTT/EDTA prep were spun down at 1500 rpm for 10 minutes at 4ºC to collect IECs. For isolation of lamina propria (LP) cells, tissue pieces remaining after the DTT/EDTA step were homogenized by chopping and incubated for 40 min at 37ºC with Collagenase VIII (2 mg/ml; Sigma) and DNase (1 mg/ml; Sigma) in R10 media (1x RPMI 1640, 10% FBS, 1x Pen/Strep, 1x NEAA, 1mM, Sodium pyruvate and 2.5 mM 2-b-ME). LP cells were then purified on a 40%/75% Percoll gradient by centrifugation for 20 min at 25ºC and 600g with no brake.

Colon cells were stained with Fc Block (Clone 2.4G2) and fluorescent-labeled antibodies in FACS buffer (1x PBS, 2% FBS and 2mM EDTA) on ice in 1.5 ml microcentrifuge tubes. Samples were acquired on Attune NxT flow cytometer (Life Technologies) and analyzed with FlowJo software. Cells were sorted on either a BD FACS Aria or Aria II (BD Biosciences).

Immunofluorescence staining

For immunostaining, colon tissues were fixed in in 4% PFA overnight at 4^{o}C. Tissue was then put through several cold 1x PBS washes including an overnight incubation, and then embedded in O.C.T. (Tissue-Tek) and frozen with 2-methyl butane chilled with liquid nitrogen. Tissue sections were blocked at RT for 30 minutes with 10% mouse serum in 1x PBS and 0.05% Tween-20. Antibodies were diluted in 2% BSA/PBS/Tween-20 and incubated for 30 min at RT.

Real time PCR

cDNA synthesis was performed with iScript reverse transcription (RT) Supermix (Bio-Rad) according to manufacturer's instructions. cDNA amplification was analyzed with SsoAdvanced Universal SYBR Green Supermix (Bio-Rad) in a Biorad CFX qPCR instrument.

ELISAs

For CXC chemokine ELISAs, sorted cells were incubated in H5H for 18h at 4^{o}C and supernatants were collected for ELISA. ELISA were performed according to manufacturer's protocol (CXCL1: Mouse CXCL1/KC DuoSet ELISA, CXCL2: Mouse CXCL2/MIP-2 DuoSet ELISA, CXCL5: Mouse LIX DuoSet ELISA, R&D systems).

Briefly, a 96-well high-binding assay plate (Corning) was coated with capture antibody in 1x PBS overnight at 4°C. After 3 washes with 1x PBS, 1% BSA in 1x PBS blocking solution was added to the plate and incubated at RT for 1 hr. After 3 washes with 1x PBS/Tween-20, samples or standard were diluted in 1% diluent dilution and incubated at RT for 2 hrs, followed by detection antibody at RT for 2hrs and streptavidin-HRP at RT for 2 hrs, with 3x wash in between each step. After the final 3 washes, 100 µl of a TMB single solution (Life Tech) was added to the plate and the chemiluminescence signal was stopped with 2N Sulfuric acid and read at 450 nm.

Ladarixin treatment

Ladarixin (MedChemExpress) was first diluted in DMSO at 100mg/ml and then diluted 1:100 in 0.5% of carboxymethyl cellulose PBS solution. Ladarixin was delivered orally at 15mg/kg daily, staring from d1 p.i. till sacrifice.

Figures

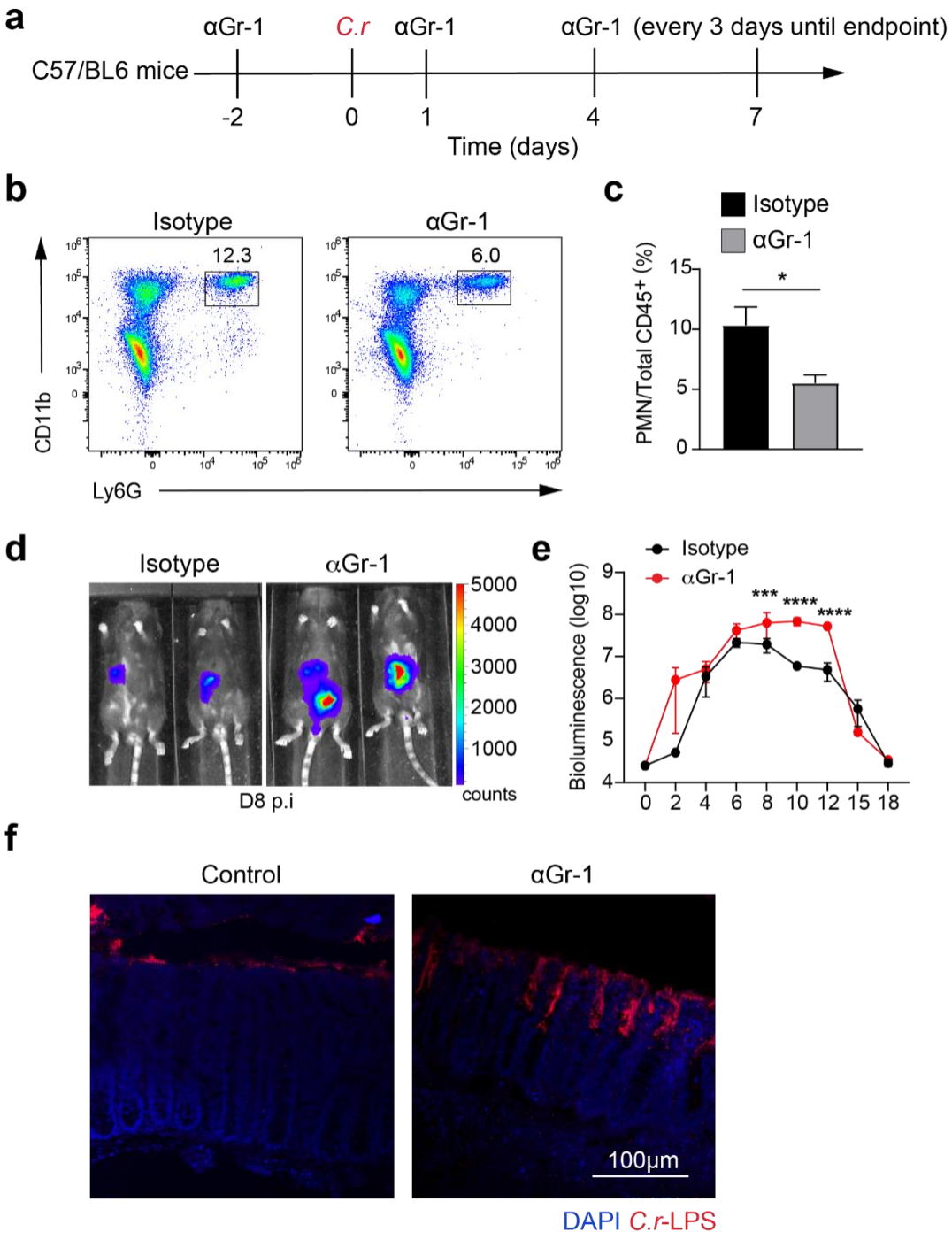

Fig. 1: Neutrophils contribute to upper crypt protection during C.r infection.

a-f BL/6 mice were treated with αGr-1 or isotype (IgG2b) control antibody on day -2, then infected with *C.r* on day 0 and received continual αGr-1 or isotype control treatment every 3 days post-infection (p.i). **a** Schematic of experimental design. **b, c** Colon cells from *C.r*-infected isotype control-treated (black) or αGr-1-treated (grey) mice were harvested on day 8 p.i., stained for Ly6G, CD11b, CD45 and L/D dye, and analyzed by flow cytometry. **c** Ratio of $Ly6G^{+}CD11b^{+}CD45^{+}$ PMNs per total $CD45^{+}$ cells. **d** Whole body imaging (day 8) and **e** colonization kinetics of *C.r* (luciferase-expressing strain)-infected mice treated with either isotype control (black) or αGr-1 (red) was performed on indicated days. **f** Colons from *C.r*-infected isotype control-treated or αGr-1-treated mice were isolated and stained for *C.r*-LPS (red) and DAPI (blue). Results are representative of two independent experiments (n=3 per group). Error bars indicate standard deviation. **c** *$p \leq 0.05$ using Student's t-test comparing isotype control and αGr-1–treated mice. **e** Two-way ANOVA ***$p \leq 0.001$ and ****$p \leq 0.0001$ comparing isotype control and αGr-1–treated mice.

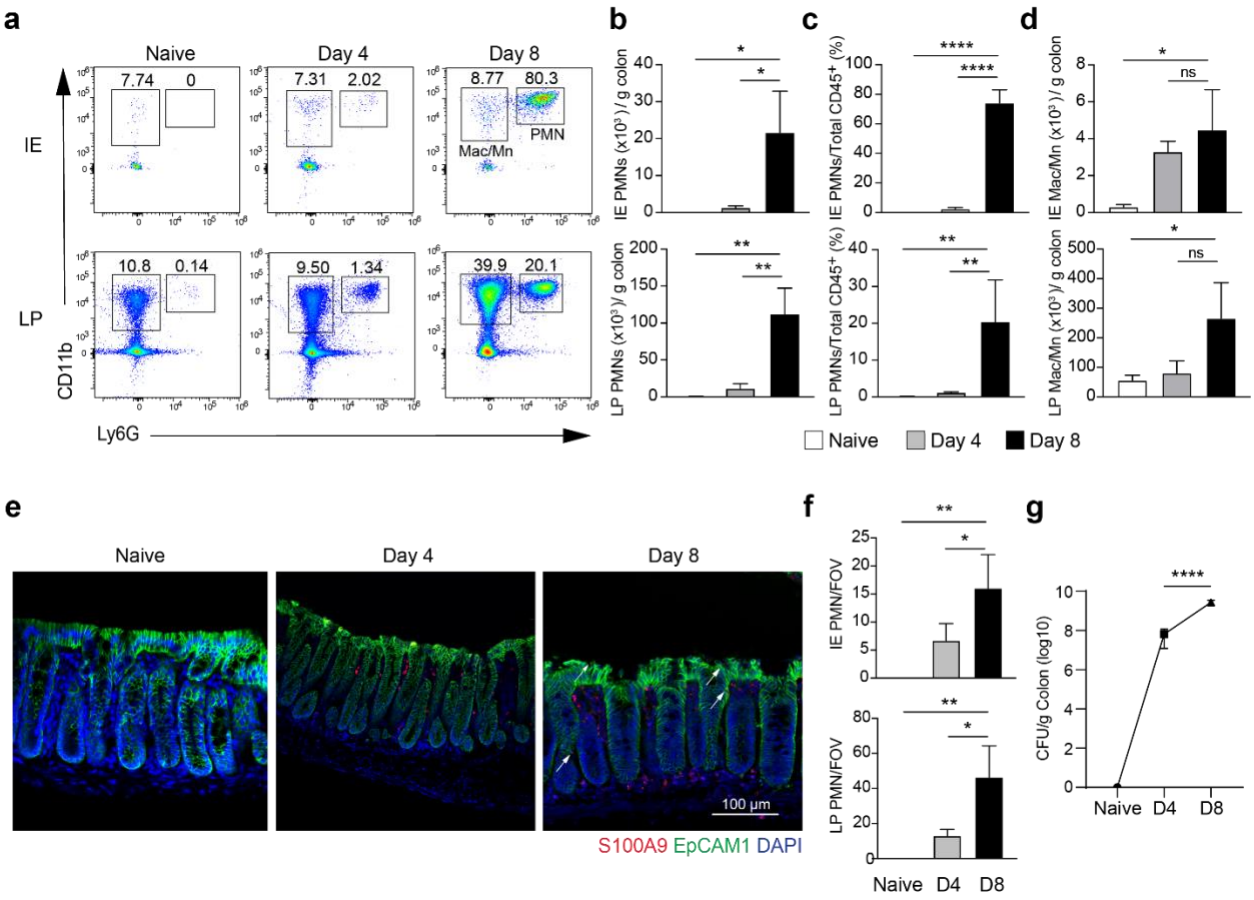

Fig. 2: Neutrophils are recruited to the colonic epithelium and lamina propria during *C.r* infection.

a-d Colon cells from IE (intraepithelial) and LP (lamina propria) regions were isolated from naïve (white) and *C.r*-infected BL/6 mice on day 4 (grey) and day 8 (black). Cells were stained for Ly6G, CD11b, CD45 and L/D dye and analyzed by flow cytometry for $Ly6G^{+}CD11b^{+}CD45^{+}$ PMNs and $Ly6G^{-}CD11b^{+}CD45^{+}$ macrophages/monocytes. Numbers represent **b** PMNs per gram of colon, **c** ratio of PMNs per total $CD45^{+}$ cells and **d** macrophages/monocytes per gram of colon. **e-g** Colons were isolated from naive and *C.r*-infected mice on D4 and D8 p.i. **e-f** Colon tissue was stained for S100A9 (red), EpCAM1 (green) and DAPI (blue). White arrows depict $S100a9^{+}$ PMNs associated with

the epithelium. **f** Quantitation of S100a9^{+} PMNs in IE and LP regions. **g** Log_{10} CFU in the colons from naïve, day 4 and day 8 *C.r*-infected mice. Results are representative of three (**a-d**) or two (**e-g**) independent experiments (n=3 mice per time point). Error bars indicate standard deviation. **a-g** Two-way ANOVA; *$p \leq 0.05$, **$p \leq 0.01$, ***$p \leq 0.001$ and ****$p \leq 0.0001$ comparing naïve and *C.r*-infected mice.

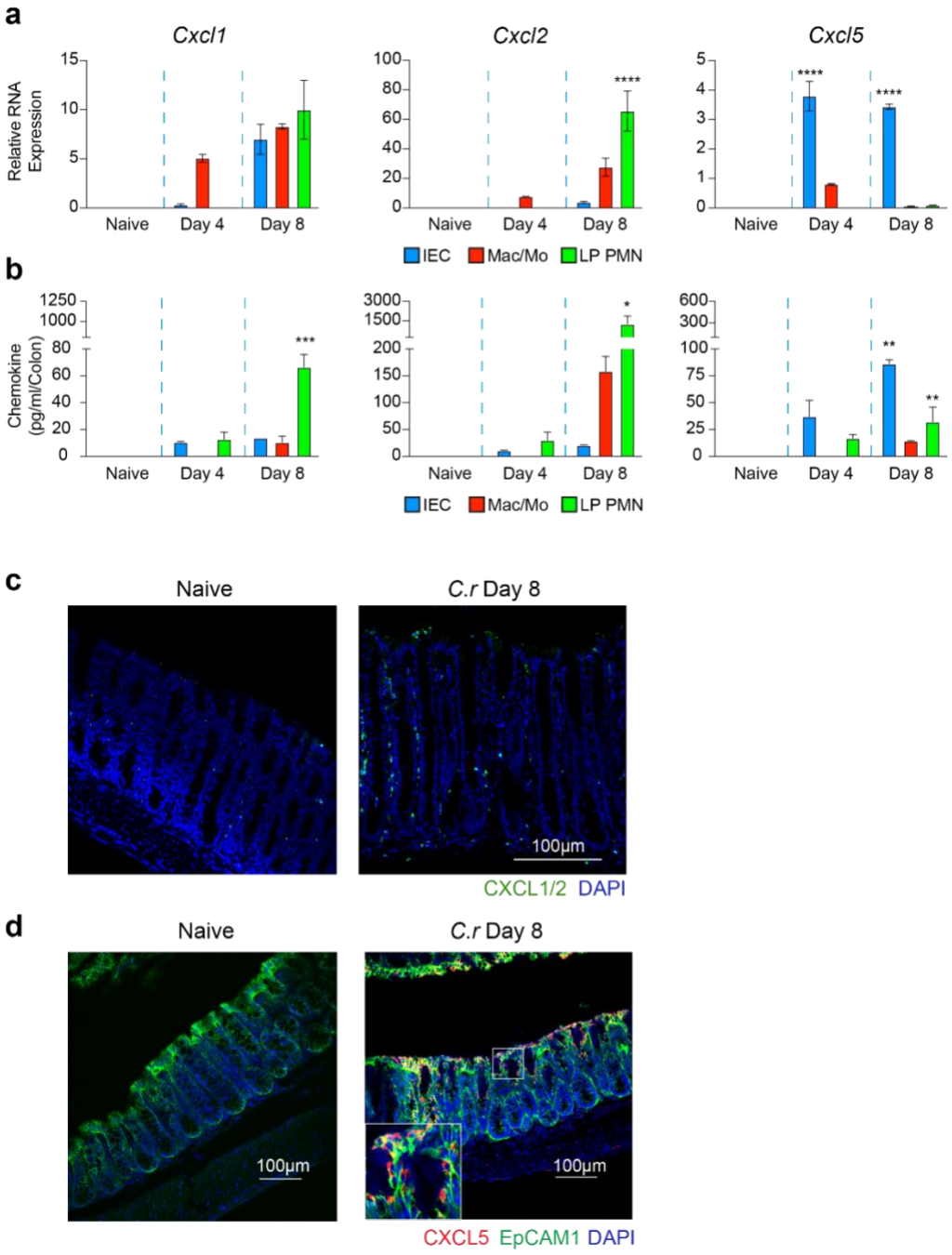

Fig. 3: Dynamics of neutrophil-recruiting CXC chemokine expression and cellular source during *C.r* infection.

a, b Colon cells from IE (intraepithelial) and LP (lamina propria) regions were isolated from naïve and *C.r*-infected mice on day 4 and day 8 p.i. Colon tissue was stained with Ly6G, CD11b, CD45, EpCAM1 and L/D dye and sorted on $EpCAM1^{+}CD45^{-}$ intestinal epithelial cells (IEC; blue). Cells from lamina propria are sorted on $CD11b^{+}$ $Ly6G^{-}$ Mac/Mo (red) and $CD11b^{+}$ $Ly6G^{+}$ PMNs (green). **a** Relative chemokine mRNA expression normalized with GAPDH mRNA was analyzed using qRT-PCR. **b** Sorted IECs and LP PMNs were cultured for 24 hrs and supernatant was analyzed for chemokine protein expression per gram of colon tissue by ELISA. **c, d** Colon tissue was isolated from naïve and day 8 *C.r*-infected mice and stained for CXCL1/2 (green) (**c**) or CXCL5 (red) (**d**) and EpCAM1 (green) DAPI (blue). Results are representative of two independent experiments (n=3 mice per time point). Error bars indicate standard deviation. **a, b** Two-way ANOVA analysis; $*p \leq 0.05$, $**p \leq 0.01$, $***p \leq 0.001$ and $****p \leq 0.0001$ comparing naïve and *C.r*-infected mice. nd= not detected.

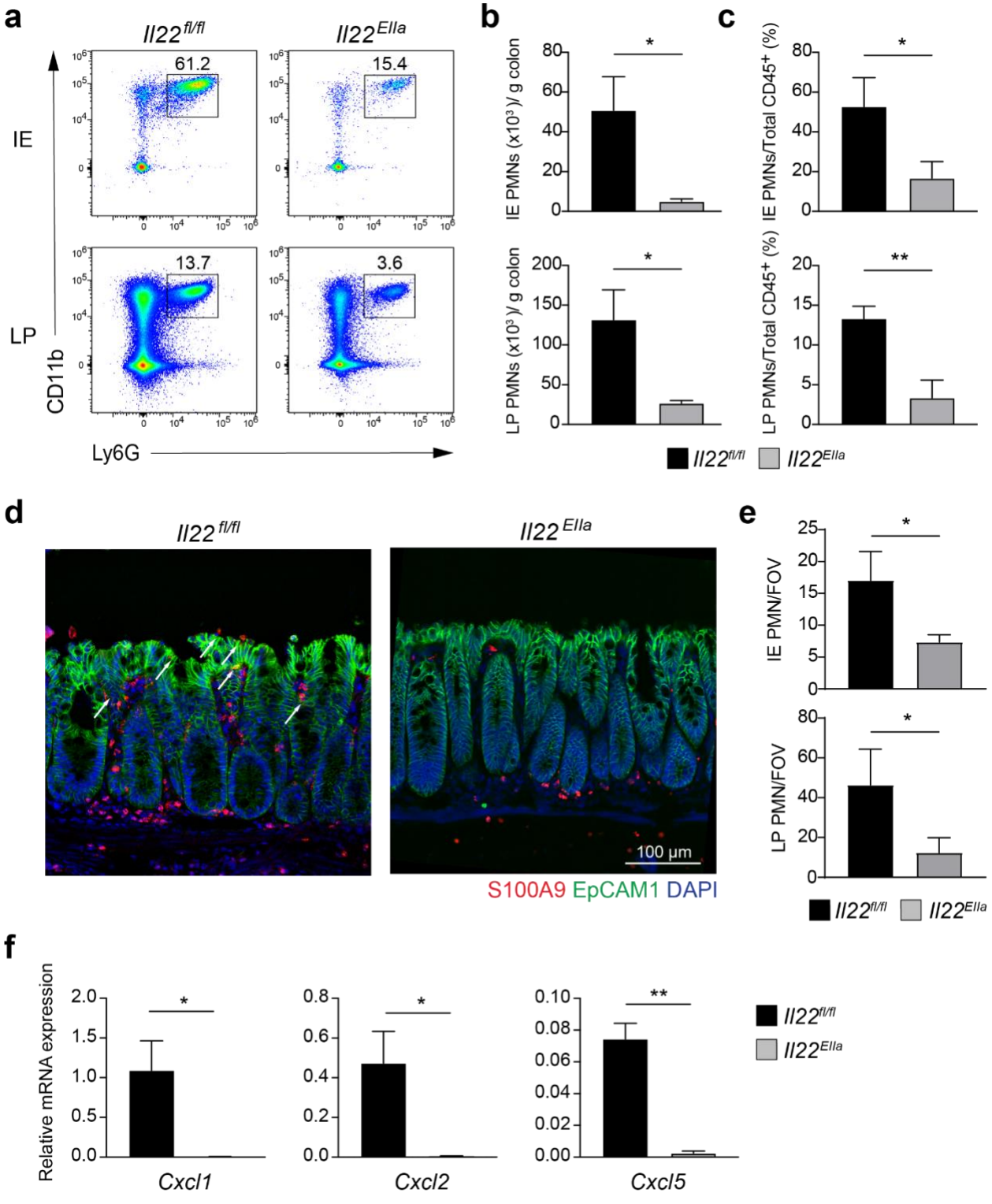

Fig. 4: IL-22 promotes neutrophil recruitment to the colon during *C.r* infection.

a-c Colon cells from IE (intraepithelial) and LP (lamina propria) regions were isolated from day 7 *C.r*-infected *Il22*$^{fl/fl}$ (Control; black) and *Il22*^{Ella} (*EIIa-cre* x *Il22*$^{fl/fl}$/gKO; grey) mice, stained for Ly6G, CD11b, CD45 and L/D dye and analyzed by flow cytometry. **b** Number of Ly6G^{+}CD11b^{+}CD45^{+} PMNs per gram of colon. **c** Ratio of PMNs per total CD45^{+} cells. **d, e** Colon tissue from day 7 *C.r*-infected *Il22*$^{fl/fl}$ (control; black) and *Il22*^{Ella} mice (gKO; grey) was harvested and stained for S100A9 (red), EpCAM1 (green) and DAPI (blue). **e** Quantitation of S100a9^{+} PMNs in IE and LP regions. **f** Colon cells from D7 *C.r*-infected *Il22*$^{fl/fl}$ (Control; black) and *Il22*^{EIIa} (*Il22*^{Ella} gKO; grey) mice was stained for EpCAM1, CD45 and L/D dye. Epcam1^{+}CD45^{-}L/D dye^{-} intestinal epithelial cells (IECs) were sorted and relative *Cxcl1*, *Cxcl2* and *Cxcl5* mRNA expression normalized with GAPDH mRNA was analyzed using qRT-PCR. Results are representative of two independent experiments (n=3 mice per group). Error bars indicate standard deviation. Student t test; *$p \leq 0.05$ and , **$p \leq 0.01$ comparing *C.r*-infected *Il22*$^{fl/fl}$ and *Il22*^{Ella} gKO mice.

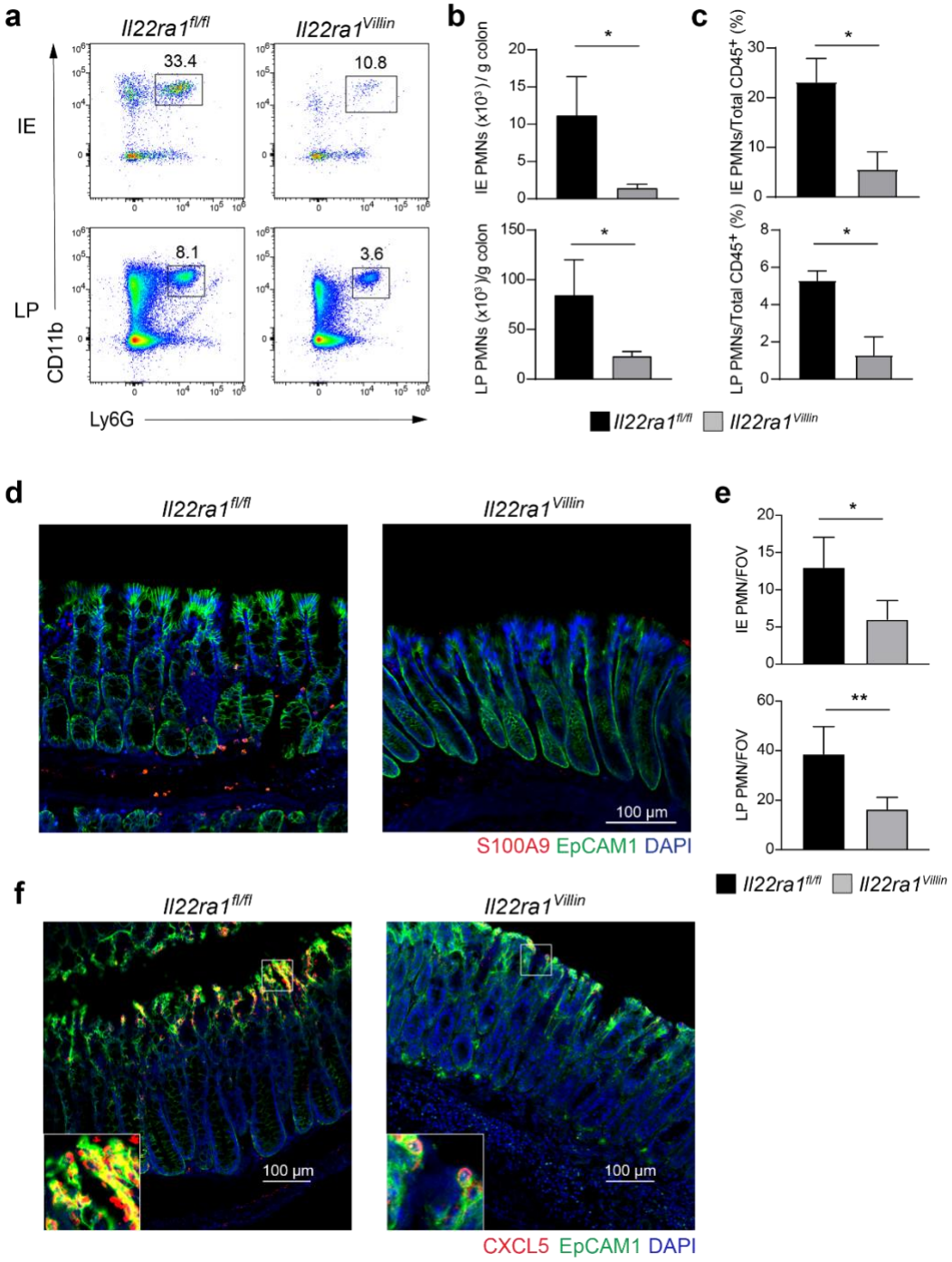

Fig. 5: IL-22RA1 signaling in colonic epithelial cells promotes neutrophil recruitment to the epithelium during *C.r* infection.

a-c Colon cells from IE (intraepithelial) and LP (lamina propria) regions were isolated from D6 *C.r*-infected *Il22ra1*$^{fl/fl}$ (Control; black) and *Il22ra1*^{Villin} (*Villin-cre* x *Il22ra1*$^{fl/fl}$/IEC cKO; grey) mice, stained for Ly6G, CD11b, CD45 and L/D dye and analyzed by flow cytometry. **b** Number of Ly6G^{+}CD11b^{+}CD45^{+} PMNs per gram of colon. **c** Ratio of PMNs per total CD45^{+} cells. **d, e** Colon tissue from D6 *C.r*-infected *Il22ra1*$^{fl/fl}$ (control; black) and *Il22ra1*^{Villin} mice (IEC cKO; grey) was harvested and stained for S100A9 (red), EpCAM1 (green) and DAPI (blue). **e** Quantitation of S100a9^{+} PMNs in IE and LP regions. **f** Colon tissue from D6 *C.r*-infected *Il22ra1*$^{fl/fl}$ (control) and *Il22ra1*^{Villin} mice (IEC cKO) was harvested and stained for CXCL5 (red), EpCAM1 (green) and DAPI (blue). Results are representative of two independent experiments (n=3 mice per group). Error bars indicate standard deviation. Student's t test; *p $\leq$ 0.05 and **p $\leq$ 0.01 comparing *C.r*-infected *Il22ra1*$^{fl/fl}$ and *Il22ra1*^{Villin} cKO mice.

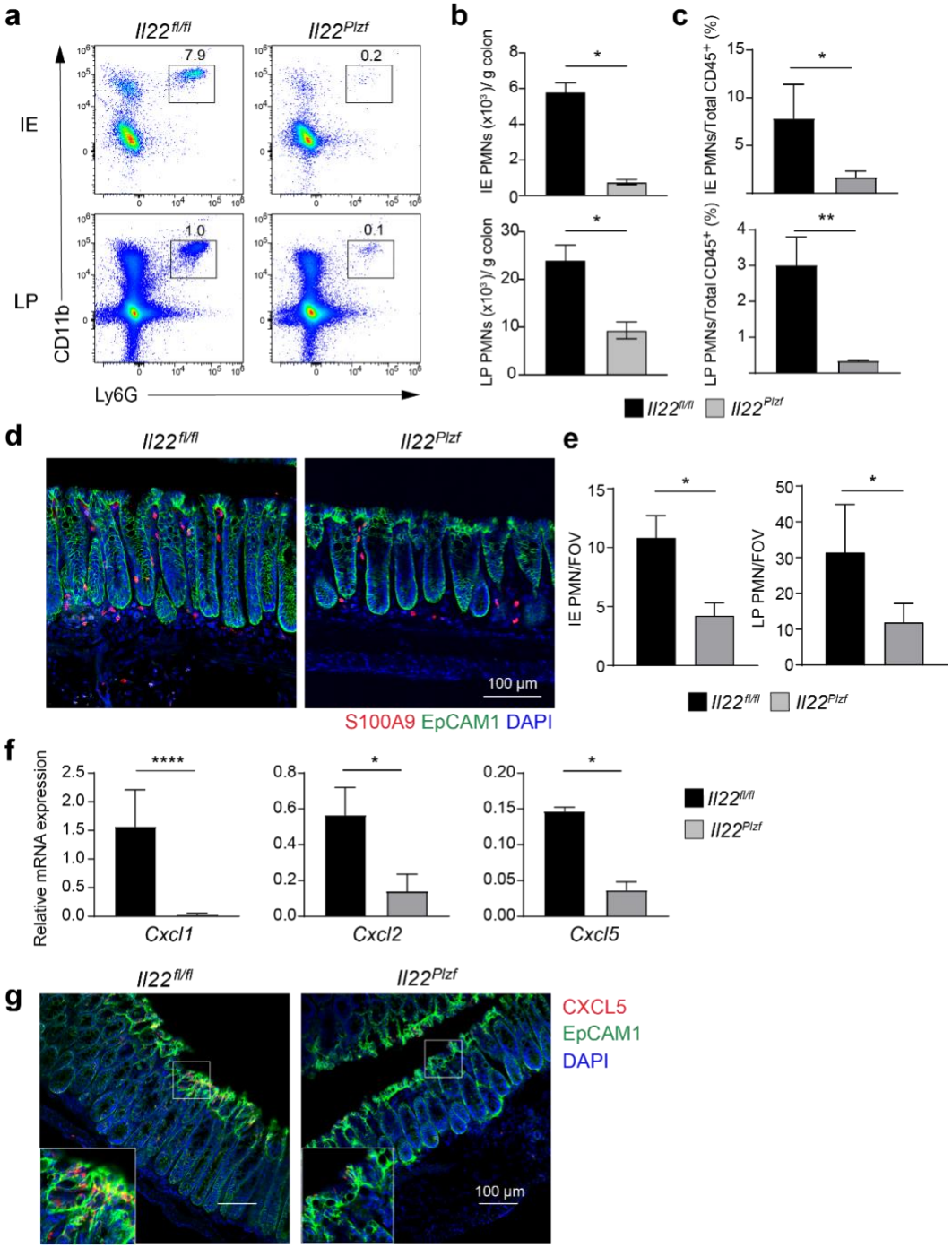

Fig. 6: IL-22–producing innate cells contribute to neutrophil recruitment during *C.r* infection.

a-c Colon cells from IE (intraepithelial) and LP (lamina propria) regions were isolated from D6 *C.r*-infected *Il22*$^{fl/fl}$ (Control; black) and *Il22*^{Plzf} (*Zbtb16/Plzf-cre* x *Il22ra1*$^{fl/fl}$/Innate-specific cKO; grey) mice, stained for Ly6G, CD11b, CD45 and L/D dye and analyzed by flow cytometry. **b** Number of Ly6G^{+}CD11b^{+}CD45^{+} PMNs per gram of colon. **c** Ratio of PMNs per total CD45^{+} cells. **d, e** Colon tissue from D6 *C.r*-infected *Il22*$^{fl/fl}$ (control; black) and *Il22*^{Plzf} mice (cKO; grey) was harvested and stained for S100A9 (red), EpCAM1 (green) and DAPI (blue). **e** Quantitation of S100a9^{+} PMNs in IE and LP regions. **f** Colon cells from D6 *C.r*-infected *Il22*$^{fl/fl}$ (control; black) and *Il22*^{Plzf} (cKO; grey) mice were stained for EpCAM1, CD45 and DAPI. Epcam1^{+}CD45^{-}L/D dye^{-} intestinal epithelial cells (IECs) were sorted and relative *Cxcl1*, *Cxcl2* and *Cxcl5* mRNA expression normalized with GAPDH mRNA was analyzed using qRT-PCR. **g** Colon tissue from D6 *C.r*-infected *Il22*$^{fl/fl}$ and *Il22*^{Plzf} mice was stained for CXCL5, EpCAM1 and DAPI. Results are representative of two independent experiments (n=3 mice per group). Error bars indicate standard deviation. Student's t test; *p ≤ 0.05, **p ≤ 0.01 and ****p ≤ 0.0001 comparing *C.r*-infected *Il22*$^{fl/fl}$ and *Il22*^{Plzf} cKO mice.

Supplementary Figures

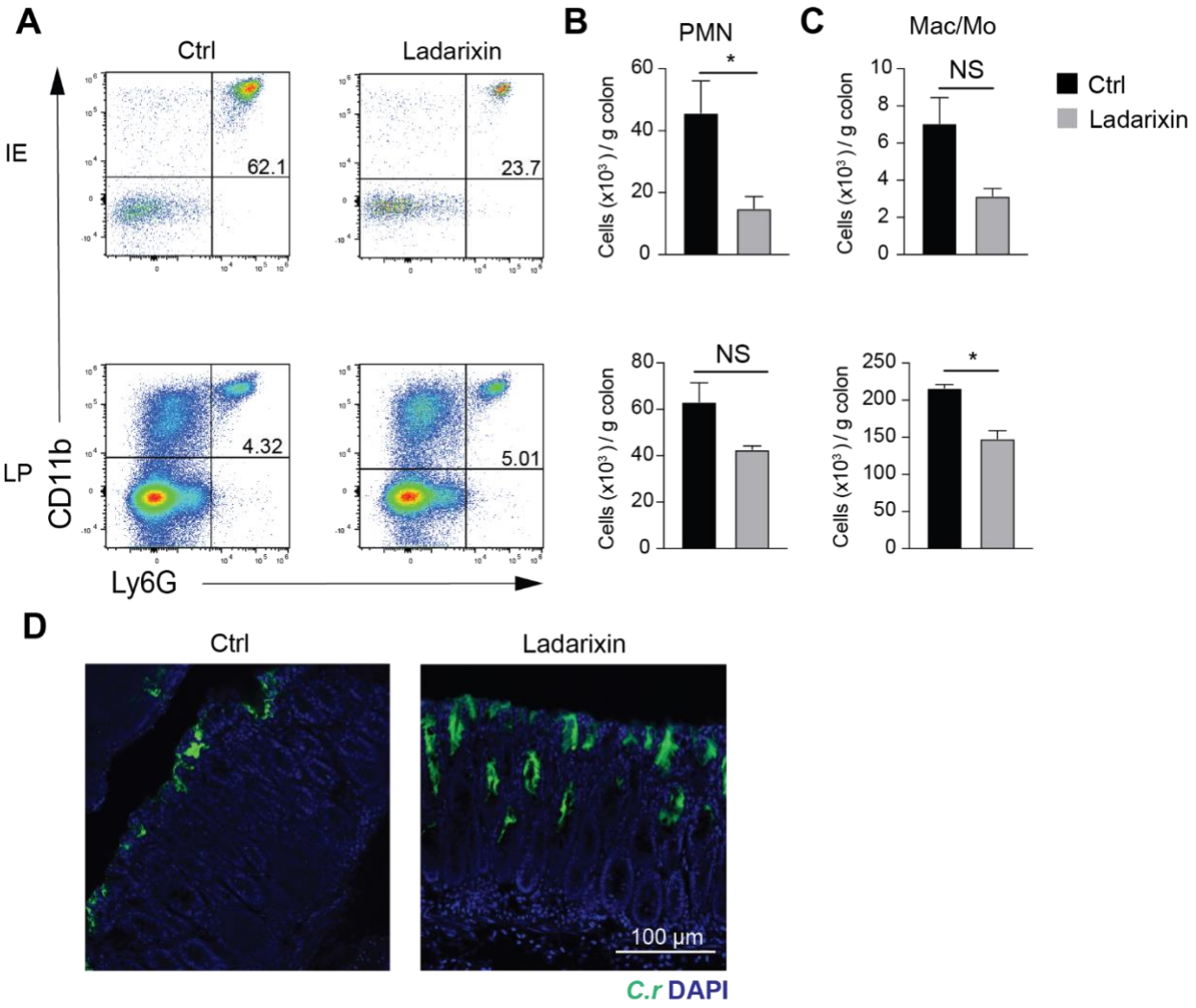

Fig. S1 CXCR2 is required for PMN recruitment and cryptal protection

A-C Colon cells from IE (intraepithelial) and LP (lamina propria) regions were isolated from D7 *C.r*-infected mice treated with either PBS or Ladarixin, stained for Ly6G, CD11b, CD45 and L/D dye and analyzed by flow cytometry. **B** Number of $Ly6G^{+}CD11b^{+}CD45^{+}$ PMNs per gram of colon. **C** Number of $Ly6G^{-}CD11b^{+}CD45^{+}$ Mac/Mono per gram of colon. **D** Colon tissue from D10 GFP *C.r*-infected mice (treated with PBS or Ladarixin) was

harvested and stained for DAPI (blue) (*C.r* is visualized by GFP protein (green)). Results are representative of two independent experiments (n=3 mice per group). Error bars indicate standard deviation. Student's t test: *$p \leq 0.05$ comparing Ctrl and Ladarixin treated mice.

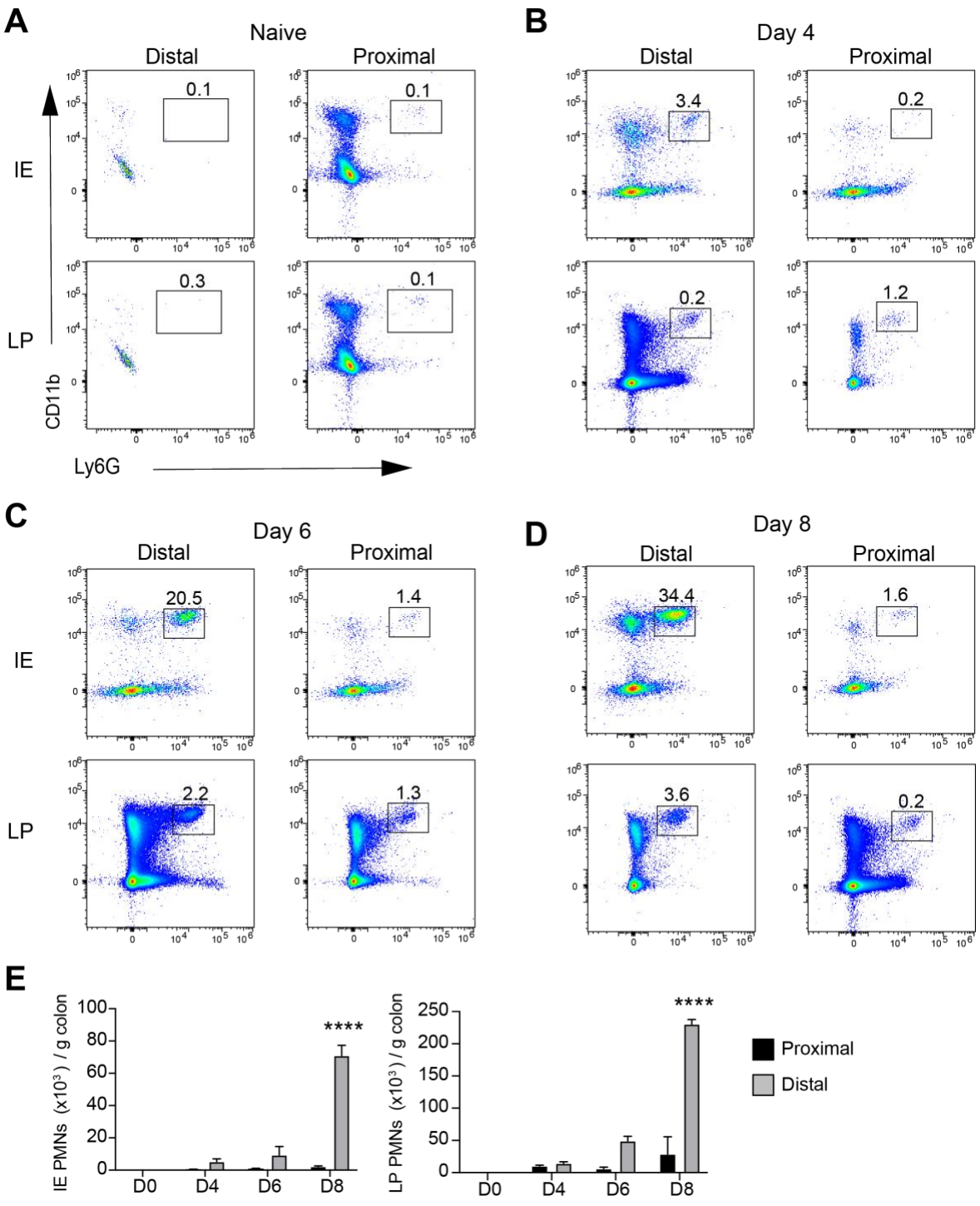

Fig. S2: PMNs are predominantly recruited to the distal colon during *C.r* infection.

Colon tissue was divided into proximal and distal parts and cells from IE (intraepithelial) and LP (lamina propria) regions were isolated from **(A)** naïve and *C.r*-infected BL/6 mice

on **(B)** D4, **(C)** D6 and **(D)** D8 post-infection. Cells were stained for Ly6G, CD11b, CD45 and L/D dye and analyzed by flow cytometry for $Ly6G^{+}CD11b^{+}CD45^{+}$ polymorphonuclear neutrophils (PMNs). **(E)** Numbers represent PMNs per gram of colon in IE and LP. Two independent experiments (n=3 mice per group). Error bars indicate standard deviation. Two-way ANOVA; ****$p \leq 0.0001$ comparing proximal and distal colon.

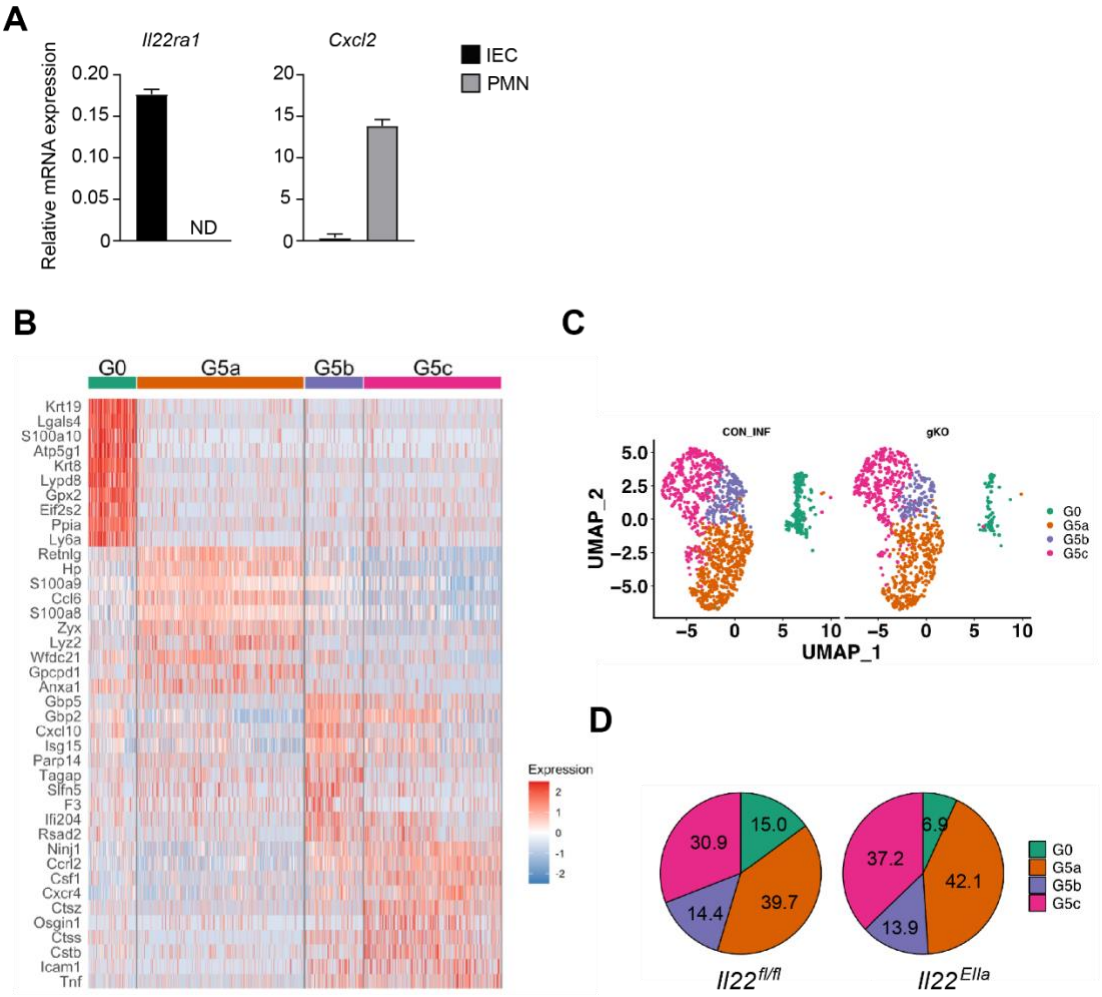

Fig. S3: Bactericidal and inflammatory matured PMNs are recruited into the colonic epithelium and their function is independent of IL-22

(A) Colonic intestinal epithelial cells (IECs) and PMNs were sorted from *C.r*-infected BL/6 mice (n=3). RNA was extracted and analyzed by qRT-PCR for *Il22ra1* and *Cxcl2*. **(B-D)** Single cell (sc)RNA-sequencing was performed on colonic PMNs from D9 *C.r*-infected WT (*Il22*$^{fl/fl}$; n=2) and *Il22* gKO (*Il22*^{Ella}; n=2) mice. **(B)** Heatmap of top differentially expressed genes in eight distinct colonic PMN subsets. **(C)** UMAP of PMN subpopulation

and **(D)** pie charts of PMN percentages of cells within each PMN subpopulation in Il22$^{fl/fl}$ and *Il22*^{Ella} mice, n=2.

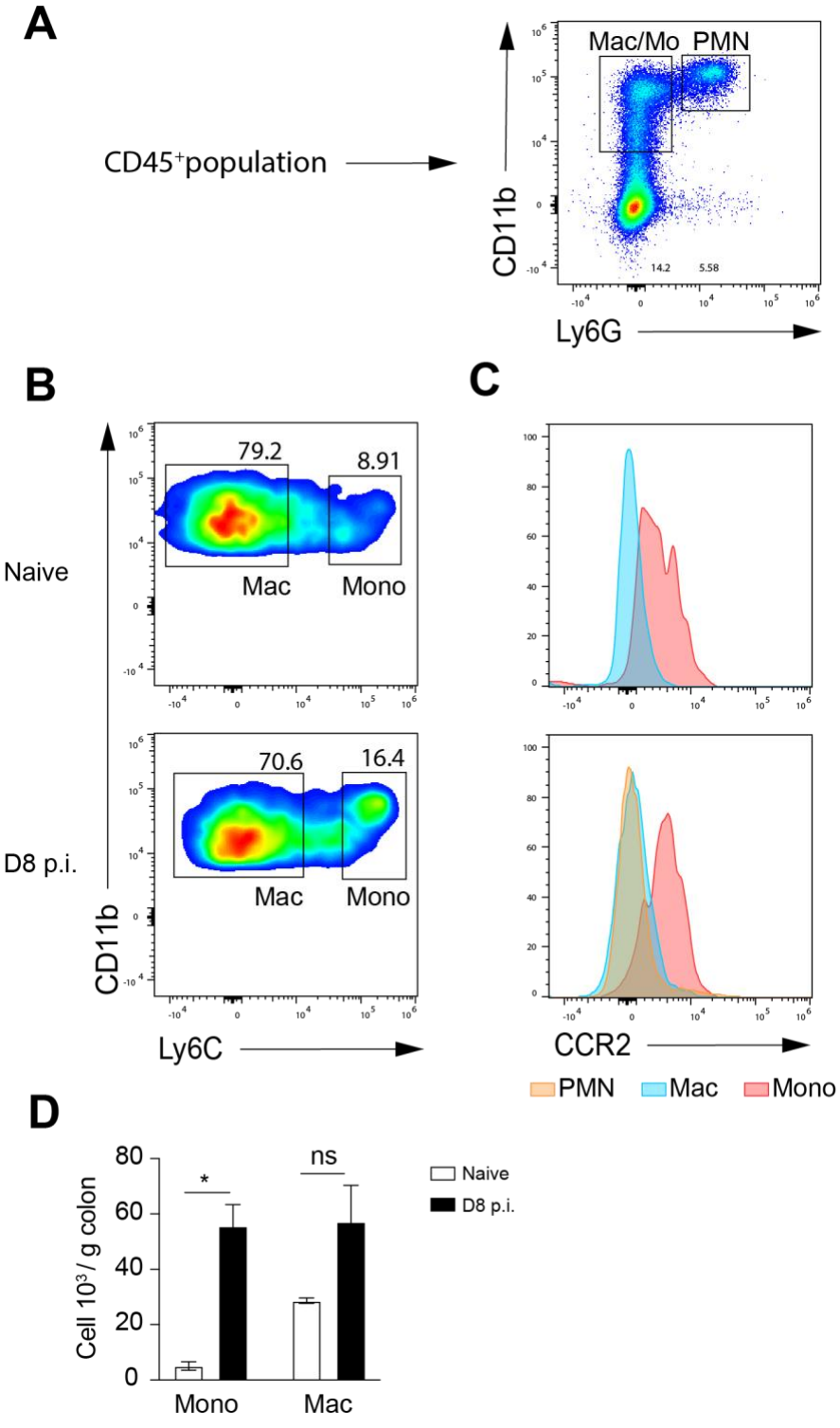

Fig. S4: CCR2^{+} monocytes are recruited to the colon during *C.r* infection

Colon cells from LP (lamina propria) regions were isolated from naïve and D8 *C.r*-infected WT mice, and stained for Ly6G, Ly6C, CD11b, CD45, CCR2 and L/D dye and analyzed by flow cytometry. **(A)** Macrophage and monocytes (Mac/Mo) are defined as live CD45^{+}CD11b^{+}Ly6G^{-} cells **(B)** macrophages (Ly6C^{-}) and monocytes (Ly6C^{+}) percentage and **(D)** numbers analyzed based on Ly6C expression **(C)** CCR2 expression and quantification of MFI on monocytes, macrophages and PMNs were analyzed by flow cytometry. Two independent experiments (n=3 mice per group). Student's Test; *$p \leq 0.05$ comparing PMN and non-PMN cells. NS= not significant.

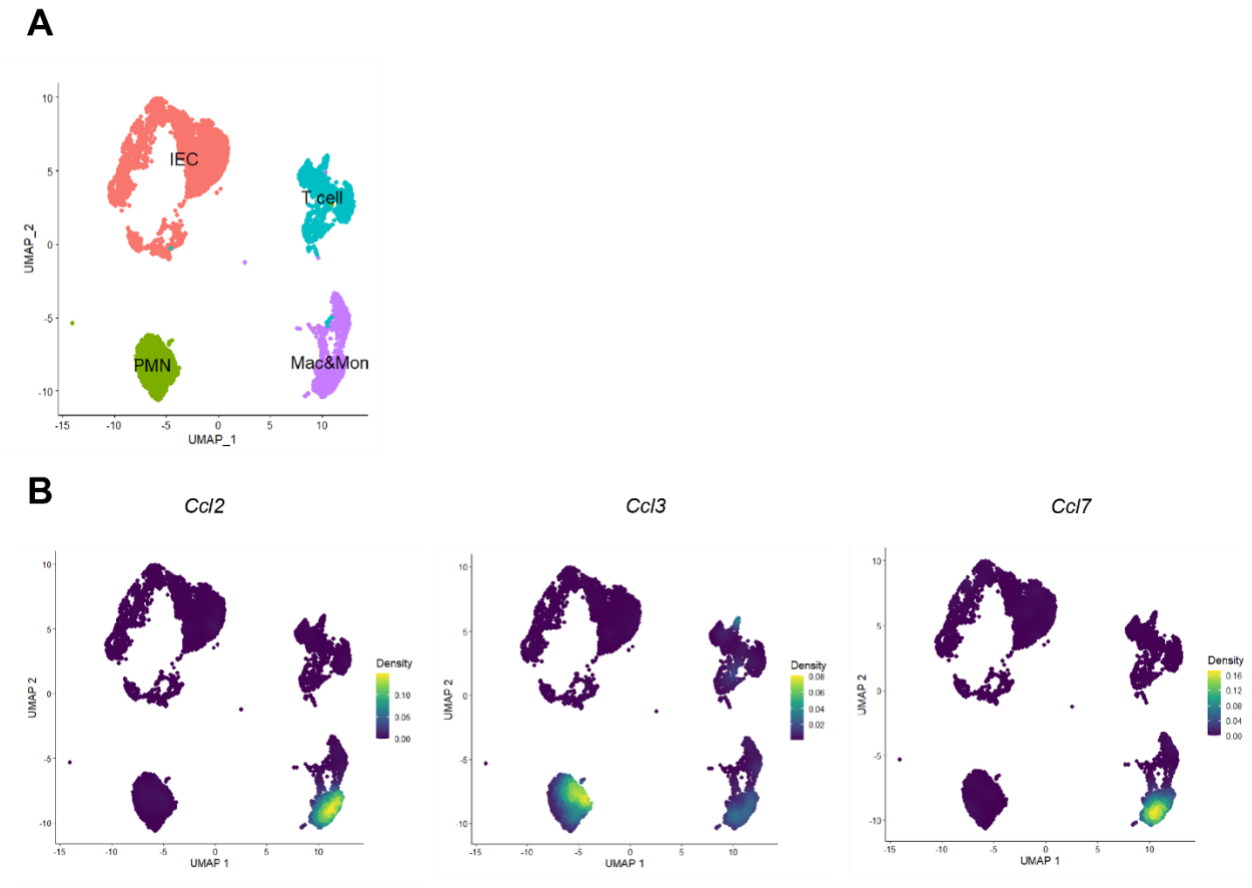

Fig. S5: Macrophages and PMNs express monocyte recruiting chemokine during C.r infection

Cells from distal colonic epithelium were isolated from D8 *C.r*-infected WT (*Il22*$^{fl/fl}$; n=2) and analyzed by scRNA-Seq **(A)** cell population from epithelium are defined and **(B)** chemokine expression was analyzed.

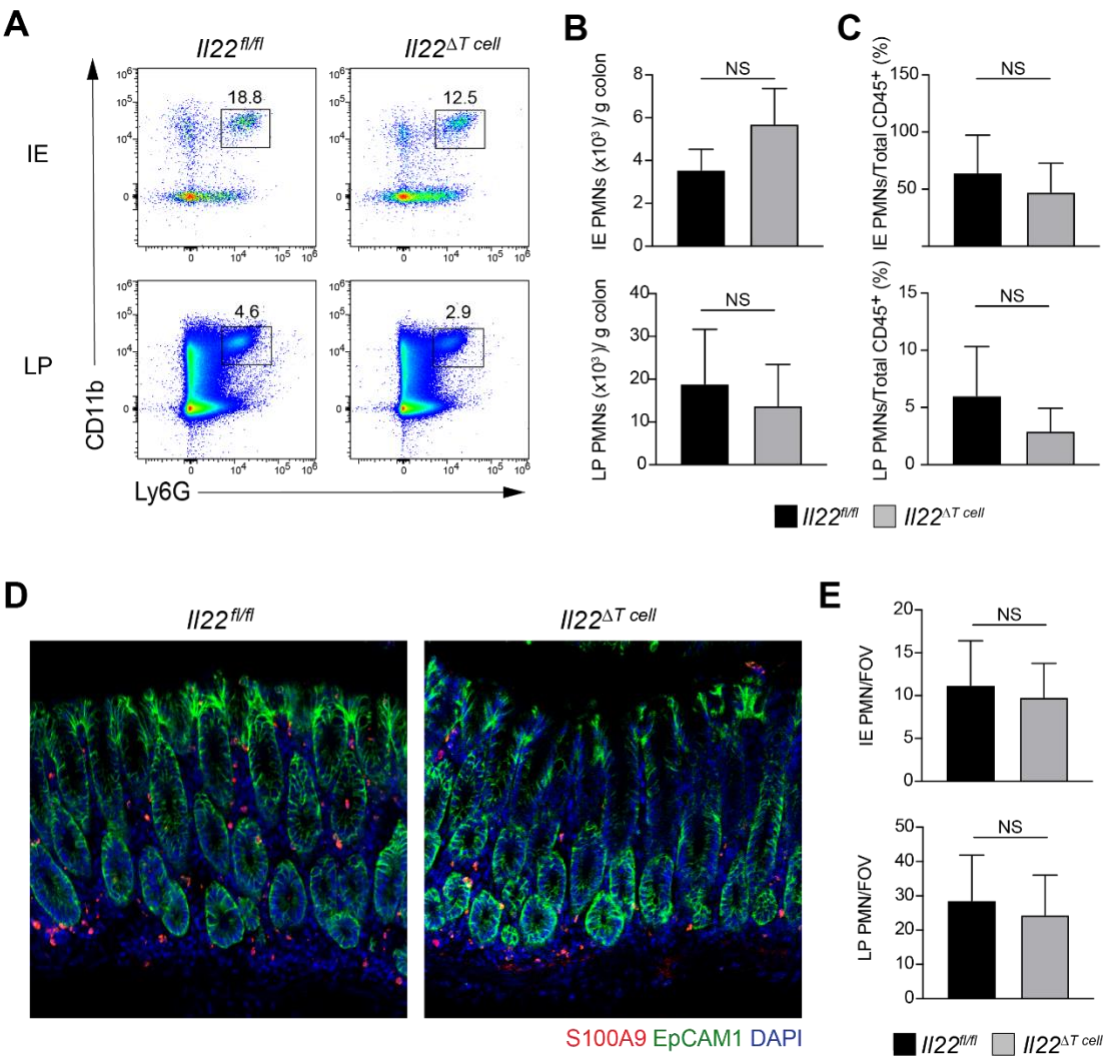

Fig. S6: PMN recruitment to colonic mucosa is independent of T cell-derived IL-22 during the late phase of *C.r* infection.

(A) Colon cells from IE (intraepithelial) and LP (lamina propria) regions were isolated from D8 *C.r*-infected *Il22*$^{fl/fl}$ (Control; black) and T cell-specific IL-22 cKO (*Il22*$^{\Delta Tcell}$; grey) mice, and stained for Ly6G, CD11b, CD45 and L/D dye and analyzed by flow cytometry. **(B)** Number of Ly6G^{+}CD11b^{+}CD45^{+} PMNs per gram of colon. **(C)** Ratio of PMNs per total CD45^{+} cells. **(D)** Colon tissue from D8 *C.r*-infected *Il22*$^{fl/fl}$ and *Il22*$^{\Delta Tcell}$ mice was

harvested and stained for S100A9 (red), EpCAM1 (green) and DAPI (blue). **(E)** Quantitation of S100a9^{+} PMNs in IE and LP regions. Results are representative of two independent experiments (n=3 mice per group). Error bars indicate standard deviation. NS= not significant based on Student's t-test.

REFERENCES

1. Liu, L. *et al.* Global, regional, and national causes of under-5 mortality in 2000–15: an updated systematic analysis with implications for the Sustainable Development Goals. *The Lancet* **388**, 3027–3035 (2016).
2. Hartland, E. L. & Leong, J. M. Enteropathogenic and enterohemorrhagic E. coli: ecology, pathogenesis, and evolution. *Front. Cell. Infect. Microbiol.* **3**, 15 (2013).
3. Silberger, D. J., Zindl, C. L. & Weaver, C. T. Citrobacter rodentium: a model enteropathogen for understanding the interplay of innate and adaptive components of type 3 immunity. *Mucosal Immunol.* **10**, 1108–1117 (2017).
4. Collins, J. W. *et al.* Citrobacter rodentium: infection, inflammation and the microbiota. *Nat. Rev. Microbiol.* **12**, 612–623 (2014).
5. Mullineaux-Sanders, C. *et al.* Citrobacter rodentium–host–microbiota interactions: immunity, bioenergetics and metabolism. *Nat. Rev. Microbiol.* **17**, 701–715 (2019).
6. Deng, W., Li, Y., Vallance, B. A. & Finlay, B. B. Locus of Enterocyte Effacement from Citrobacter rodentium: Sequence Analysis and Evidence for Horizontal Transfer among Attaching and Effacing Pathogens. *Infect. Immun.* **69**, 6323–6335 (2001).
7. Ghaem-Maghami, M. *et al.* Intimin-specific immune responses prevent bacterial colonization by the attaching-effacing pathogen Citrobacter rodentium. *Infect. Immun.* **69**, 5597–5605 (2001).
8. Frontiers | Type Three Secretion System in Attaching and Effacing Pathogens | Cellular and Infection Microbiology. https://www.frontiersin.org/articles/10.3389/fcimb.2016.00129/full.
9. Berger, C. N. *et al.* The Citrobacter rodentium type III secretion system effector EspO affects mucosal damage repair and antimicrobial responses. *PLoS Pathog.* **14**, e1007406 (2018).
10. Raczynski, A. R. *et al.* Enteric Infection with Citrobacter rodentium Induces Coagulative Liver Necrosis and Hepatic Inflammation Prior to Peak Infection and Colonic Disease. *PLoS ONE* **7**, e33099 (2012).
11. Zheng, Y. *et al.* Interleukin-22 mediates early host defense against attaching and effacing bacterial pathogens. *Nat. Med.* **14**, 282–289 (2008).
12. Basu, R. *et al.* Th22 cells are an important source of IL-22 for host protection against enteropathogenic bacteria. *Immunity* **37**, 1061–1075 (2012).
13. Zindl, C. L. *et al.* A nonredundant role for T cell-derived interleukin 22 in antibacterial defense of colonic crypts. *Immunity* **55**, 494-511.e11 (2022).

14. Burn, G. L., Foti, A., Marsman, G., Patel, D. F. & Zychlinsky, A. The Neutrophil. *Immunity* **54**, 1377–1391 (2021).

15. Sumagin, R., Robin, A. Z., Nusrat, A. & Parkos, C. A. Transmigrated neutrophils in the intestinal lumen engage ICAM-1 to regulate the epithelial barrier and neutrophil recruitment. *Mucosal Immunol.* **7**, 905–915 (2014).

16. Gierlikowska, B., Stachura, A., Gierlikowski, W. & Demkow, U. Phagocytosis, Degranulation and Extracellular Traps Release by Neutrophils—The Current Knowledge, Pharmacological Modulation and Future Prospects. *Front. Pharmacol.* **12**, (2021).

17. Spehlmann, M. E. *et al.* CXCR2-dependent mucosal neutrophil influx protects against colitis-associated diarrhea caused by an attaching/effacing lesion-forming bacterial pathogen. *J. Immunol. Baltim. Md 1950* **183**, 3332–3343 (2009).

18. Zarbock, A. & Stadtmann, A. CXCR2: From Bench to Bedside. *Front. Immunol.* **3**, (2012).

19. Flannigan, K. L. *et al.* IL-17A-mediated neutrophil recruitment limits expansion of segmented filamentous bacteria. *Mucosal Immunol.* **10**, 673–684 (2017).

20. Ohtsuka, Y., Lee, J., Stamm, D. S. & Sanderson, I. R. MIP-2 secreted by epithelial cells increases neutrophil and lymphocyte recruitment in the mouse intestine. *Gut* **49**, 526–533 (2001).

21. Shieh, J.-M., Tsai, Y.-J., Tsou, C.-J. & Wu, W.-B. CXCL1 Regulation in Human Pulmonary Epithelial Cells by Tumor Necrosis Factor. *Cell. Physiol. Biochem.* **34**, 1373–1384 (2014).

22. Girbl, T. *et al.* Distinct Compartmentalization of the Chemokines CXCL1 and CXCL2 and the Atypical Receptor ACKR1 Determine Discrete Stages of Neutrophil Diapedesis. *Immunity* **49**, 1062-1076.e6 (2018).

23. Sun, D. & Shi, M. Neutrophil swarming toward Cryptococcus neoformans is mediated by complement and leukotriene B4. *Biochem. Biophys. Res. Commun.* **477**, 945–951 (2016).

24. Lentini, G. *et al.* Neutrophils Enhance Their Own Influx to Sites of Bacterial Infection via Endosomal TLR-Dependent Cxcl2 Production. *J. Immunol.* **204**, 660–670 (2020).

25. In vivo imaging reveals unique neutrophil transendothelial migration patterns in inflamed intestines | Mucosal Immunology. https://www.nature.com/articles/s41385-018-0069-5.

26. Ahlfors, H. *et al.* IL-22 Fate Reporter Reveals Origin and Control of IL-22 Production in Homeostasis and Infection. *J. Immunol.* **193**, 4602–4613 (2014).

27. Keir, M. E., Yi, T., Lu, T. T. & Ghilardi, N. The role of IL-22 in intestinal health and disease. *J. Exp. Med.* **217**, e20192195 (2020).

28. Bando, J. K. & Colonna, M. Innate lymphoid cell function in the context of adaptive immunity. *Nat. Immunol.* **17**, 783–789 (2016).

29. Sugimoto, K. *et al.* IL-22 ameliorates intestinal inflammation in a mouse model of ulcerative colitis. *J. Clin. Invest.* JCI33194 (2008) doi:10.1172/JCI33194.

30. Pham, T. A. N. *et al.* Epithelial IL-22RA1-Mediated Fucosylation Promotes Intestinal Colonization Resistance to an Opportunistic Pathogen. *Cell Host Microbe* **16**, 504–516 (2014).

31. Lindemans, C. A. *et al.* Interleukin-22 promotes intestinal-stem-cell-mediated epithelial regeneration. *Nature* **528**, 560–564 (2015).

32. Bevins, C. L. & Salzman, N. H. Paneth cells, antimicrobial peptides and maintenance of intestinal homeostasis. *Nat. Rev. Microbiol.* **9**, 356–368 (2011).

33. Wiles, S., Pickard, K. M., Peng, K., MacDonald, T. T. & Frankel, G. In vivo bioluminescence imaging of the murine pathogen Citrobacter rodentium. *Infect. Immun.* **74**, 5391–5396 (2006).

34. Mattos, M. S. *et al.* CXCR1 and CXCR2 Inhibition by Ladarixin Improves Neutrophil-Dependent Airway Inflammation in Mice. *Front. Immunol.* **11**, (2020).

35. Szabady, R. & McCormick, B. Control of Neutrophil Inflammation at Mucosal Surfaces by Secreted Epithelial Products. *Front. Immunol.* **4**, (2013).

36. Lee, E., Schiller, L. R. & Fordtran, J. S. Quantification of colonic lamina propria cells by means of a morphometric point-counting method. *Gastroenterology* **94**, 409–418 (1988).

37. Yang, L. & Pei, Z. Bacteria, inflammation, and colon cancer. *World J. Gastroenterol. WJG* **12**, 6741–6746 (2006).

38. Crepin, V. F. *et al.* Tir Triggers Expression of CXCL1 in Enterocytes and Neutrophil Recruitment during Citrobacter rodentium Infection. *Infect. Immun.* **83**, 3342–3354 (2015).

39. Kienle, K. *et al.* Neutrophils self-limit swarming to contain bacterial growth in vivo. *Science* **372**, eabe7729 (2021).

40. Stacey, M. A. *et al.* Neutrophils Recruited by IL-22 in Peripheral Tissues Function as TRAIL-Dependent Antiviral Effectors against MCMV. *Cell Host Microbe* **15**, 471–483 (2014).

41. Xie, X. *et al.* Single-cell transcriptome profiling reveals neutrophil heterogeneity in homeostasis and infection. *Nat. Immunol.* **21**, 1119–1133 (2020).

42. Parks, O. B., Pociask, D. A., Hodzic, Z., Kolls, J. K. & Good, M. Interleukin-22 Signaling in the Regulation of Intestinal Health and Disease. *Front. Cell Dev. Biol.* **3**, (2016).

43. Kamada, N. *et al.* Humoral Immunity in the Gut Selectively Targets Phenotypically Virulent Attaching-and-Effacing Bacteria for Intraluminal Elimination. *Cell Host Microbe* **17**, 617–627 (2015).

44. Ellison, R. T. & Giehl, T. J. Killing of gram-negative bacteria by lactoferrin and lysozyme. *J. Clin. Invest.* **88**, 1080–1091 (1991).

45. Masschalck, B., Van Houdt, R., Van Haver, E. G. R. & Michiels, C. W. Inactivation of Gram-Negative Bacteria by Lysozyme, Denatured Lysozyme, and Lysozyme-Derived Peptides under High Hydrostatic Pressure. *Appl. Environ. Microbiol.* **67**, 339–344 (2001).
46. Corbin, B. D. *et al.* Metal Chelation and Inhibition of Bacterial Growth in Tissue Abscesses. *Science* **319**, 962–965 (2008).
47. Saha, P. *et al.* PAD4-dependent NETs generation are indispensable for intestinal clearance of Citrobacter rodentium. *Mucosal Immunol.* **12**, 761–771 (2019).
48. Mei, J. *et al.* CXCL5 Regulates Chemokine Scavenging and Pulmonary Host Defense to Bacterial Infection. *Immunity* **33**, 106–117 (2010).

THE ROLE OF IL-22 MEDIATED ANTIMICROBIAL PEPTIDES AND PMN EFFECTOR MOLECULES DURING *CITROBACTER RODENTIUM* INFECTION

by

BAIYI CAI, JEFFREY R. SINGER, DANIEL J. SILBERGER, WOLFGANG NACKEN, CARLENE L. ZINDL AND CASEY T. WEAVER

Introduction

Intestinal mucosal surfaces are occasionally subject to pathogen challenge by organisms such as enteropathogenic *E. coli* (EPEC) and enterohemorrhagic *E. coli* (EHEC)[1]. In order to efficiently defend the colon from bacterial invasion, coordination between the intestinal epithelium and the host immune system is required to mount an effective antimicrobial response to limit bacterial expansion, and eventually eliminate invading pathogens[2,3].

Citrobacter rodentium (*C.r*) is a mouse pathogen that models EPEC and EHEC, which are common human pathogens that causes around 300,000 annual fatalities worldwide[4]. Intestinal epithelial cells (IECs) are the first line of defense against *C.r* and produce antimicrobial-molecules, including antimicrobial peptides (AMPs)[5,6] and iNOS[7] to inhibit bacterial expansion. IL-22 is indispensable for the host protection against *C.r* and mice with IL-22 deficiency succumb to the infection and have *C.r* invasion deep into the colonic crypt, suggesting a deficit in immune protection in the crypt[8,9]. IL-22 has been extensively reported to induce AMP and iNOS production from IECs[10,11], yet the specific role of these IEC derived antimicrobial-molecules in host protection, and specifically crypt protection, remains unknown.

AMPs are produced by IECs and also by polymorphonuclear neutrophils (PMNs) during infection[12], including the regenerating islet-derived protein (Reg) family members Reg3β and Reg3γ, β-defensins (S100A8 and S100A9) and Lipocalin-2 (Lcn2)[12]. AMPs are bactericidal small peptides that are regarded as one of the oldest mechanisms of immune defense found in organisms from protozoa to mammals[13]. AMPs can directly kill bacteria or limit their growth through different pathways: they can directly bind to the cell membrane and destroy its structure to kill targets; they can also disrupt metabolism of

target cells, by inhibiting protein biosynthesis and chelating essential metals[13,14]. IBD patients often have elevated Lcn2 and calprotectin level (heterodimer formed by S100A8 and S100A9) in fecal samples is used as a IBD activity marker[15,16], highlighting the relevance of AMPs during intestinal inflammation.

Reg3β and Reg3γ binds to lipid A and peptidoglycan respectively to mediate bacterial killing[5,17,18]. Lcn2 binds with bacterial siderophores that chelates Fe^{3+}, and S100A9 can bind with S100A8 to form calprotectin to chelate Mn^{2+} and Zn^{2+}[19,20]. These metal elements bear important roles in pathogen survival: Mn and Fe are critical elements in superoxide dismutase which is often used by pathogens to resist oxidative stress, in order to promote self-survival[14]. Meanwhile, Zn^{2+} can serve both a catalytic and structural role within proteins and is required for bacteria growth[14]. Studies have shown that IL-22 promotes AMP Lcn2 and S100a9 production from epithelial cells in various models[21–23]. AMPs are often assumed as the downstream effector molecules that support the protective function of IL-22[8,10], yet few studies have investigated the specific role of AMPs mediate host protection against *C.r* infection, and whether AMPs from different cellular sources (IEC versus PMN) are redundant or if they have unique roles during infection.

Intestinal epithelial cells can also produce inducible nitric oxide synthase (iNOS or NOS2) in response to infection[24]. iNOS catalyzes the production of several reactive nitrogen intermediates including nitrite, NO and S-nitrosoglutathione, which is bactericidal[24]. Mice with iNOS deficiency show elevated bacterial load[7], suggesting that iNOS may be protective against *C.r*, but it's unclear whether iNOS contribute to colonic crypt protection.

PMNs are indispensable for host protection against *C.r*. Mice lacking the PMN chemokine receptor CXCR2 fail to recruit PMNs into the colon and suffer from delayed *C.r* clearance,

exacerbated diarrhea, and crypt invasion by *C.r*[25], suggesting that PMNs can both control the bacterial load and prevent *C.r* from spreading to the epithelial crypts. PMNs utilize three distinctive major killing mechanisms: degranulation, phagocytosis, and neutrophil extracellular traps (NETs) formation[26]. Reactive oxygen species (ROS) production is required for all three PMN killing mechanisms as ROS are released by granules to the surrounding area, killing engulfed targets during phagocytosis, and causing chromatin decondensation to form NET[27]. NOX2 is the catalytic, membrane-bound subunit of NADPH oxidase that catalyzes the ROS production pathway[28]. Neutrophil elastase (NE) is the other critical molecule involved in PMN-mediated killing[29]. NE can digest targets within PMNs during phagocytosis and binds to neutrophil NETs to destroy trapped targets[29]. It is unclear if there is a unique role of these individual bactericidal molecules in bacterial killing versus crypt protection.

In this study, we specified the regional and cellular distribution of AMPs in the colon during *C.r* infection: we found that Reg3 family proteins are expressed in the proximal colon by IECs, while S100 series proteins are produced in the distal colon by PMNs and IECs. Mice with S100A9 and LCN2 deficiency have delayed clearance and higher early bacterial loads respectively. We also found that NOX2 mediated ROS production is required for host protection against *C.r*, as NOX2 deficient mice succumb to *C.r* infection. Conversely, NE was required for early control of bacterial load and upper crypt protection. These data suggest that AMP production and PMN recruitment work synergistically to provide host defense against *C.r* infection.

Results

Regional distribution of AMPs during *C.r* infection in the colon

C.r colonizes the distal colon during infection and induces AMP production[30]. To assess the regional distribution and dynamics of *C.r* induced *Reg3b, Reg3g, S100a8,* and *S100a9* during infection, we infected C57BL/6 mice and divided collected colon tissue into proximal, middle, and distal regions and compared AMP expression between these regions in naïve and *C.r* infected mice. In naïve mice, we found low levels of *Reg3b* and *Reg3g* expression in the proximal colon, but no expression in the middle or distal colon (Fig. 1a, left panels). There was no detectable *S100a8* or *S100a9* expression in any location in naïve mice (Fig. 1b, left 2 panels). At day 8 post infection (d8 p.i), we observed a substantial increase of *Reg3b* and *Reg3g* expression in the proximal colon (Fig. 1a, right 2 panels), in contrast to *S100a8* and *S100a9,* which were upregulated in the middle and distal colon, also believed to be the regions of *C.r* colonization. (Fig. 1b, right 2 panels).

C.r attachments are generally restricted to surface epithelium but not cryptal epithelium during infection[4,31]. We next compared the expression of Reg3b/g and S100a8/9 between surface and crypt epithelial cells at d8 of *C.r* infection by laser microdissection of distal colon tissue sections (Fig. 1c, d). Both Reg3b/g and S100a8/9 were found to be expressed by surface epithelial cells (Fig. 1e. f). Reg3b/g are expressed by crypt epithelial cells at a significantly lower level than surface epithelial cells, and S100A8/9 was almost undetectable in crypt epithelial cells (Fig. 1e). These data show that Reg3b/g molecules are mostly produced by proximal colon, while S100A8/9 are mostly made by cells from the distal colon. Surface epithelial cells are the major source of epithelial derived AMPs.

PMNs are the major source of AMP during *C.r* infection

Both IECs and PMNs are sources of AMP during infection[12]. Next, we investigated the cellular source of AMPs during *C.r* infection. We isolated cells from the distal colon of

day 8 *C.r* infected mice by FACS and analyzed AMP expression. We found *Reg3b* expression in IECs ($EpCAM1^+$, $CD45^-$) and non PMN immune cells, including eosinophils ($CD45^+$, $CD11b^+$, Siglec F^+) and γδT ($CD45^+$, $TCR\gamma\delta^+$) cells, despite its low expression in the distal colon (Fig. 1a). *S100a8* and *Lcn2* were produced almost exclusively by PMNs ($CD45^+$, $CD11b^+$, $Ly6G^+$). (Fig. 2a) Immunofluorescence staining shows that both S100A8 and Lcn2 producing cells have a typical PMN polymorphonuclear structure and are found in the lamina propria region of the colon, suggesting they are PMNs. Surface IECs appeared to have low levels of S100A8 expression. (Fig. 2b) We further validated the cellular expression of S100A8 by performing *in-situ* hybridization on colon tissue from d8 post *C.r* infected mice. Most *S100a8* expressing cells co-expressed *Mpo*, a classic PMN marker (Fig. 2c). Collectively, these data show that PMNs are the major source of S100A8 and Lcn2 during *C.r* infection, while IECs produced more Reg3b.

Lipocalin 2 limits bacterial load at early phase of *C.r* infection

Lcn2 limits bacterial growth by sequestering iron-containing siderophores of the bacteria[20], and is thought to be part of IL-22 mediated host immunity[21]. To examine the role of Lcn2 during *C.r* infection, we infected both WT and Lcn2 deficient (Lcn2 KO) mice with a luminescent strain of *C.r* (ICC180) and quantified the bacterial load through real time imaging from live mice. Compared with controls, mice with Lcn2 deficiency have notably higher *C.r* load at d3 post infection (Fig. 3a, b), suggesting a defect in limiting early *C.r* expansion. Both groups were able to clear the infection after 3 weeks with no fatalities (Fig. 3c). Next, we assessed the role of Lcn2 in crypt protection against *C.r* by infecting both WT and Lcn2 KO mice with *C.r* GFP to visualize bacterial distribution at d10 p.i by immunofluorescence staining of distal colon sections. We observed that attachment of *C.r*

is located at the epithelial luminal surface in both WT and Lcn2 KO animals and the distribution pattern is comparable between the two strains (Fig 3d). Together, these data show that Lcn2 contributes to early control of *C.r* growth but is dispensable for crypt protection at later stages of infection.

S100A9 promotes *C.r* clearance during late infection

S100A9 limits bacterial growth by sequestering zinc, and is thought to be another part of the IL-22 mediated host immune response[21]. To specify the role of S100A9 during *C.r* infection, we infected both WT and S100A9 deficient mice with a luminescent strain of *C.r* (ICC180) and quantified the bacteria through real time imaging from live mice. S100A9 KO mice have delayed clearance and an elongated peak of *C.r* colonization (d10-d17) compared with WT mice (d6) (Fig. 4a, b). S100A9 mice appear to be unable to completely clear the infection, showing a very small but persistent *C.r* presence in the colon up to d40 post infection (data not shown), although this is not associated with infection related fatalities (Fig. 4c). These data collectively show that S100A9 is required for bacterial clearance during later phases of *C.r* infection.

Neutrophil elastase (NE) and host ROS production is required for immunity against *C.r*

PMNs utilize NE to eliminate engulfed or NET trapped targets[32,33]. NOX2 mediated ROS production is another important aspect of PMN's bactericidal function[34]. To specify the role of NE and NOX2 in PMN mediated antibacterial activity, we infected WT mice, ELANE KO (neutrophil elastase knockout) mice and NOX2 KO mice with a luminescent *C.r* strain and monitored the bacterial load during *C.r* infection. We found ELANE KO

mice have significant higher *C.r* load at very early stages of infection (d3 p.i) compared with WT mice (Fig. 5a and b). In contrast, NOX2 KO mice were equivalent to WT controls early in infection but displayed a higher *C.r* load during laterrs stage of infection (d13 p.i)(Fig. 5c). Notably, a portion NOX2 KO mice succumbed to the infection, while WT and ELANE mice survived (Fig. 5d). Next, we tested the role NE and NOX2 in colonic crypt protection. ELANE KO mice, NOX2 KO mice and WT mice were infected by *C.r* and bacterial attachment was analyzed at day 10 p.i. by immunofluorescence staining. We found no significant difference in the distribution of *C.r* attachment between WT and NOX2 KO mice, with both displaying C.r staining at the luminal surface epithelial cells (Fig. 5e). In marked contrast, *C.r* invaded into the upper crypt regions of the colon in ELANE KO mice (Fig. 5e). To summarize, NE is required to limit early *C.r* load and for crypt protection against *C.r* expansion. NOX2 mediated ROS protection contributes to later *C.r* expansion and protects the host from fatality caused by *C.r* infection.

iNOS production limits bacterial load during early *C.r* infection

iNOS can be induced by IL-22 and drives ROS production at the epithelium to kill bacteria[11,24]. To test whether iNOS contributes to host protection during *C.r* infection, we infected WT and NOS2 (alias for iNOS) KO mice with a luminescent strain of *C.r* and monitored bacterial load. We found that NOS2 mice have a significantly increased *C.r* load at d6 of infection compared with WT mice (Fig. 6a and b). This was associated with a trend towards increased weight loss in NOS2 KO mice, although this was not significant (Fig. 6c) and no fatalities were observed (Fig. 6d). We next tested if iNOS protect epithelial crypts from *C.r* invasion by infecting NOS2 KO mice and mice treated with an iNOS chemical inhibitor L-N$^{\omega}$-Methylarginine (L-NMA), along with WT mice, and assessing

C.r attachment at d10 p.i. All three groups of mice showed *C.r* attachment to the surface epithelium but *C.r* was not observed deeper into colonic crypts. In summary, these data suggest that iNOS can limit early bacterial expansion but does not significantly contribute to *C.r* clearance, or crypt protection from *C.r* expansion.

Discussion

In this study we have defined the role of several antimicrobial response molecules during *C.r* infection. IL-22 induced AMP production, PMN response and iNOS have been speculated to be protective against *C.r* infection, but it is unknown how these molecules modulate *C.r* infection. Here, we demonstrated during early infection (d3 p.i.), PMN and IEC- derived Lcn2, PMN derived NE, and IE drived iNOS production all limit bacterial expansion. S100A8 and ROS production restrain the bacterial load during late infection and ROS specifically protects the host from *C.r* mediated fatality. These results provide insight details of the mechanism of antimicrobial function during *C.r* infection.

Reg3b and Reg3g promote antimicrobial responses against various pathogens including *C.r*. Interestingly, we found that Reg3b and Reg3g are expressed at a much higher levels in the proximal colon, where *C.r* does not colonize, compared to the distal colon where *C.r* is found. Induction of Reg proteins by *C.r* is in agreeance with a previous study showing *C.r* upregulates Reg3b/g expression from IECs, which depends on *C.r* type III secretion system effector EspO[35]. Reg3b and Reg3g target Gram-negative and positive pathogen respectively[5]. Reg3b has been shown to limit *Salmonella* infection in the colon, whilst Reg3g can promote intestinal mucus production and prevent IECs from directly contacting with potential pathogens[36]. Reg3g has been shown to have play a limited role in *C.r* colonization. However, the direct role of Reg3b on *C.r* remains largely unknown, and the

mechanisms by which Reg3b and Reg3g are produced at sites physically distant from bacterial infection, and whether proximal production of Reg3b/g can remotely affect distal *C.r* infection required further investigation.

We found both Lcn2 and S100A9 contributed to host protection against *C.r*. Both AMPs sequester metals in the colon to form nutritional immunity[14]: *C.r* growth is strongly inhibited when metal elements are removed from media *in vitro* (unpublished data), further validating the essential role of metals in *C.r* metabolism and growth. Colonic pathogens use the host as a major source of metal: *S. aureus* utilizes host hemoglobin as a heme iron source through surface IsDB protein[37]. A recent study revealed that *E.coli* uses injectosome to directly obtain nutrients from host cells[38], potentially including iron. In our study, Lcn2 deficiency only leads to early increase of *C.r* load, suggesting either the bacteria adapted a new, non Lcn2 controlled, pathway to obtain Fe, or the host evolved a compensatory immune response to control *C.r* growth.

Our data showed that defects in neutrophil molecules Nos2, NE and Lcn2 lead to an increased early bacterial load in *C.r* infection, but this did not translate to an increase in mortality and only NE deficiency resulted in increased crypt invasion at later stages of disease. NE is a PMN specific serine protease that can directly kill bacteria or contribute NET formation[39]. PMN NET has been shown to be formed and contribute to host defense during *C.r* infection[33]. This suggest that NE mediated NET may be one of the key components in cryptal protection by trapping and killing *C.r* that can potentially spread to the crypts. These findings suggest that there are multiple mechanisms of bacterial control by neutrophils and defects in any one of these results in an appreciable increase in bacterial

colonization, but ultimately each mechanism can be compensated for to achieve an equivalent level of bacterial control.

Methods

Primers

Gene	Forward primer	Reverse primer
Gapdh	ACCACAGTCCATGCCATCAC	CACCACCCTGTTGCTGTAGCC
S100a8	CCCGTCTTCAAGACATCGTTTG	ATATCCAGGGACCCAGCCCTAG
S100a9	CCCTGACACCCTGAGCAAGAAG	TTTCCCAGAACAAAGGCCATTGAG
Reg3b	ATACCCTCCGCACGCATTAGTT	AGGCCAGTTCTGCATCAAACCA
Reg3g	TCCTTTCTCAGGTGCAAGGTGA	TTGGCAGGCCATATCTGCATCA
Lcn2	GCTACAATGTCACCTCCATC	CCTGGAGCTTGGAACAAAT
Nos2	GACAGCACAGAATGTTCCAG	TGGCCAGATGTTCCTCTATT

Mice

C57BL/6 (WT; JAX 000664), LCN2 KO (JAX 024630), NOS2 KO (JAX 002609), ELANE KO (JAX 006112), and NOX2 KO (JAX 002365) mice were purchased from Jackson Laboratory (JAX). S100A9 KO are provided by Dr. Wolfgang Nacken from the University of Münster. In all experiments, littermates were used as controls and experimental adult animals (8-12 wk old) were co-caged in groups of 2-7 mice. Both sexes were used per experimental group whenever possible. All mouse strains were bred and maintained at UAB in SPF environment in accordance with IACUC guidelines.

Citrobacter rodentium infection

Citrobacter rodentium (*C.r*) strain, DBS100 (ATCC 51459) was used for all kinetics experiments. For whole-body imaging experiments, the bioluminescent *C.r* strain ICC180 (derived from DBS100) was used (Wiles et al., 2006) (generously provided by Dr. Gad Frankel and Siouxsie Wiles, Imperial College London). For some histology staining of *C.r*, a strain of C.r expressing GFP (derived from DBS100) was used[40] (kindly provided by Dr.

Bruce A. Vallance).Animals were imaged for bioluminescence using an IVIS-100 Imaging System (Xenogen). For *C.r* inoculation: A fresh, single colony was grown in 10 ml LB overnight at 37ºC with agitation for 12-14 hrs. Next day, 1 ml of overnight culture was added to 250 ml LB, incubated at 37ºC with agitation for 4-5 hrs and then stopped when OD600 reached 1.0 on ThermoFisher SPECTRONIC™ 200 spectrophotometer. Bacteria was pelleted at 25ºC, 3000 rpm for 15 minutes and then resuspended in 5 ml sterile 1x PBS. Mice were inoculated in a total volume of 100 µl via gastric gavage.

Isolation of Intestinal cells

Intestinal tissues were flushed, opened longitudinally and then cut into strips of 0.5 cm length. Tissue pieces were incubated for 40 min at 37ºC with 1 mM DTT (Sigma) and 2 mM EDTA (Invitrogen) in H5H media (1x HBSS, 5% FBS, 20 mM Hepes, and 2.5 mM 2-b-ME), cells from the DTT/EDTA prep were spun down at 1500 rpm for 10 minutes at 4ºC to collect IECs. For isolation of lamina propria (LP) cells, tissue pieces remaining after the DTT/EDTA step were homogenized by chopping and incubated for 40 min at 37ºC with Collagenase VIII (1 mg/ml; Sigma) and DNase (1 mg/ml; Sigma) in R10 media (1x RPMI 1640, 10% FBS, 1x Pen/Strep, 1x NEAA, 1mM, Sodium pyruvate and 2.5 mM 2-b-ME). LP cells were then purified on a 40%/75% Percoll gradient by centrifugation for 20 min at 25ºC and 600g with no brake.

Colon cells were stained with Fc Block (Clone 2.4G2) and fluorescent-labeled antibodies in FACS buffer (1x PBS, 2% FBS and 2mM EDTA) on ice in 1.5 ml microcentrifuge tubes. Samples were acquired on Attune NxT flow cytometer (Life Technologies) and analyzed with FlowJo software. Cells were sorted on either a BD FACS Aria or Aria II (BD Biosciences).

Immunofluorescence staining

For immunostaining, colon tissues were fixed in in 4% PFA overnight at 4ºC. Tissue was then put through several cold 1x PBS washes including an overnight incubation, and then embedded in O.C.T. (Tissue-Tek) and frozen with 2-methyl butane chilled with liquid nitrogen. Tissue sections were blocked at RT for 30 minutes with 10% mouse serum in 1x PBS and 0.05% Tween-20. Antibodies were diluted in 2% BSA/PBS/Tween-20 and incubated for 30 min at RT.

Real time PCR

cDNA synthesis was performed with iScript reverse transcription (RT) Supermix (Bio-Rad) according to manufacturer's instructions. cDNA amplification was analyzed with SsoAdvanced Universal SYBR Green Supermix (Bio-Rad) in a Biorad CFX qPCR instrument.

Laser microdissection

Unfixed colon tissue was frozen in O.C.T. compound (Tissue-Tek) in liquid nitrogen-cooled 2-methyl butane (Sigma). Ten-micron sections were melted onto PEN-membrane glass slides (Leica) and stained with Cresyl Violet dye (Ambion). Stained epithelial cells (150,000-250,000 mm2 per cap) were captured into microcentrifuge tubes using a Leica LMD6 instrument. RNA was extracted using the miRNeasy Micro RNA isolation kit (Qiagen).

Figures

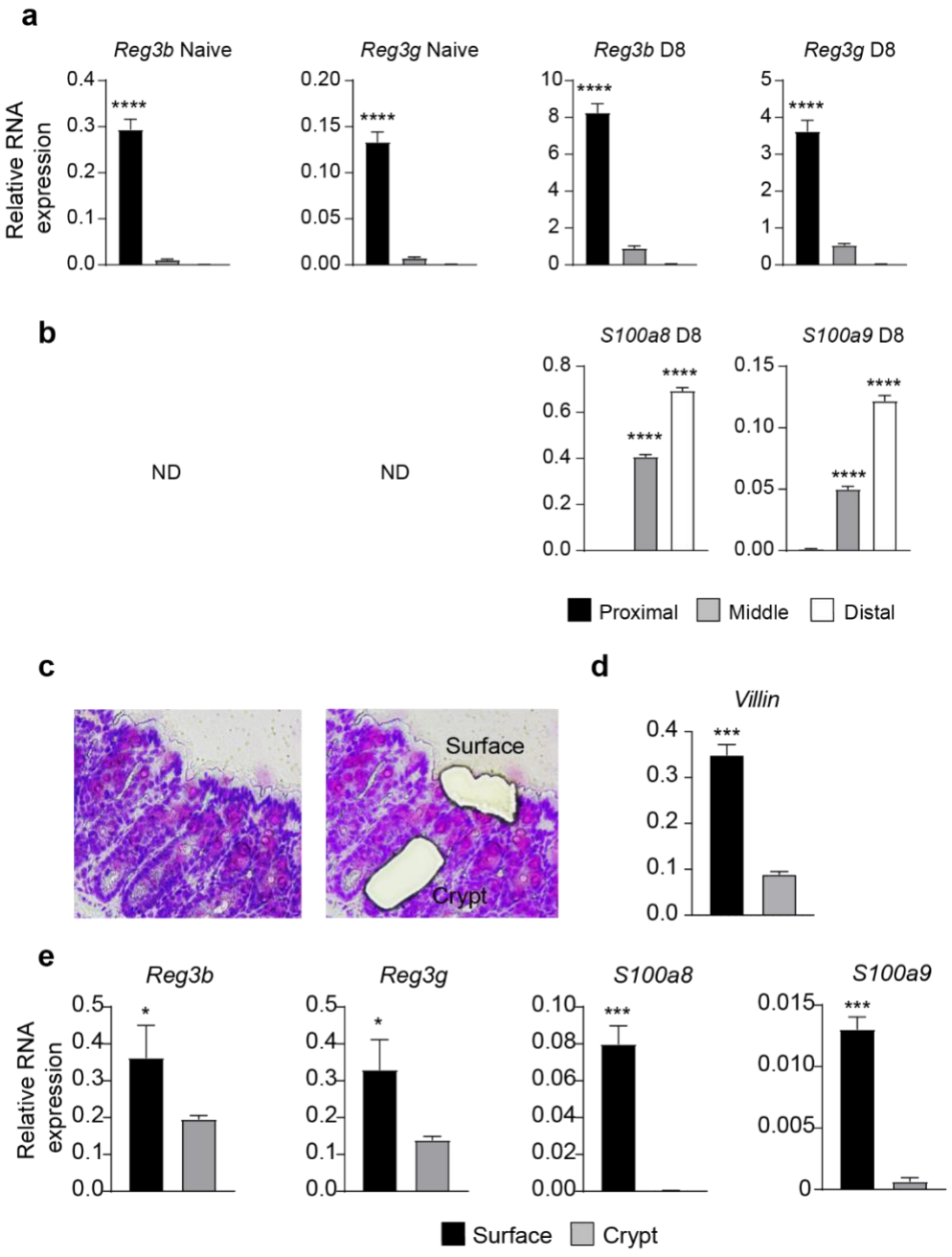

Figure 1. Regional dynamics and distribution of *Reg3b*, *Reg3g*, *S100a8* and *S100a9*

a, b Proximal and distal colons were isolated from naïve and *C.r*-infected mice on day 8 p.i. Colon tissue and relative *Reg3b/g* (**a**) and *S100a8/9* (**b**) mRNA expression normalized

with GAPDH mRNA was analyzed using qRT-PCR. **c, d, e** Distal colon tissue was isolated from day 8 *C.r*-infected mice and surfaced and cryptal epithelial cells were isolated using laser microdissection (**c**). mRNA expression of *Villin* (**d**) and AMPs (**e**) were analyzed using qRT-PCR.

Results are representative of two independent experiments (n=3 mice per time point). Error bars indicate standard deviation. **a, b** Two-way ANOVA analysis; ****p $\leq$ 0.0001 comparing naïve and *C.r*-infected mice. nd= not detected. **d, e** Student's t-test; *p $\leqslant$ 0.05, ***p $\leqslant$ 0.001. n=3, two independent experiment

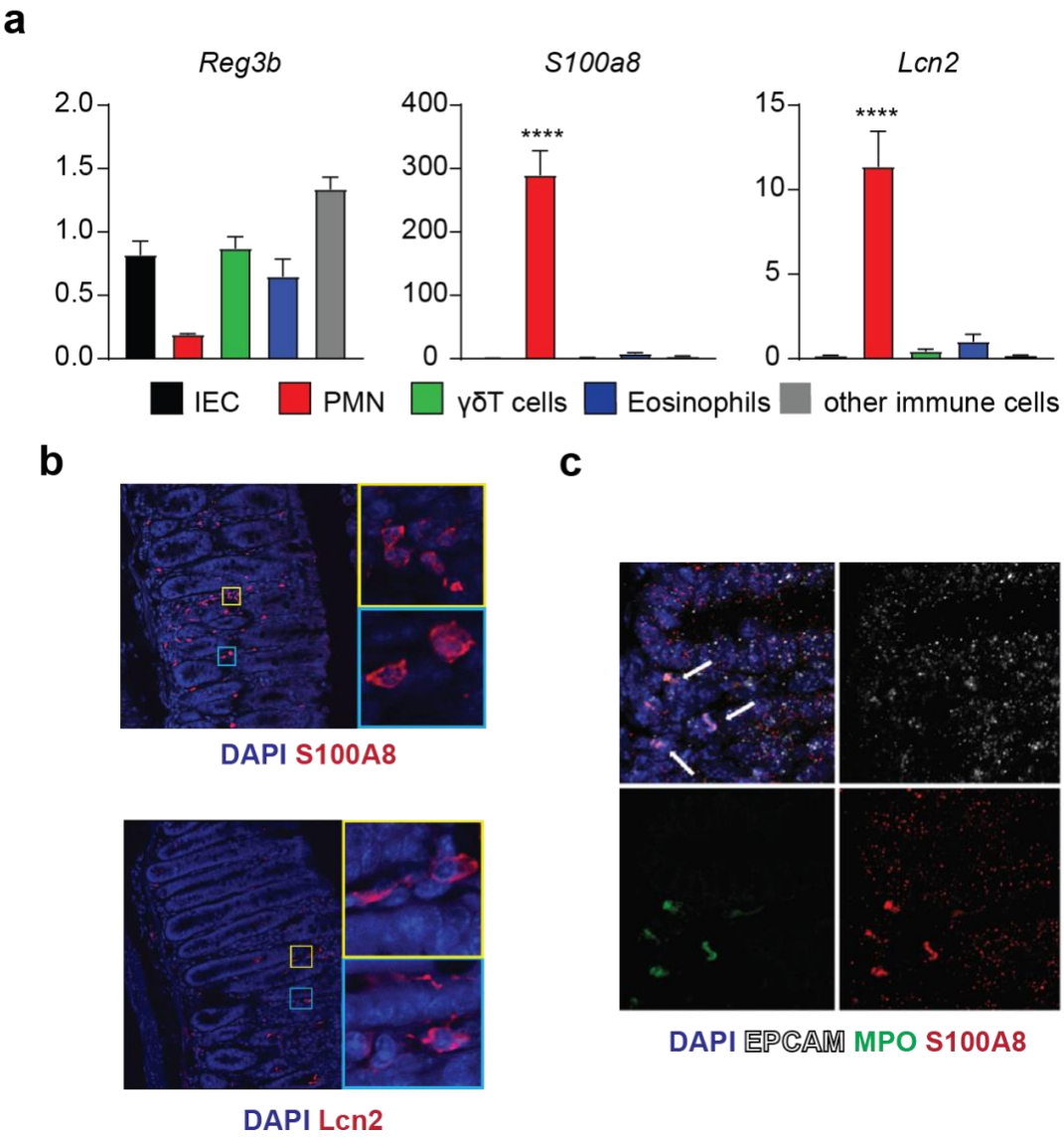

Figure 2. Cellular source of *Reg3b*, *S100a8* and *Lcn2* during *C.r* infection

a Colon cells from intestinal epithelium were isolated from day 8 p.i. Colon tissue was stained with Siglet-F, TCRgd, Ly6G, CD11b, CD45, EpCAM1 and L/D dye and sorted on $EpCAM1^{+}CD45^{-}$ intestinal epithelial cells (IEC; black), $CD11b^{+}$ $Ly6G^{+}$ PMNs (red),

CD45+, TCRgd^{+} γδT cells (green), CD45^{+} Siglet-F^{+} Eosinophils (blue), and remaining CD45^{+} cells were also collected (grey). **b** Distal colon tissue from day 8 C.r-infected C57BL/6 mice was harvested and stained for S100A9 or Lcn2 (red), and DAPI (blue). **c**. Distal colon tissue from day 8 C.r-infected C57BL/6 mice was harvested and S100a9 (Red), EpCAM1 (White), MPO (Green) and DAPI (blue) expression were stained using *in-situ* hybridization probe. Two-way ANOVA ****p ≤ 0.0001 comparing AMP expression between PMN and other cells. n=3 two independent experiment

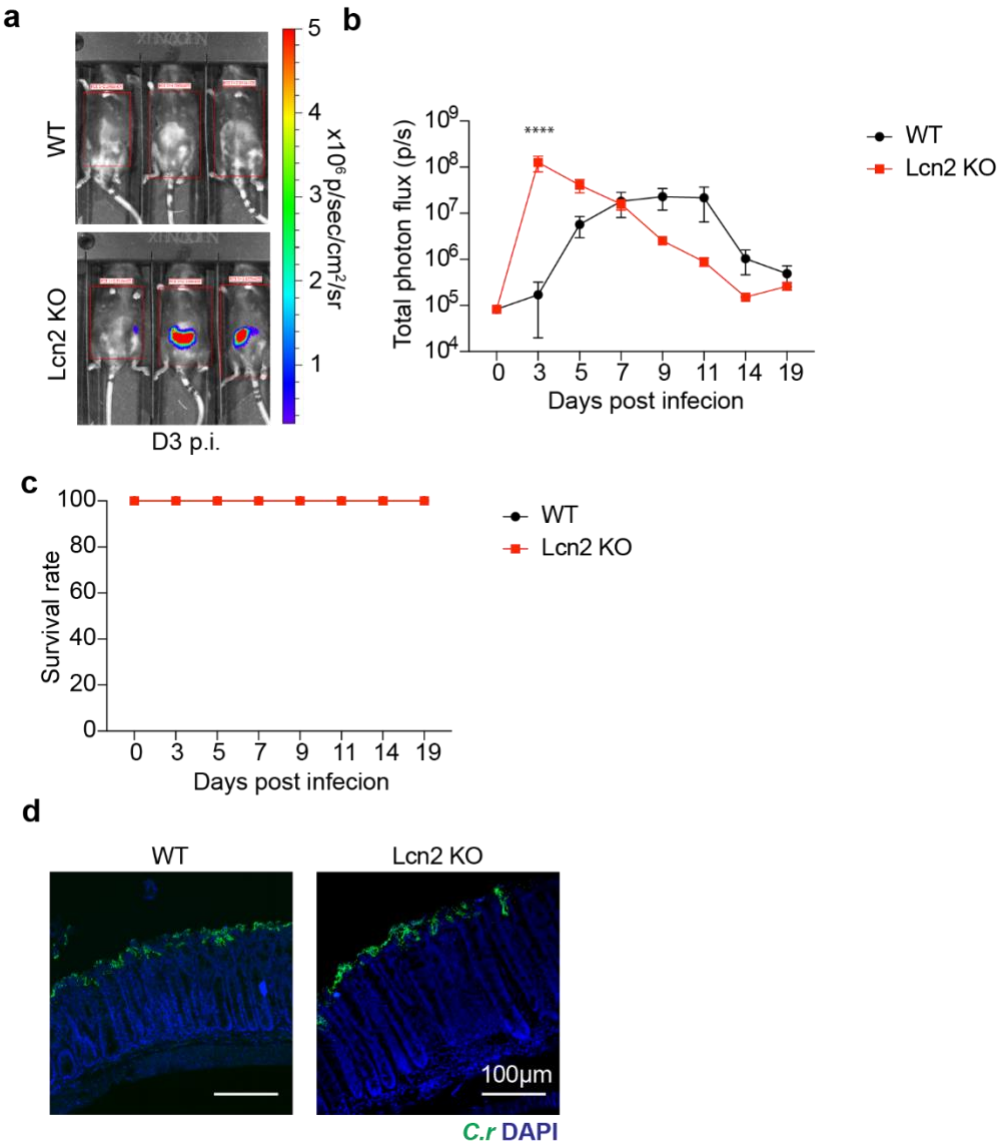

Figure 3. Lcn2 limits early bacterial load during *C.r* infection

a-c C57BL/6 or Lcn2 KO mice were infected with *C.r* and whole-body imaging (day 3) (**a**) and colonization kinetics (**b**) was performed on indicated days (n=5 per group). Mice survival rate was recorded (**c**). Colons from GFP *C.r*-infected WT and Lcn2 mice were isolated at day 10 post infection and stained for *C.r*-GFP (green) and DAPI (blue) (n=3 per group) (**d**). Results are representative of two independent experiments (n=3 per group).

Error bars indicate standard deviation. **b** Two-way ANOVA ****$p \leq 0.0001$ comparing WT and Lcn2 KO mice.

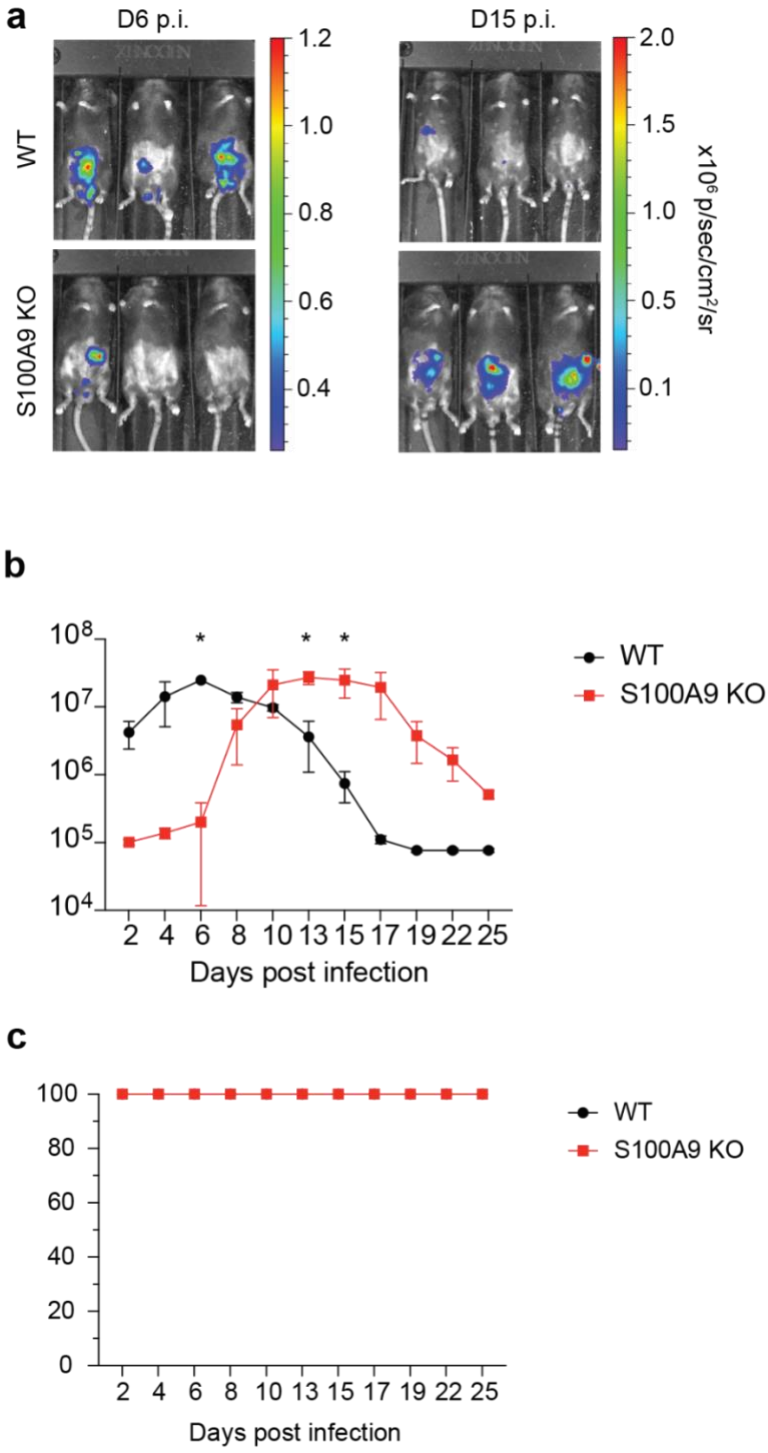

Figure 4. S100a9 limits late bacterial load and promote *C.r* clearance

a-c C57BL/6 or S100A9 KO mice were infected with lux-*C.r* and whole-body imaging (day 6 and day 15 p.i.) (**a**) and colonization kinetics (**b**) was performed on indicated days.

Mice survival rate was recorded (**c**). Results are representative of two independent experiments (n=3 per group). Error bars indicate standard deviation. **b** Two-way ANOVA *$p \leq 0.05$ comparing WT and S100A9 KO mice.

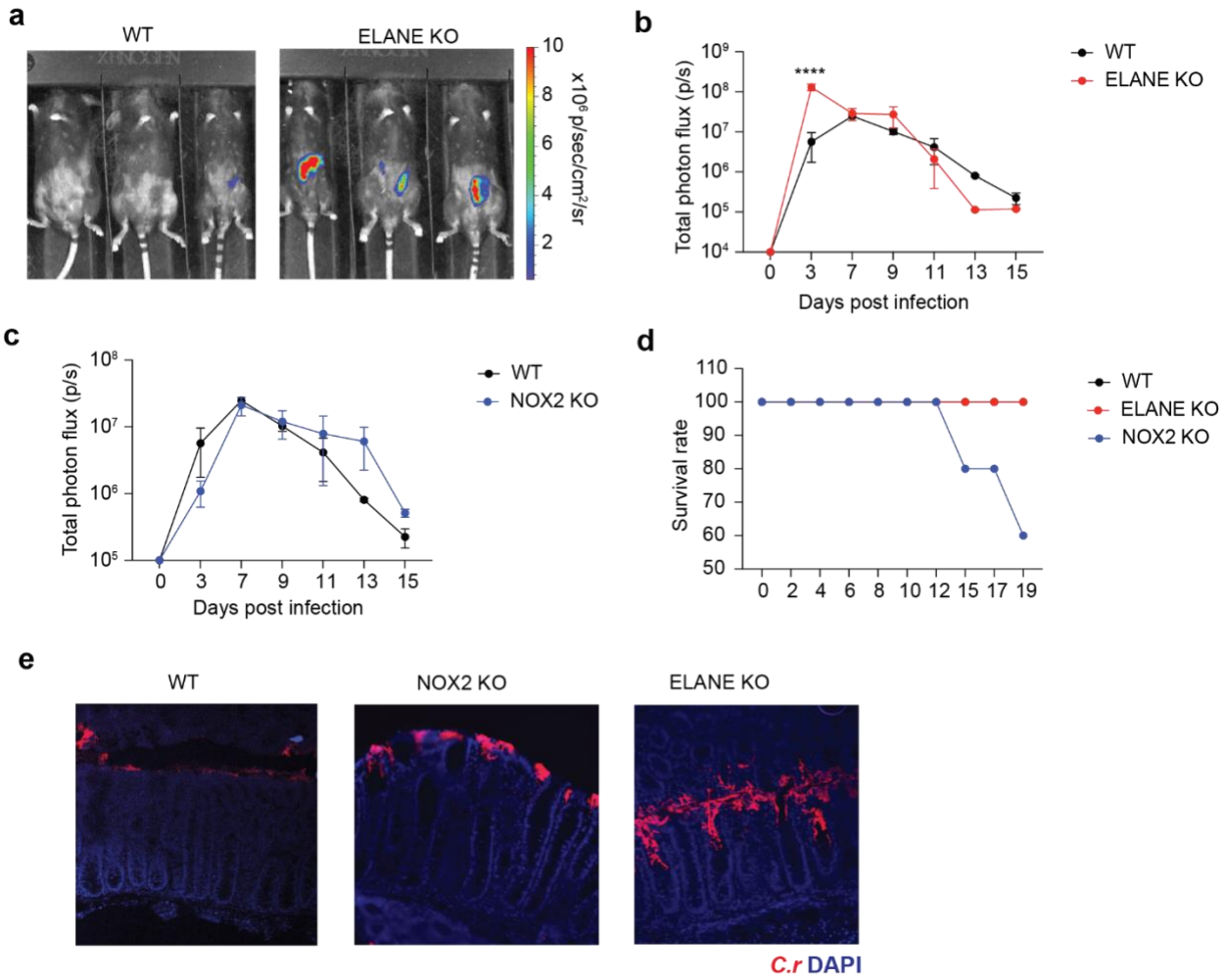

Figure 5. Neutrophil elastase and NOX2 mediated ROS production protect the host from elevated *C.r* load, crypt invasion and infection-induced fatality

a-d C57BL/6, ELANE KO, and NOX2 KO mice were infected with lux-*C.r* and whole-body imaging of WT and ELANE KO mice (day 3 p.i.) (**a**) and colonization kinetics of WT, ELANE KO mice (**b**) and NOX2 KO mice (**c**) was performed on indicated days. Mice survival rate was recorded (**d**). Results are representative of two independent experiments (n=3 per group). Colons from *C.r*-infected WT, NOX2 KO and ELANE KO mice were isolated at d10 post infection and stained for *C.r*-LPS (red) and DAPI (blue) Error bars

indicate standard deviation. **b** Two-way ANOVA ****$p \leq 0.0001$ comparing WT and ELANE KO mice.

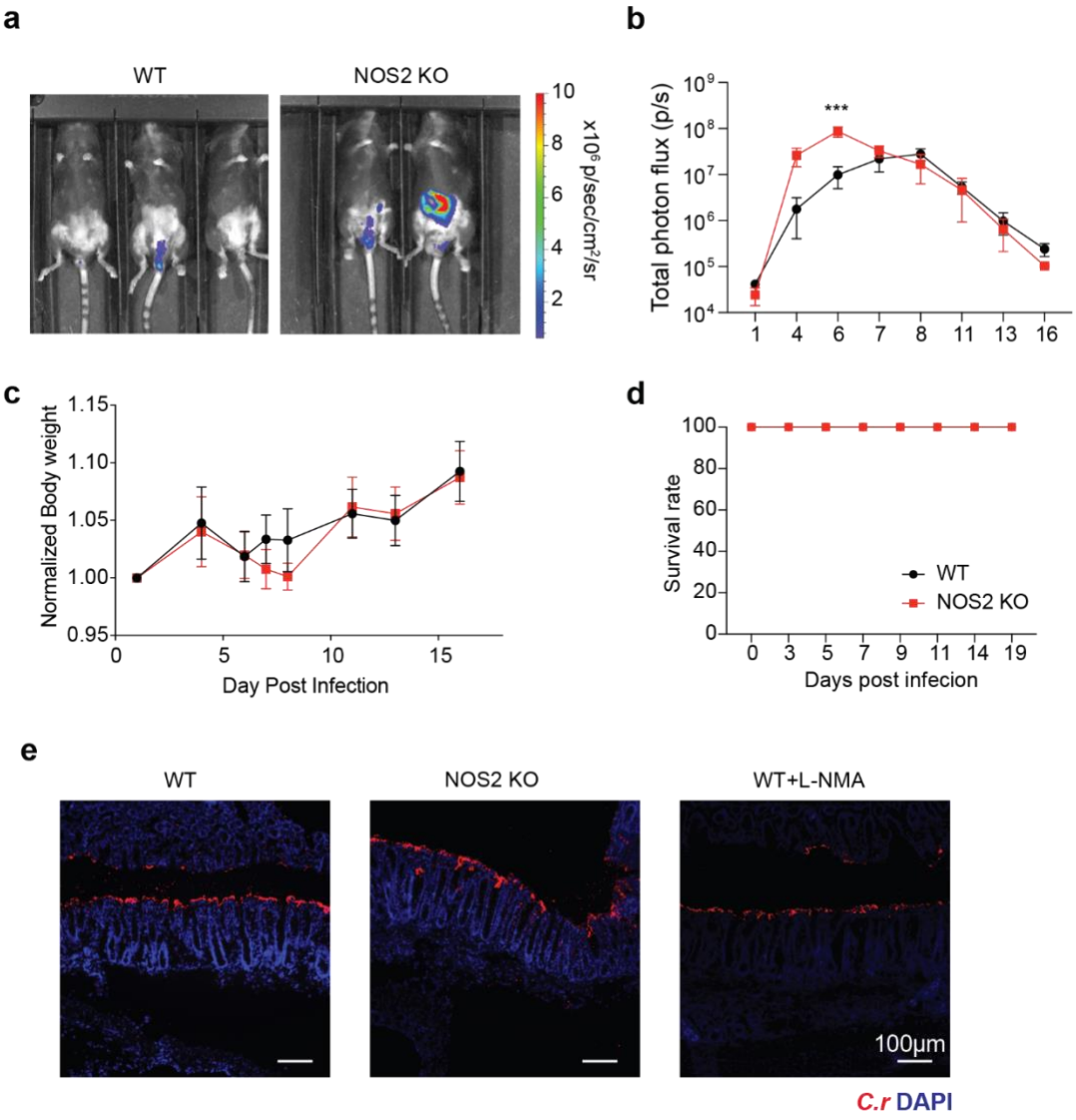

Figure 6. NOS2 production limits *C.r* load during early infection

a-c C57BL/6 or NOS2 KO mice were infected with *C.r* and whole-body imaging (day 6) (**a**) and colonization kinetics (**b**) was performed on indicated days. Mice body weight (**c**) and survival rate was recorded (**d**). Colons from *C.r*-infected WT, NOS2 KO mice, or WT mice treated with NOS2 inhibitor L-NMA were isolated at d8 post infection and stained for *C.r*-LPS (red) and DAPI (blue) (**e**). Results are representative of two independent experiments (n=3 per group). Error bars indicate standard deviation. **b** Two-way ANOVA ***$p \leq 0.001$ comparing WT and NOS2 KO mice.

REFERENCES

1. Hartland, E. L. & Leong, J. M. Enteropathogenic and enterohemorrhagic E. coli: ecology, pathogenesis, and evolution. *Front. Cell. Infect. Microbiol.* **3**, 15 (2013).
2. Peterson, L. W. & Artis, D. Intestinal epithelial cells: regulators of barrier function and immune homeostasis. *Nat. Rev. Immunol.* **14**, 141–153 (2014).
3. Mowat, A. M. & Agace, W. W. Regional specialization within the intestinal immune system. *Nat. Rev. Immunol.* **14**, 667–685 (2014).
4. Silberger, D. J., Zindl, C. L. & Weaver, C. T. Citrobacter rodentium: a model enteropathogen for understanding the interplay of innate and adaptive components of type 3 immunity. *Mucosal Immunol.* **10**, 1108–1117 (2017).
5. van Ampting, M. T. J. *et al.* Intestinally Secreted C-Type Lectin Reg3b Attenuates Salmonellosis but Not Listeriosis in Mice. *Infect. Immun.* **80**, 1115–1120 (2012).
6. Lee, M. J. *et al.* Interleukin-6 Induces S100A9 Expression in Colonic Epithelial Cells through STAT3 Activation in Experimental Ulcerative Colitis. *PLOS ONE* **7**, e38801 (2012).
7. Woo, V. *et al.* Commensal segmented filamentous bacteria-derived retinoic acid primes host defense to intestinal infection. *Cell Host Microbe* **29**, 1744-1756.e5 (2021).
8. Zheng, Y. *et al.* Interleukin-22 mediates early host defense against attaching and effacing bacterial pathogens. *Nat. Med.* **14**, 282–289 (2008).
9. Basu, R. *et al.* Th22 cells are an important source of IL-22 for host protection against enteropathogenic bacteria. *Immunity* **37**, 1061–1075 (2012).
10. Keir, M. E., Yi, T., Lu, T. T. & Ghilardi, N. The role of IL-22 in intestinal health and disease. *J. Exp. Med.* **217**, e20192195 (2020).
11. Wang, C. *et al.* Interleukin-22 drives nitric oxide-dependent DNA damage and dysplasia in a murine model of colitis-associated cancer. *Mucosal Immunol.* **10**, 1504–1517 (2017).
12. Muniz, L. R., Knosp, C. & Yeretssian, G. Intestinal antimicrobial peptides during homeostasis, infection, and disease. *Front. Immunol.* **3**, (2012).
13. Huan, Y., Kong, Q., Mou, H. & Yi, H. Antimicrobial Peptides: Classification, Design, Application and Research Progress in Multiple Fields. *Front. Microbiol.* **11**, (2020).
14. Hood, M. I. & Skaar, E. P. Nutritional immunity: transition metals at the pathogen–host interface. *Nat. Rev. Microbiol.* **10**, 525–537 (2012).

15. Bjarnason, I. The Use of Fecal Calprotectin in Inflammatory Bowel Disease. *Gastroenterol. Hepatol.* **13**, 53–56 (2017).

16. Stallhofer, J. *et al.* Lipocalin-2 Is a Disease Activity Marker in Inflammatory Bowel Disease Regulated by IL-17A, IL-22, and TNF-α and Modulated by IL23R Genotype Status. *Inflamm. Bowel Dis.* **21**, 2327–2340 (2015).

17. Hendrikx, T. *et al.* Bacteria engineered to produce IL-22 in intestine induce expression of REG3G to reduce ethanol-induced liver disease in mice. *Gut* **68**, 1504–1515 (2019).

18. Wang, L. *et al.* Intestinal REG3 Lectins Protect against Alcoholic Steatohepatitis by Reducing Mucosa-Associated Microbiota and Preventing Bacterial Translocation. *Cell Host Microbe* **19**, 227–239 (2016).

19. Corbin, B. D. *et al.* Metal Chelation and Inhibition of Bacterial Growth in Tissue Abscesses. *Science* **319**, 962–965 (2008).

20. Flo, T. H. *et al.* Lipocalin 2 mediates an innate immune response to bacterial infection by sequestrating iron. *Nature* **432**, 917–921 (2004).

21. Coorens, M. *et al.* Innate lymphoid cell type 3–derived interleukin-22 boosts lipocalin-2 production in intestinal epithelial cells via synergy between STAT3 and NF-κB. *J. Biol. Chem.* **294**, 6027–6041 (2019).

22. Carrión, M. *et al.* IL-22/IL-22R1 axis and S100A8/A9 alarmins in human osteoarthritic and rheumatoid arthritis synovial fibroblasts. *Rheumatol. Oxf. Engl.* **52**, 2177–2186 (2013).

23. Zhuang, Y. *et al.* A pro-inflammatory role for Th22 cells in Helicobacter pylori-associated gastritis. *Gut* **64**, 1368–1378 (2015).

24. Mühl, H., Bachmann, M. & Pfeilschifter, J. Inducible NO synthase and antibacterial host defence in times of Th17/Th22/T22 immunity: iNOS and Th17/Th22/T22-like immunity. *Cell. Microbiol.* **13**, 340–348 (2011).

25. Martin, C. *et al.* Chemokines acting via CXCR2 and CXCR4 control the release of neutrophils from the bone marrow and their return following senescence. *Immunity* **19**, 583–593 (2003).

26. Burn, G. L., Foti, A., Marsman, G., Patel, D. F. & Zychlinsky, A. The Neutrophil. *Immunity* **54**, 1377–1391 (2021).

27. Nguyen, G. T., Green, E. R. & Mecsas, J. Neutrophils to the ROScue: Mechanisms of NADPH Oxidase Activation and Bacterial Resistance. *Front. Cell. Infect. Microbiol.* **7**, (2017).

28. El-Benna, J., Dang, P. M.-C., Gougerot-Pocidalo, M.-A., Marie, J.-C. & Braut-Boucher, F. p47phox, the phagocyte NADPH oxidase/NOX2 organizer: structure, phosphorylation and implication in diseases. *Exp. Mol. Med.* **41**, 217–225 (2009).

29. Honda, M. & Kubes, P. Neutrophils and neutrophil extracellular traps in the liver and gastrointestinal system. *Nat. Rev. Gastroenterol. Hepatol.* **15**, 206–221 (2018).

30. Wiles, S., Pickard, K. M., Peng, K., MacDonald, T. T. & Frankel, G. In vivo bioluminescence imaging of the murine pathogen Citrobacter rodentium. *Infect. Immun.* **74**, 5391–5396 (2006).

31. Buschor, S. *et al.* Innate immunity restricts Citrobacter rodentium A/E pathogenesis initiation to an early window of opportunity. *PLoS Pathog.* **13**, e1006476 (2017).

32. Belaaouaj, A. azzaq, Kim, K. S. & Shapiro, S. D. Degradation of Outer Membrane Protein A in Escherichia coli Killing by Neutrophil Elastase. *Science* **289**, 1185–1187 (2000).

33. Saha, P. *et al.* PAD4-dependent NETs generation are indispensable for intestinal clearance of Citrobacter rodentium. *Mucosal Immunol.* **12**, 761–771 (2019).

34. Rada, B. *et al.* Role of Nox2 in elimination of microorganisms. *Semin. Immunopathol.* **30**, 237–253 (2008).

35. Berger, C. N. *et al.* The Citrobacter rodentium type III secretion system effector EspO affects mucosal damage repair and antimicrobial responses. *PLoS Pathog.* **14**, e1007406 (2018).

36. Loonen, L. M. P. *et al.* REG3γ-deficient mice have altered mucus distribution and increased mucosal inflammatory responses to the microbiota and enteric pathogens in the ileum. *Mucosal Immunol.* **7**, 939–947 (2014).

37. Torres, V. J., Pishchany, G., Humayun, M., Schneewind, O. & Skaar, E. P. Staphylococcus aureus IsdB Is a Hemoglobin Receptor Required for Heme Iron Utilization. *J. Bacteriol.* **188**, 8421–8429 (2006).

38. Pal, R. R. *et al.* Pathogenic E. coli Extracts Nutrients from Infected Host Cells Utilizing Injectisome Components. *Cell* **177**, 683-696.e18 (2019).

39. Papayannopoulos, V., Metzler, K. D., Hakkim, A. & Zychlinsky, A. Neutrophil elastase and myeloperoxidase regulate the formation of neutrophil extracellular traps. *J. Cell Biol.* **191**, 677–691 (2010).

40. Bergstrom, K. S. B. *et al.* Muc2 Protects against Lethal Infectious Colitis by Disassociating Pathogenic and Commensal Bacteria from the Colonic Mucosa. *PLoS Pathog.* **6**, e1000902 (2010).

Discussion and future remarks

IL-22 is indispensable for host protection against attaching-effacing pathogens in the intestine[30,66]. In this study we examined the role of IL-22 from innate and adaptive sources in host protection against *C.r* infection. Using a novel IL-22 reporter mouse, we found innate cells, mostly ILC3s, provide robust IL-22 production during early *C.r* infection whilst IL-22 producing $CD4^+$ T cells become the dominant source of IL-22 during late infection. It was initially thought that IL-22 from adaptive sources is redundant in host protection against *C.r*[66]. However, our study demonstrates that IL-22 from both innate and adaptive sources are required for host protection: IL-22 from innate cells protects the colon during early infection by limiting *C.r* load and initiating protective PMN recruitment into the colon; $CD4^+$ T cell produced IL-22 protects the host during late infection and uniquely prevents colonic crypts from *C.r* invasion. We found that IL-22 induces genes related to host defense and barrier function, such as AMPs, PMN recruiting chemokines and mucin-related molecules.

Our studies show that IL-22 from innate cells controls *C.r* during early infection, as *Il22*^{Plzf} mice had a significantly elevated bacterial burden at d3 of infection. This was associated with a reduction in PMN recruiting chemokines CXCL1, CXCL2 and CXCL5 from IECs, and resulting neutropenia in the colon during C.r infection. PMNs are important phagocytes that act to limit bacterial load[176], and our study shows that mice with PMN deficiency, as well as mice deficient in a number of genes involved in PMN function, including *Elane*, *S100a9*, *Lcn2* and *Nos2*, have increased *C.r* burden, implying that the early response to *C.r* is coordinated by innate cell-derived IL-22, IECs, and PMNs, and functions primarily to control bacterial colonization and expansion. A defect in any arm of this early immune

response leads to an increase in susceptibility to infection: *Il22*^{Plzf} mice unable to produce innate-derived IL-22 and *Il22ra1*^{Villin} mice unable to signal through IL-22RA in IECs showed reduced PMN infiltration and increased mortality, and PMN-deficient animals displayed increased crypt invasion. This highlights the fact that multiple levels of defense are required to maintain epithelial barrier function. Interestingly, while Elane-deficient mice showed increased colonic epithelial crypt invasion by *C.r*, S100A9-, Lcn2- and Nos2-deficient mice did not, indicating that increased bacterial load does not always correlate with crypt invasion. Further work will be necessary to elucidate the mechanisms by which PMNs and IECs are able to prevent crypt colonization.

One interesting discovery is our finding that both IECs and PMNs are sources of the AMPs LCN2, S100A8 and S100A9. It was believed that one aspect of the IL-22–mediated immune response was its contribution to AMP production from IECs[177]. However, our data establishes that PMNs are the major contributor of AMPs during C.r infection. AMPs are known to be important for host protection, and our data shows that LCN2 KO and S100A9 KO mice display defects in controlling bacterial burden. It remains unclear whether AMPs from IECs and PMNs are redundant, or they work synergistically to limit bacteria growth. Though PMNs express much higher levels of AMPs, they are geographically distant from the surface epithelium and colonizing bacteria. Conversely, IECs have lower expression levels of AMPs compared with PMNs, but they appear in much higher numbers and are in direct contact with attached pathogens. Most of the AMPs we found in the colon are metal chelating molecules that act by limiting the access of essential metals to bacteria, thus disturbing their metabolism. It is possible that AMPs produced by IECs first create a ‘metal drought’ at the epithelial surface to restrict *C.r* growth and expansion during very early

infection when fewer PMNs are present, and this mechanism is further augmented by AMPs produced by subsequently recruited PMNs. Future experiments using bone marrow chimeras or conditional AMP knockout models will be helpful to further specify the role of AMPs from different cellular sources in host protection against *C.r*.

Our study specify the cellular sources of PMN recruiting chemokine during *C.r* infection: CXCL1 and CXCL2 are predominantly produced by PMNs and CXCL5 is exclusively produced by IECs. These chemokines all bind to the PMN surface receptor CXCR2 and promote PMN migration to the target tissue through chemokine gradients[178]. However, these chemokines also have unique and non-redundant functions, despite all being CXCR2 ligands. CXCL1 decorates the apical surface of endothelial cells to promote PMN adhesion and activation[136]. CXCL2 can bind to ACKR1 receptors between endothelial junctions and the extracellular matrix to promote PMN transendothelial migration[136]. These findings are supported by a study conducted in the small intestine, where PMNs were found to be only able to cross the vessel at the region high in CXC chemokine gradients, in order to be recruited to the surface epithelium[179]. These data suggest that local PMN chemokine distribution largely dictates PMN migration by not only forming chemical gradients but also binding to surrounding cells to facilitate PMN movement in between tissue cells. In our study, we found most of the CXCL1- and CXCL2-producing cells are located at the bottom of the mucosa with some located at surface epithelium, suggesting that PMNs may create a local chemokine 'hot spot' to promote self-recruitment from blood vessels into the lamina propria. Further experiment using mice CXCL1/CXCL2 conditional knockout in PMNs will potentially solve the mechanism for PMNs to utilize CXCL1 and CXCL2 to promote self-recruitment through a feed-forward loop.

We also found that surface epithelial cells are the exclusive source of CXCL5 in the colon. The specific role of CXCL5 in the colon is largely unknown, but it can act either as a direct neutrophil recruiting agent through CXCR2 signaling, or a local chemokine gradient modifier by binding with DARC[180], to increase local CXCL1 and CXCL2 concentration. It is possible that CXCL5 is facilitating PMN transendothelial migration from capillaries that stretch to the surface epithelium by creating a strong local chemokine gradient. In this case PMNs could reach the surface epithelium much faster through a shorter route. Future studies using our newly created CXCL5 conditional knockout mouse will examine the significance of epithelial CXCR5 expression. Our hypothesis is that mice with CXCL5 deficiency in IECs may fail to recruit PMNs to and across the surface epithelium, resulting in impaired protection.

In the later stages of infection, $CD4^+$ T cells become the dominant source of IL-22 and these cells target crypt IECs to induce host defense genes and maintain epithelial barrier function. IL-22 production is seen in both Th22 and Th17 cells in the colon. IL-17, the canonical Th17 cytokine, is also known to induced epithelial derived PMN chemokines CXCL1 and CXCL2 to promote PMN recruitment in respond to SFB infection[181]. The role of IL-17 in this model and whether there is any functional overlap with IL-22 is unclear. IL-17A and IL-17F deficient mice have increased bacterial loads and delayed clearance during *C.r* infection, but do not show increased mortality[65], suggesting that any protective functions of these cytokines can be compensated for, likely by IL-22. It is worth noting that in contrast to IL-22, IL-17 expression in the colon during *C.r* infection only starts to increase significantly at the peak of infection (d8 p.i.)[65]. In this case, IL-22 from innate sources is the major cytokine during early infection to induce IEC-derived CXCL1,

CXCL2 and CXCL5 to initiated PMN recruitment, and is subsequently supplemented by T cell derived IL-17 and IL-22 during later stages of infection. Though IL-17 and IL-22 can both act on IECs to induce chemokine production, our data show that the function of IL-22 is not redundant, as *Il22*^{CD4} mice have reduced *Cxcl1* and *Cxcl2* expression from IECs during *C.r* infection. Interestingly, while *Il22*^{CD4} mice show increased susceptibility to *C.r* infection, around 50% of mice survive, raising the question of whether CD4^{+} T cell derived IL-17 can compensate for the absence of IL-22 in surviving animals. The specific role of IL-17 mediate chemokine production and PMN recruitment in *C.r* model remains to be further studied.

Our study shows that CD4^{+} IL-22^{+} cells can systemically activate both surface and crypt epithelial STAT3 phosphorylation, where innate-driven IL-22 production acts on only surface IECs during *C.r* infection. *Il22*^{CD4} mice also suffer from crypt invasion, suggesting a unique role for T cell derived IL-22 to protect the crypt from *C.r* infection. The mechanism for such crypt protection remains mostly unknown, but our study shows that PMN or neutrophil elastase depletion results in *C.r* invasion into the upper crypt of the colon, suggesting a potential link between IL-22–mediated PMN recruitment and protection of crypt from bacterial colonization. Surprisingly, we found that *Il22*^{CD4} have comparable PMN counts in the LP and IE compared with WT mice during peak infection, despite having reduced chemokine production from IECs. This can be explained by the fact that *Il22*^{CD4} mice retain a robust innate-derived IL-22 response which could effectively initiate PMN recruitment, and PMN auto-recruitment through CXCL1 and CXCL2 production becomes the dominant mechanism later on, rendering CD4^{+} T cell derived IL-22 somewhat redundant. However, IEC derived chemokines, especially CXCL5, still

create local gradients at the surface epithelium and are very likely to impact local PMN activation and transepithelial migration.

Future studies aim to resolve the discrepancy in our findings stated above. We first plan to expand our observation timepoint to d11-13 p.i., where we see a peak in the number of $CD4^+$ $IL\text{-}22^+$ cells and PMN recruitment, as well as possibly using a lower dose of *C.r* to examine $Il22^{CD4}$ mice while avoiding increased mortality and systemic inflammation. We also hypothesize that chemokines driven by T cell derived IL-22 may also promote PMN transepithelial migration into the lumen. This will be tested using mucus staining and lightsheet microscopy analysis of colon tissue to track PMN in the lumen and compared PMN transepithelial migration between WT and $Il22^{CD4}$ mice. We anticipate that $Il22^{CD4}$ mice may have reduced epithelial bound PMN and less PMN migration into the lumen, due to the reduction of IEC-derived CXC chemokines.

Mouse intestinal infection and inflammation models are strongly affected and heavily dependent on the composition of the intestinal microbiota. Whilst not specifically addressed in this study, control of host microbiota is key for consistent outcomes using the *C.r* infection model (data not shown). The typical *C.r* infection last 3 weeks in C57BL/6 mice with an infection peak at d6-8 p.i. Differences in *C.r* infection patterns among C57BL/6 mice sourced from different animal vendors have been observed, in terms of time point of peak infection, bacterial load, and infection duration[182]. Such discrepancies between vendors is believed to result from altered colonic short chain fatty acid production caused by bacteria in *Firmicutes* and other phyla[182]. Alterations of *C.r* infection curves and susceptibility in mice with changes in microflora could negatively impact the accurate and consistent assessment of the immune response, and care must be taken when comparing

results from different laboratories. Other commensal bacteria including *Bifidobacterium breve*[183], SFB[184] and *Helicobacter*[185] have been shown to attenuates *C.r* inflammation. So far, mice from Jackson laboratory (JAX) have been shown to be the most consistent and permissible for *C.r* infection model use.

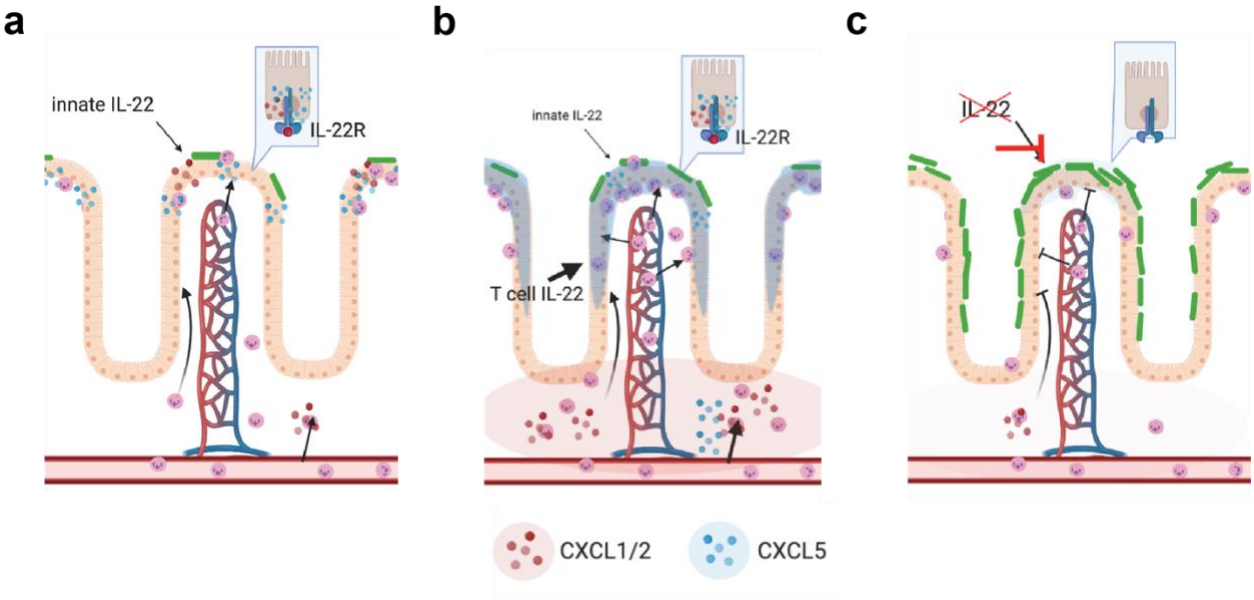

Figure 1. Model of IL-22 mediated PMN recruitment during *C.r* infection

a During early infection (d4 p.i.), IL-22 produced by innate immune cells activates epithelial IL-22 receptor to promote the production of CXCR ligands CXCL1, CXCL2 and CXCL5. In this stage IECs are the major source of CXCR2 ligand and initiate the early wave of PMN recruitment into the colon **b** As infection progress to d8 p.i., IL-22 production is augmented largely by infiltrating T cells that produce a higher dose of IL-22 and systematically activates both surface and cryptal IECs. At this stage PMNs produce self-recruiting chemokine CXCL1 and CXCL2 to amplify their presence in the lamina propria. However, IECs remain to be an exclusive source of CXCL5 and create a unique CXCL5 gradients at the colonic surface and upper crypt to potentially facilitate PMN translocation to the epithelium. **c** In the absence of IL-22, IECs are no longer able to provide robust production of CXCR2 ligand and fail to recruit normal number of PMN in the colon. This leads to a reduction of antibacterial property of the colon and allows *C.r* to overgrow and infiltrate the colonic crypt, which eventually leads to death of the host animal.

REFERENCES

1. Liu, L. *et al.* Global, regional, and national causes of under-5 mortality in 2000–15: an updated systematic analysis with implications for the Sustainable Development Goals. *The Lancet* **388**, 3027–3035 (2016).
2. Kotloff, K. L. *et al.* Burden and aetiology of diarrhoeal disease in infants and young children in developing countries (the Global Enteric Multicenter Study, GEMS): a prospective, case-control study. *Lancet Lond. Engl.* **382**, 209–222 (2013).
3. Escherichia coli, Diarrheagenic - Chapter 4 - 2020 Yellow Book | Travelers' Health | CDC. https://wwwnc.cdc.gov/travel/yellowbook/2020/travel-related-infectious-diseases/escherichia-coli-diarrheagenic.
4. Robins-Browne, R. M. & Hartland, E. L. Escherichia coli as a cause of diarrhea. *J. Gastroenterol. Hepatol.* **17**, 467–475 (2002).
5. Clarke, S. C., Haigh, R. D., Freestone, P. P. E. & Williams, P. H. Virulence of Enteropathogenic Escherichia coli, a Global Pathogen. *Clin. Microbiol. Rev.* **16**, 365–378 (2003).
6. Franzin, F. M. & Sircili, M. P. Locus of Enterocyte Effacement: A Pathogenicity Island Involved in the Virulence of Enteropathogenic and Enterohemorragic Escherichia coli Subjected to a Complex Network of Gene Regulation. *BioMed Res. Int.* **2015**, 534738 (2015).
7. Santos, F. F. *et al.* The Type III Secretion System (T3SS)-Translocon of Atypical Enteropathogenic Escherichia coli (aEPEC) Can Mediate Adherence. *Front. Microbiol.* **10**, (2019).
8. Gaytán, M. O., Martínez-Santos, V. I., Soto, E. & González-Pedrajo, B. Type Three Secretion System in Attaching and Effacing Pathogens. *Front. Cell. Infect. Microbiol.* **6**, 129 (2016).
9. Knutton, S., Baldwin, T., Williams, P., Manjarrez-Hernandez, A. & Aitken, A. The Attaching and Effacing Virulence Property of Enteropathogenic Escherichia coli. *Zentralblatt Für Bakteriol.* **278**, 209–217 (1993).
10. Goosney, D. L. *et al.* Enteropathogenic E. coli translocated intimin receptor, Tir, interacts directly with α-actinin. *Curr. Biol.* **10**, 735–738 (2000).
11. Savkovic, S. D., Koutsouris, A. & Hecht, G. Activation of NF-kappaB in intestinal epithelial cells by enteropathogenic Escherichia coli. *Am. J. Physiol.* **273**, C1160-1167 (1997).
12. Subramanian, S. *et al.* Characterization of epithelial IL-8 response to inflammatory bowel disease mucosal E. coli and its inhibition by mesalamine. *Inflamm. Bowel Dis.* **14**, 162–175 (2008).

13. Ledwaba, S. E. *et al.* Enteropathogenic Escherichia coli Infection Induces Diarrhea, Intestinal Damage, Metabolic Alterations, and Increased Intestinal Permeability in a Murine Model. *Front. Cell. Infect. Microbiol.* **10**, (2020).

14. Xu, J.-G., Cheng, B.-K. & Jing, H.-Q. Escherichia Coli O157 : H7 and Shiga-like-toxin-producing Escherichia Coli in China. *World J. Gastroenterol.* **5**, 191–194 (1999).

15. Jones, N. L. *et al.* Escherichia coli Shiga toxins induce apoptosis in epithelial cells that is regulated by the Bcl-2 family. *Am. J. Physiol. Gastrointest. Liver Physiol.* **278**, G811-819 (2000).

16. Obrig, T. G. & Karpman, D. Shiga Toxin Pathogenesis: Kidney Complications and Renal Failure. *Curr. Top. Microbiol. Immunol.* **357**, 105–136 (2012).

17. Guan, Q. A Comprehensive Review and Update on the Pathogenesis of Inflammatory Bowel Disease. *J. Immunol. Res.* **2019**, 7247238 (2019).

18. Kaplan, G. G. The global burden of IBD: from 2015 to 2025. *Nat. Rev. Gastroenterol. Hepatol.* **12**, 720–727 (2015).

19. Szigethy, E., McLafferty, L. & Goyal, A. Inflammatory bowel disease. *Child Adolesc. Psychiatr. Clin. N. Am.* **19**, 301–318, ix (2010).

20. Gryboski, J. D. Ulcerative colitis in children 10 years old or younger. *J. Pediatr. Gastroenterol. Nutr.* **17**, 24–31 (1993).

21. Baumgart, D. C. & Sandborn, W. J. Inflammatory bowel disease: clinical aspects and established and evolving therapies. *Lancet Lond. Engl.* **369**, 1641–1657 (2007).

22. Abraham, C. & Cho, J. H. Inflammatory Bowel Disease. *N. Engl. J. Med.* **361**, 2066–2078 (2009).

23. Gajendran, M., Loganathan, P., Catinella, A. P. & Hashash, J. G. A comprehensive review and update on Crohn's disease. *Dis.--Mon. DM* **64**, 20–57 (2018).

24. Nell, S., Suerbaum, S. & Josenhans, C. The impact of the microbiota on the pathogenesis of IBD: lessons from mouse infection models. *Nat. Rev. Microbiol.* **8**, 564–577 (2010).

25. Nishida, A. *et al.* Gut microbiota in the pathogenesis of inflammatory bowel disease. *Clin. J. Gastroenterol.* **11**, 1–10 (2018).

26. Ni, J., Wu, G. D., Albenberg, L. & Tomov, V. T. Gut microbiota and IBD: causation or correlation? *Nat. Rev. Gastroenterol. Hepatol.* **14**, 573–584 (2017).

27. Liu, J. Z. *et al.* Association analyses identify 38 susceptibility loci for inflammatory bowel disease and highlight shared genetic risk across populations. *Nat. Genet.* **47**, 979–986 (2015).

28. Yamamoto, S. & Ma, X. Role of Nod2 in the development of Crohn's disease. *Microbes Infect. Inst. Pasteur* **11**, 912–918 (2009).

29. Mangan, P. R. *et al.* Transforming growth factor-β induces development of the TH17 lineage. *Nature* **441**, 231–234 (2006).

30. Basu, R. *et al.* Th22 cells are an important source of IL-22 for host protection against enteropathogenic bacteria. *Immunity* **37**, 1061–1075 (2012).

31. Barthold, S. W., Coleman, G. L., Bhatt, P. N., Osbaldiston, G. W. & Jonas, A. M. The etiology of transmissible murine colonic hyperplasia. in *Laboratory Animal Science* vol. 26 (1976).

32. Silberger, D. J., Zindl, C. L. & Weaver, C. T. Citrobacter rodentium: a model enteropathogen for understanding the interplay of innate and adaptive components of type 3 immunity. *Mucosal Immunol.* **10**, 1108–1117 (2017).

33. Deng, W. *et al.* Dissecting virulence: Systematic and functional analyses of a pathogenicity island. *Proc. Natl. Acad. Sci.* **101**, 3597–3602 (2004).

34. Mallick, E. M. *et al.* A novel murine infection model for Shiga toxin–producing *Escherichia coli*. *J. Clin. Invest.* **122**, 4012–4024 (2012).

35. Wiles, S., Hanage, W. P., Frankel, G. & Robertson, B. Modelling infectious disease - time to think outside the box? *Nat. Rev. Microbiol.* **4**, 307–312 (2006).

36. Collins, J. W. *et al.* Citrobacter rodentium: infection, inflammation and the microbiota. *Nat. Rev. Microbiol.* **12**, 612–623 (2014).

37. Umanski, T., Rosenshine, I. & Friedberg, D. Thermoregulated expression of virulence genes in enteropathogenic Escherichia coli. *Microbiol. Read. Engl.* **148**, 2735–2744 (2002).

38. Alsharif, G. *et al.* Host attachment and fluid shear are integrated into a mechanical signal regulating virulence in Escherichia coli O157:H7. *Proc. Natl. Acad. Sci.* **112**, 5503–5508 (2015).

39. Reading, N. C., Rasko, D. A., Torres, A. G. & Sperandio, V. The two-component system QseEF and the membrane protein QseG link adrenergic and stress sensing to bacterial pathogenesis. *Proc. Natl. Acad. Sci.* **106**, 5889–5894 (2009).

40. Nakanishi, N. *et al.* Regulation of virulence by butyrate sensing in enterohaemorrhagic Escherichia coli. *Microbiol. Read. Engl.* **155**, 521–530 (2009).

41. Buschor, S. *et al.* Innate immunity restricts Citrobacter rodentium A/E pathogenesis initiation to an early window of opportunity. *PLoS Pathog.* **13**, e1006476 (2017).

42. Lopez, C. A. *et al.* Virulence factors enhance Citrobacter rodentium expansion through aerobic respiration. *Science* **353**, 1249–1253 (2016).

43. Wiles, S. *et al.* Organ specificity, colonization and clearance dynamics in vivo following oral challenges with the murine pathogen Citrobacter rodentium. *Cell. Microbiol.* **6**, 963–972 (2004).

44. Cepeda-Molero, M. *et al.* Attaching and effacing (A/E) lesion formation by enteropathogenic E. coli on human intestinal mucosa is dependent on non-LEE effectors. *PLoS Pathog.* **13**, e1006706 (2017).

45. Hopkins, E. G. D., Roumeliotis, T. I., Mullineaux-Sanders, C., Choudhary, J. S. & Frankel, G. Intestinal Epithelial Cells and the Microbiome Undergo Swift

Reprogramming at the Inception of Colonic Citrobacter rodentium Infection. *mBio* **10**, e00062-19 (2019).

46. Wiles, S., Dougan, G. & Frankel, G. Emergence of a 'hyperinfectious' bacterial state after passage of Citrobacter rodentium through the host gastrointestinal tract. *Cell. Microbiol.* **7**, 1163–1172 (2005).

47. Shenoy, A. R., Furniss, R. C. D., Goddard, P. J. & Clements, A. Modulation of Host Cell Processes by T3SS Effectors. *Curr. Top. Microbiol. Immunol.* **416**, 73–115 (2018).

48. Pal, R. R. *et al.* Pathogenic E. coli Extracts Nutrients from Infected Host Cells Utilizing Injectisome Components. *Cell* **177**, 683-696.e18 (2019).

49. Maaser, C. *et al.* Clearance of Citrobacter rodentium Requires B Cells but Not Secretory Immunoglobulin A (IgA) or IgM Antibodies. *Infect. Immun.* **72**, 3315–3324 (2004).

50. Belzer, C., Liu, Q., Carroll, M. C. & Bry, L. The role of specific IgG and complement in combating a primary mucosal infection of the gut epithelium. *Eur. J. Microbiol. Immunol.* **1**, 311–318 (2011).

51. Kamada, N. *et al.* Humoral Immunity in the Gut Selectively Targets Phenotypically Virulent Attaching-and-Effacing Bacteria for Intraluminal Elimination. *Cell Host Microbe* **17**, 617–627 (2015).

52. Kamada, N. *et al.* Regulated virulence controls the ability of a pathogen to compete with the gut microbiota. *Science* **336**, 1325–1329 (2012).

53. Sano, T. *et al.* An IL-23R/IL-22 Circuit Regulates Epithelial Serum Amyloid A to Promote Local Effector Th17 Responses. *Cell* **163**, 381–393 (2015).

54. Atarashi, K. *et al.* Th17 Cell Induction by Adhesion of Microbes to Intestinal Epithelial Cells. *Cell* **163**, 367–380 (2015).

55. Kim, Y.-G. *et al.* The Nod2 Sensor Promotes Intestinal Pathogen Eradication via the Chemokine CCL2-Dependent Recruitment of Inflammatory Monocytes. *Immunity* **34**, 769–780 (2011).

56. Gibson, D. L. *et al.* MyD88 signalling plays a critical role in host defence by controlling pathogen burden and promoting epithelial cell homeostasis during Citrobacter rodentium-induced colitis. *Cell. Microbiol.* **10**, 618–631 (2008).

57. Spehlmann, M. E. *et al.* CXCR2-dependent mucosal neutrophil influx protects against colitis-associated diarrhea caused by an attaching/effacing lesion-forming bacterial pathogen. *J. Immunol. Baltim. Md 1950* **183**, 3332–3343 (2009).

58. Schreiber, H. A. *et al.* Intestinal monocytes and macrophages are required for T cell polarization in response to Citrobacter rodentium. *J. Exp. Med.* **210**, 2025–2039 (2013).

59. Manta, C. *et al.* CX3CR1+ macrophages support IL-22 production by innate lymphoid cells during infection with Citrobacter rodentium. *Mucosal Immunol.* **6**, 177–188 (2013).

60. Grohmann, U. *et al.* Positive Regulatory Role of IL-12 in Macrophages and Modulation by IFN-γ. *J. Immunol.* **167**, 221–227 (2001).

61. Lin, Y.-D., Arora, J., Diehl, K., Bora, S. A. & Cantorna, M. T. Vitamin D Is Required for ILC3 Derived IL-22 and Protection From Citrobacter rodentium Infection. *Front. Immunol.* **10**, (2019).

62. Satoh-Takayama, N. *et al.* Microbial flora drives interleukin 22 production in intestinal NKp46+ cells that provide innate mucosal immune defense. *Immunity* **29**, 958–970 (2008).

63. Bry, L., Brigl, M. & Brenner, M. B. CD4+-T-Cell Effector Functions and Costimulatory Requirements Essential for Surviving Mucosal Infection with Citrobacter rodentium. *Infect. Immun.* **74**, 673–681 (2006).

64. Simmons, C. P. *et al.* Central role for B lymphocytes and CD4+ T cells in immunity to infection by the attaching and effacing pathogen Citrobacter rodentium. *Infect. Immun.* **71**, 5077–5086 (2003).

65. Ishigame, H. *et al.* Differential Roles of Interleukin-17A and -17F in Host Defense against Mucoepithelial Bacterial Infection and Allergic Responses. *Immunity* **30**, 108–119 (2009).

66. Zheng, Y. *et al.* Interleukin-22 mediates early host defense against attaching and effacing bacterial pathogens. *Nat. Med.* **14**, 282–289 (2008).

67. Aujla, S. J. *et al.* IL-22 mediates mucosal host defense against Gram-negative bacterial pneumonia. *Nat. Med.* **14**, 275–281 (2008).

68. Xie, M. H. *et al.* Interleukin (IL)-22, a novel human cytokine that signals through the interferon receptor-related proteins CRF2-4 and IL-22R. *J. Biol. Chem.* **275**, 31335–31339 (2000).

69. Ouyang, W., Rutz, S., Crellin, N. K., Valdez, P. A. & Hymowitz, S. G. Regulation and Functions of the IL-10 Family of Cytokines in Inflammation and Disease. *Annu. Rev. Immunol.* **29**, 71–109 (2011).

70. Bleicher, L. *et al.* Crystal structure of the IL-22/IL-22R1 complex and its implications for the IL-22 signaling mechanism. *FEBS Lett.* **582**, 2985–2992 (2008).

71. Dudakov, J. A., Hanash, A. M. & van den Brink, M. R. M. Interleukin-22: Immunobiology and Pathology. *Annu. Rev. Immunol.* **33**, 747–785 (2015).

72. Chen, J., Caspi, R. R. & Po Chong, W. IL-20 receptor cytokines in autoimmune diseases. *J. Leukoc. Biol.* **104**, 953–959 (2018).

73. Shouval, D. S. *et al.* Interleukin 10 Receptor Signaling: Master Regulator of Intestinal Mucosal Homeostasis in Mice and Humans. *Adv. Immunol.* **122**, 177–210 (2014).

74. Parks, O. B., Pociask, D. A., Hodzic, Z., Kolls, J. K. & Good, M. Interleukin-22 Signaling in the Regulation of Intestinal Health and Disease. *Front. Cell Dev. Biol.* **3**, (2016).

75. Satpathy, A. T. *et al.* Notch2-dependent classical dendritic cells orchestrate intestinal immunity to attaching-and-effacing bacterial pathogens. *Nat. Immunol.* **14**, 937–948 (2013).

76. Rutz, S., Eidenschenk, C. & Ouyang, W. IL-22, not simply a Th17 cytokine. *Immunol. Rev.* **252**, 116–132 (2013).

77. Works, M. G. *et al.* Inhibition of TYK2 and JAK1 Ameliorates Imiquimod-Induced Psoriasis-like Dermatitis by Inhibiting IL-22 and the IL-23/IL-17 Axis. *J. Immunol.* **193**, 3278–3287 (2014).

78. Banerjee, S., Biehl, A., Gadina, M., Hasni, S. & Schwartz, D. M. JAK–STAT Signaling as a Target for Inflammatory and Autoimmune Diseases: Current and Future Prospects. *Drugs* **77**, 521–546 (2017).

79. Pickert, G. *et al.* STAT3 links IL-22 signaling in intestinal epithelial cells to mucosal wound healing. *J. Exp. Med.* **206**, 1465–1472 (2009).

80. Lejeune, D. *et al.* Interleukin-22 (IL-22) activates the JAK/STAT, ERK, JNK, and p38 MAP kinase pathways in a rat hepatoma cell line. Pathways that are shared with and distinct from IL-10. *J. Biol. Chem.* **277**, 33676–33682 (2002).

81. Wittkopf, N. *et al.* Activation of Intestinal Epithelial Stat3 Orchestrates Tissue Defense during Gastrointestinal Infection. *PLoS ONE* **10**, e0118401 (2015).

82. Oshima, H. *et al.* Stat3 is indispensable for damage-induced crypt regeneration but not for Wnt-driven intestinal tumorigenesis. *FASEB J. Off. Publ. Fed. Am. Soc. Exp. Biol.* **33**, 1873–1886 (2019).

83. Boniface, K. *et al.* IL-22 inhibits epidermal differentiation and induces proinflammatory gene expression and migration of human keratinocytes. *J. Immunol. Baltim. Md 1950* **174**, 3695–3702 (2005).

84. Zindl, C. L. *et al.* IL-22–producing neutrophils contribute to antimicrobial defense and restitution of colonic epithelial integrity during colitis. *Proc. Natl. Acad. Sci.* **110**, 12768–12773 (2013).

85. Barone, F. *et al.* IL-22 regulates lymphoid chemokine production and assembly of tertiary lymphoid organs. *Proc. Natl. Acad. Sci.* **112**, 11024–11029 (2015).

86. Stacey, M. A. *et al.* Neutrophils Recruited by IL-22 in Peripheral Tissues Function as TRAIL-Dependent Antiviral Effectors against MCMV. *Cell Host Microbe* **15**, 471–483 (2014).

87. Lindemans, C. A. *et al.* Interleukin-22 promotes intestinal-stem-cell-mediated epithelial regeneration. *Nature* **528**, 560–564 (2015).

88. Luperchio, S. A. *et al.* Citrobacter rodentium, the Causative Agent of Transmissible Murine Colonic Hyperplasia, Exhibits Clonality: Synonymy of C. rodentium and Mouse-Pathogenic Escherichia coli. *J. Clin. Microbiol.* **38**, 4343–4350 (2000).

89. Zha, J.-M. *et al.* Interleukin 22 Expands Transit-Amplifying Cells While Depleting Lgr5+ Stem Cells via Inhibition of Wnt and Notch Signaling. *Cell. Mol. Gastroenterol. Hepatol.* **7**, 255–274 (2019).

90. Chiang, H.-Y. *et al.* IL-22 initiates an IL-18-dependent epithelial response circuit to enforce intestinal host defence. *Nat. Commun.* **13**, 874 (2022).

91. Grivennikov, S. *et al.* IL-6 and Stat3 Are Required for Survival of Intestinal Epithelial Cells and Development of Colitis-Associated Cancer. *Cancer Cell* **15**, 103–113 (2009).

92. Zwarycz, B. *et al.* IL22 Inhibits Epithelial Stem Cell Expansion in an Ileal Organoid Model. *Cell. Mol. Gastroenterol. Hepatol.* **7**, 1–17 (2018).

93. Johansson, M. E. V. & Hansson, G. C. Immunological aspects of intestinal mucus and mucins. *Nat. Rev. Immunol.* **16**, 639–649 (2016).

94. Arshad, T., Mansur, F., Palek, R., Manzoor, S. & Liska, V. A Double Edged Sword Role of Interleukin-22 in Wound Healing and Tissue Regeneration. *Front. Immunol.* **11**, 2148 (2020).

95. Liang, S. C. *et al.* IL-22 Induces an Acute-Phase Response. *J. Immunol.* **185**, 5531–5538 (2010).

96. Stacey, M. A. *et al.* Neutrophils Recruited by IL-22 in Peripheral Tissues Function as TRAIL-Dependent Antiviral Effectors against MCMV. *Cell Host Microbe* **15**, 471–483 (2014).

97. Zhuang, Y. *et al.* A pro-inflammatory role for Th22 cells in Helicobacter pylori-associated gastritis. *Gut* **64**, 1368–1378 (2015).

98. Van Belle, A. B. *et al.* IL-22 is required for imiquimod-induced psoriasiform skin inflammation in mice. *J. Immunol. Baltim. Md 1950* **188**, 462–469 (2012).

99. Hendrikx, T. *et al.* Bacteria engineered to produce IL-22 in intestine induce expression of REG3G to reduce ethanol-induced liver disease in mice. *Gut* **68**, 1504–1515 (2019).

100. Lo, B. C. *et al.* IL-22 Preserves Gut Epithelial Integrity and Promotes Disease Remission during Chronic *Salmonella* Infection. *J. Immunol.* **202**, 956–965 (2019).

101. Carrión, M. *et al.* IL-22/IL-22R1 axis and S100A8/A9 alarmins in human osteoarthritic and rheumatoid arthritis synovial fibroblasts. *Rheumatol. Oxf. Engl.* **52**, 2177–2186 (2013).

102. Chen, Z., Downing, S. & Tzanakakis, E. S. Four Decades After the Discovery of Regenerating Islet-Derived (Reg) Proteins: Current Understanding and Challenges. *Front. Cell Dev. Biol.* **7**, (2019).

103. van Ampting, M. T. J. *et al.* Intestinally Secreted C-Type Lectin Reg3b Attenuates Salmonellosis but Not Listeriosis in Mice. *Infect. Immun.* **80**, 1115–1120 (2012).

104. Cash, H. L., Whitham, C. V., Behrendt, C. L. & Hooper, L. V. Symbiotic Bacteria Direct Expression of an Intestinal Bactericidal Lectin. *Science* **313**, 1126–1130 (2006).

105. Loonen, L. M. P. *et al.* REG3γ-deficient mice have altered mucus distribution and increased mucosal inflammatory responses to the microbiota and enteric pathogens in the ileum. *Mucosal Immunol.* **7**, 939–947 (2014).

106. Hood, M. I. & Skaar, E. P. Nutritional immunity: transition metals at the pathogen–host interface. *Nat. Rev. Microbiol.* **10**, 525–537 (2012).

107. Flo, T. H. *et al.* Lipocalin 2 mediates an innate immune response to bacterial infection by sequestrating iron. *Nature* **432**, 917–921 (2004).

108. Shabani, F., Farasat, A., Mahdavi, M. & Gheibi, N. Calprotectin (S100A8/S100A9): a key protein between inflammation and cancer. *Inflamm. Res.* **67**, 801–812 (2018).

109. Corbin, B. D. *et al.* Metal Chelation and Inhibition of Bacterial Growth in Tissue Abscesses. *Science* **319**, 962–965 (2008).

110. Gao, H. *et al.* S100A9-induced release of interleukin (IL)-6 and IL-8 through toll-like receptor 4 (TLR4) in human periodontal ligament cells. *Mol. Immunol.* **67**, 223–232 (2015).

111. Simard, J.-C. *et al.* S100A8 and S100A9 Induce Cytokine Expression and Regulate the NLRP3 Inflammasome via ROS-Dependent Activation of NF-κB1. *PLoS ONE* **8**, e72138 (2013).

112. Németh, T., Sperandio, M. & Mócsai, A. Neutrophils as emerging therapeutic targets. *Nat. Rev. Drug Discov.* **19**, 253–275 (2020).

113. Smith, J. A. Exercise Immunology and Neutrophils. *Int. J. Sports Med.* **18**, S46–S55 (1997).

114. Dancey, J. T., Deubelbeiss, K. A., Harker, L. A. & Finch, C. A. Neutrophil kinetics in man. *J. Clin. Invest.* **58**, 705–715 (1976).

115. Hidalgo, A., Chilvers, E. R., Summers, C. & Koenderman, L. The Neutrophil Life Cycle. *Trends Immunol.* **40**, 584–597 (2019).

116. Pillay, J. *et al.* In vivo labeling with 2H2O reveals a human neutrophil lifespan of 5.4 days. *Blood* **116**, 625–627 (2010).

117. Prame Kumar, K., Nicholls, A. J. & Wong, C. H. Y. Partners in crime: neutrophils and monocytes/macrophages in inflammation and disease. *Cell Tissue Res.* **371**, 551–565 (2018).

118. Li, Y. *et al.* The regulatory roles of neutrophils in adaptive immunity. *Cell Commun. Signal.* **17**, 147 (2019).

119. Vietinghoff, S. von & Ley, K. Homeostatic Regulation of Blood Neutrophil Counts. *J. Immunol.* **181**, 5183–5188 (2008).

120. Ng, L. G., Ostuni, R. & Hidalgo, A. Heterogeneity of neutrophils. *Nat. Rev. Immunol.* **19**, 255–265 (2019).

121. Adrover, J. M., Nicolás-Ávila, J. A. & Hidalgo, A. Aging: A Temporal Dimension for Neutrophils. *Trends Immunol.* **37**, 334–345 (2016).

122. Martin, C. *et al.* Chemokines acting via CXCR2 and CXCR4 control the release of neutrophils from the bone marrow and their return following senescence. *Immunity* **19**, 583–593 (2003).

123. Ussov, W. Y., Aktolun, C., Myers, M. J., Jamar, F. & Peters, A. M. Granulocyte margination in bone marrow: comparison with margination in the spleen and liver. *Scand. J. Clin. Lab. Invest.* **55**, 87–96 (1995).

124. Saverymuttu, S. H., Peters, A. M., Keshavarzian, A., Reavy, H. J. & Lavender, J. P. The kinetics of 111Indium distribution following injection of 111Indium labelled autologous granulocytes in man. *Br. J. Haematol.* **61**, 675–685 (1985).

125. Ley, K., Laudanna, C., Cybulsky, M. I. & Nourshargh, S. Getting to the site of inflammation: the leukocyte adhesion cascade updated. *Nat. Rev. Immunol.* **7**, 678–689 (2007).

126. Fox, S., Leitch, A. E., Duffin, R., Haslett, C. & Rossi, A. G. Neutrophil Apoptosis: Relevance to the Innate Immune Response and Inflammatory Disease. *J. Innate Immun.* **2**, 216–227 (2010).

127. Sumagin, R., Robin, A. Z., Nusrat, A. & Parkos, C. A. Transmigrated neutrophils in the intestinal lumen engage ICAM-1 to regulate the epithelial barrier and neutrophil recruitment. *Mucosal Immunol.* **7**, 905–915 (2014).

128. Häger, M., Cowland, J. B. & Borregaard, N. Neutrophil granules in health and disease. *J. Intern. Med.* **268**, 25–34 (2010).

129. Fournier, B. M. & Parkos, C. A. The role of neutrophils during intestinal inflammation. *Mucosal Immunol.* **5**, 354–366 (2012).

130. Kansas, G. S. Selectins and their ligands: current concepts and controversies. *Blood* **88**, 3259–3287 (1996).

131. The role of JAM-A and PECAM-1 in modulating leukocyte infiltration in inflamed and ischemic tissues - Nourshargh - 2006 - Journal of Leukocyte Biology - Wiley Online Library. https://jlb.onlinelibrary.wiley.com/doi/full/10.1189/jlb.1105645.

132. McEver, R. P. & Cummings, R. D. Perspectives series: cell adhesion in vascular biology. Role of PSGL-1 binding to selectins in leukocyte recruitment. *J. Clin. Invest.* **100**, 485–491 (1997).

133. Nourshargh, S., Krombach, F. & Dejana, E. The role of JAM-A and PECAM-1 in modulating leukocyte infiltration in inflamed and ischemic tissues. *J. Leukoc. Biol.* **80**, 714–718 (2006).

134. Pontejo, S. M. & Murphy, P. M. Chemokines act as phosphatidylserine-bound "find-me" signals in apoptotic cell clearance. *PLOS Biol.* **19**, e3001259 (2021).

135. Salas, A. *et al.* Rolling Adhesion through an Extended Conformation of Integrin αLβ2 and Relation to α I and β I-like Domain Interaction. *Immunity* **20**, 393–406 (2004).

136. Girbl, T. *et al.* Distinct Compartmentalization of the Chemokines CXCL1 and CXCL2 and the Atypical Receptor ACKR1 Determine Discrete Stages of Neutrophil Diapedesis. *Immunity* **49**, 1062-1076.e6 (2018).

137. Vestweber, D. Regulation of endothelial cell contacts during leukocyte extravasation. *Curr. Opin. Cell Biol.* **14**, 587–593 (2002).

138. Wang, S. *et al.* Venular basement membranes contain specific matrix protein low expression regions that act as exit points for emigrating neutrophils. *J. Exp. Med.* **203**, 1519–1532 (2006).

139. Patel, D. F. & Snelgrove, R. J. The multifaceted roles of the matrikine Pro-Gly-Pro in pulmonary health and disease. *Eur. Respir. Rev.* **27**, (2018).

140. Hughes, C. E. & Nibbs, R. J. B. A guide to chemokines and their receptors. *Febs J.* **285**, 2944–2971 (2018).

141. Zarbock, A. & Stadtmann, A. CXCR2: From Bench to Bedside. *Front. Immunol.* **3**, (2012).

142. Samuelsson, B. Leukotrienes: mediators of immediate hypersensitivity reactions and inflammation. *Science* **220**, 568–575 (1983).

143. Dorward, D. A. *et al.* The Role of Formylated Peptides and Formyl Peptide Receptor 1 in Governing Neutrophil Function during Acute Inflammation. *Am. J. Pathol.* **185**, 1172–1184 (2015).

144. Sumida, H. *et al.* Interplay between CXCR2 and BLT1 facilitates neutrophil infiltration and resultant keratinocyte activation in a murine model of imiquimod-induced psoriasis. *J. Immunol. Baltim. Md 1950* **192**, 4361–4369 (2014).

145. Khajah, M. *et al.* Fer Kinase Limits Neutrophil Chemotaxis toward End Target Chemoattractants. *J. Immunol. Author Choice* **190**, 2208–2216 (2013).

146. Cheng, Y., Ma, X., Wei, Y. & Wei, X.-W. Potential roles and targeted therapy of the CXCLs/CXCR2 axis in cancer and inflammatory diseases. *Biochim. Biophys. Acta BBA - Rev. Cancer* **1871**, 289–312 (2019).

147. Zu, Y. L. *et al.* p38 mitogen-activated protein kinase activation is required for human neutrophil function triggered by TNF-alpha or FMLP stimulation. *J. Immunol. Baltim. Md 1950* **160**, 1982–1989 (1998).

148. Reutershan, J. *et al.* Critical role of endothelial CXCR2 in LPS-induced neutrophil migration into the lung. *J. Clin. Invest.* **116**, 695–702 (2006).

149. Dambuza, I. M. & Brown, G. D. C-type lectins in immunity: recent developments. *Curr. Opin. Immunol.* **32**, 21–27 (2015).

150. Li, K. & Underhill, D. M. C-Type Lectin Receptors in Phagocytosis. in *C-Type Lectins in Immune Homeostasis* (ed. Yamasaki, S.) 1–18 (Springer International Publishing, 2020). doi:10.1007/82_2020_198.

151. Kobayashi, N. *et al.* TIM-1 and TIM-4 Glycoproteins Bind Phosphatidylserine and Mediate Uptake of Apoptotic Cells. *Immunity* **27**, 927–940 (2007).

152. Park, S.-Y. *et al.* Rapid cell corpse clearance by stabilin-2, a membrane phosphatidylserine receptor. *Cell Death Differ.* **15**, 192–201 (2008).

153. Park, D. *et al.* BAI1 is an engulfment receptor for apoptotic cells upstream of the ELMO/Dock180/Rac module. *Nature* **450**, 430–434 (2007).

154. Tridandapani, S. *et al.* The Adapter Protein LAT Enhances Fcγ Receptor-mediated Signal Transduction in Myeloid Cells *. *J. Biol. Chem.* **275**, 20480–20487 (2000).

155. Larsen, E. C. *et al.* Differential Requirement for Classic and Novel PKC Isoforms in Respiratory Burst and Phagocytosis in RAW 264.7 Cells. *J. Immunol.* **165**, 2809–2817 (2000).

156. Freeman, S. A. & Grinstein, S. Phagocytosis: receptors, signal integration, and the cytoskeleton. *Immunol. Rev.* **262**, 193–215 (2014).

157. Marshansky, V. & Futai, M. The V-type H+-ATPase in vesicular trafficking: targeting, regulation and function. *Curr. Opin. Cell Biol.* **20**, 415–426 (2008).

158. Kinchen, J. M. & Ravichandran, K. S. Phagosome maturation: going through the acid test. *Nat. Rev. Mol. Cell Biol.* **9**, 781–795 (2008).

159. Fairn, G. D. & Grinstein, S. How nascent phagosomes mature to become phagolysosomes. *Trends Immunol.* **33**, 397–405 (2012).

160. Sheshachalam, A., Srivastava, N., Mitchell, T., Lacy, P. & Eitzen, G. Granule Protein Processing and Regulated Secretion in Neutrophils. *Front. Immunol.* **5**, (2014).

161. Brinkmann, V. *et al.* Neutrophil Extracellular Traps Kill Bacteria. *Science* **303**, 1532–1535 (2004).

162. Urban, C. F. *et al.* Neutrophil Extracellular Traps Contain Calprotectin, a Cytosolic Protein Complex Involved in Host Defense against Candida albicans. *PLOS Pathog.* **5**, e1000639 (2009).

163. Bawadekar, M. *et al.* Peptidylarginine deiminase 2 is required for tumor necrosis factor alpha-induced citrullination and arthritis, but not neutrophil extracellular trap formation. *J. Autoimmun.* **80**, 39–47 (2017).

164. Azzouz, D., Khan, M. A. & Palaniyar, N. ROS induces NETosis by oxidizing DNA and initiating DNA repair. *Cell Death Discov.* **7**, 1–10 (2021).

165. Saha, P. *et al.* PAD4-dependent NETs generation are indispensable for intestinal clearance of Citrobacter rodentium. *Mucosal Immunol.* **12**, 761–771 (2019).

166. Mehrotra, P. *et al.* IL-17 mediates neutrophil infiltration and renal fibrosis following recovery from ischemia reperfusion: compensatory role of natural killer cells in athymic rats. *Am. J. Physiol. Renal Physiol.* **312**, F385–F397 (2017).

167. Gill, S. E. *et al.* Shedding of Syndecan-1/CXCL1 Complexes by Matrix Metalloproteinase 7 Functions as an Epithelial Checkpoint of Neutrophil Activation. *Am. J. Respir. Cell Mol. Biol.* **55**, 243–251 (2016).

168. Starr, A. E., Bellac, C. L., Dufour, A., Goebeler, V. & Overall, C. M. Biochemical Characterization and N-terminomics Analysis of Leukolysin, the Membrane-type 6 Matrix Metalloprotease (MMP25). *J. Biol. Chem.* **287**, 13382–13395 (2012).

169. Van Den Steen, P. E. *et al.* Gelatinase B/MMP-9 and neutrophil collagenase/MMP-8 process the chemokines human GCP-2/CXCL6, ENA-78/CXCL5 and mouse GCP-2/LIX and modulate their physiological activities. *Eur. J. Biochem.* **270**, 3739–3749 (2003).

170. Cho, J. S. *et al.* Neutrophil-derived IL-1β is sufficient for abscess formation in immunity against Staphylococcus aureus in mice. *PLoS Pathog.* **8**, e1003047 (2012).

171. Sun, D. & Shi, M. Neutrophil swarming toward Cryptococcus neoformans is mediated by complement and leukotriene B4. *Biochem. Biophys. Res. Commun.* **477**, 945–951 (2016).

172. Kienle, K. *et al.* Neutrophils self-limit swarming to contain bacterial growth in vivo. *Science* **372**, eabe7729 (2021).

173. Chertov, O. *et al.* Identification of Human Neutrophil-derived Cathepsin G and Azurocidin/CAP37 as Chemoattractants for Mononuclear Cells and Neutrophils. *J. Exp. Med.* **186**, 739–747 (1997).

174. Knipfer, L. *et al.* A CCL1/CCR8-dependent feed-forward mechanism drives ILC2 functions in type 2–mediated inflammation. *J. Exp. Med.* **216**, 2763–2777 (2019).

175. Herold, S., Mayer, K. & Lohmeyer, J. Acute Lung Injury: How Macrophages Orchestrate Resolution of Inflammation and Tissue Repair. *Front. Immunol.* **2**, (2011).

176. Soehnlein, O. & Lindbom, L. Phagocyte partnership during the onset and resolution of inflammation. *Nat. Rev. Immunol.* **10**, 427–439 (2010).

177. Keir, M. E., Yi, T., Lu, T. T. & Ghilardi, N. The role of IL-22 in intestinal health and disease. *J. Exp. Med.* **217**, e20192195 (2020).

178. Rajarathnam, K., Schnoor, M., Richardson, R. M. & Rajagopal, S. How do chemokines navigate neutrophils to the target site: Dissecting the structural mechanisms and signaling pathways. *Cell. Signal.* **54**, 69–80 (2019).

179. Sullivan, D. P., Bui, T., Muller, W. A., Butin-Israeli, V. & Sumagin, R. In vivo imaging reveals unique neutrophil transendothelial migration patterns in inflamed intestines. *Mucosal Immunol.* **11**, 1571–1581 (2018).

180. Mei, J. *et al.* CXCL5 Regulates Chemokine Scavenging and Pulmonary Host Defense to Bacterial Infection. *Immunity* **33**, 106–117 (2010).

181. Flannigan, K. L. *et al.* IL-17A-mediated neutrophil recruitment limits expansion of segmented filamentous bacteria. *Mucosal Immunol.* **10**, 673–684 (2017).

182. Osbelt, L. *et al.* Variations in microbiota composition of laboratory mice influence Citrobacter rodentium infection via variable short-chain fatty acid production. *PLOS Pathog.* **16**, e1008448 (2020).

183. Collins, J. W. *et al.* Pre-treatment with Bifidobacterium breve UCC2003 modulates Citrobacter rodentium-induced colonic inflammation and organ specificity. *Microbiology* **158**, 2826–2834 (2012).

184. Ivanov, I. I. *et al.* Induction of intestinal Th17 cells by segmented filamentous bacteria. *Cell* **139**, 485–498 (2009).

185. Rolig, A. S., Carter, J. E. & Ottemann, K. M. Bacterial chemotaxis modulates host cell apoptosis to establish a T-helper cell, type 17 (Th17)-dominant immune response in Helicobacter pylori infection. *Proc. Natl. Acad. Sci.* **108**, 19749–19754 (2011).

APPENDIX: IACUC APPROVAL FORM

THE UNIVERSITY OF ALABAMA AT BIRMINGHAM

MEMORANDUM

DATE: 01-Feb-2021

TO: Weaver, Casey T

FROM: Robert A. Kesterson, Ph.D., Chair

Institutional Animal Care and Use Committee (IACUC)

SUBJECT: **NOTICE OF APPROVAL**

The following application was approved by the University of Alabama at Birmingham Institutional Animal Care and Use Committee (IACUC) on 01-Feb-2021.

Protocol PI:	Weaver, Casey T
Title:	Specialization of Innate and Adaptive Immune Cells in Intestinal Barrier Function
Sponsor:	National Institute of Diabetes and Digestive and Kidney Diseases/NIH/DHHS
Animal Project Number (APN):	IACUC-20728

This institution has an Animal Welfare Assurance on file with the Office of Laboratory Animal Welfare (OLAW), is registered as a Research Facility with the USDA, and is accredited by the Association for Assessment and Accreditation of Laboratory Animal Care International (AAALAC).

This protocol is due for full review by 03-Feb-2023.

Institutional Animal Care and Use Committee (IACUC)

403 Community Health on 19th | 933 19th Street South

Mailing Address:

CH19 403 | 1720 2nd Ave South | Birmingham AL 35294-2041

phone: 205.934.7692 | fax: 205.934.1188

www.uab.edu/iacuc | iacuc@uab.edu